PhD degree in Systems Medicine (curriculum in Molecular Oncology)

European School of Molecular Medicine (SEMM),

University of Milan and University of Naples “Federico II”

Settore disciplinare: med/04

Role of obesity in the development of acute promyelocytic leukemia (APL)

Paolo Falvo

IEO, Milan

Matricola n. R 11124

Supervisor: Prof. Pier Giuseppe Pelicci

IEO, Milan

Added Supervisor: Dr. Luca Mazzarella

IEO, Milan

Anno accademico 2017-2018

Table of content

List of tables and figures

List of Abbreviations

4-HNE: 4-hydroxynonenal

AA: arachidonic acid

ALL: acute lymphoid leukemia

AML: acute myeloid leukemia

APL: acute promyelocytic leukemia

ATM: ataxia telangiectasia mutated

ATO: arsenic trioxide

ATR: ataxia-telengiectasia and Rad-3 related

ATRA: *all-trans* retinoic acid

BER: base excision repair

BMI: body mass index

CLL: chronic lymphoblastic leukemia

CML: chronic myeloid leukemia

CNS: central nervous system

CR: complete remission

DDR: DNA damage response

EPA: eicosapentaenoic acid

FA: fatty acid

FAB: French-American-British classification

FAO: fatty acid oxidation

HAT: histone acetyl-transferase complexes

HDAC: histone deactylase complexes

HFD: high fat diet

HIF-1: hypoxia inducible factor-1

histone acetyl-transferase complexes (HAT)

HPC-1: hematopoietic progenitors cells-1

HPC2: hematopoietic progenitors cells-2

HR: hazard ratio

HR: homologous-direct repair

HSCs: hematopoietic stem cells

LA: linoleic acid

LKS cells: Lin^{-} Sca^{+} c-Kit^{+} cells

LT: leukotrienes

M1DG: 3-(2-deoxy-β-D-erythro-pentofuranosyl)pyrimido[1,2-α]purin-10(3H)-one

MMR: mismatch repair

MPPs: multipotent progenitors

NCOR: nuclear receptor corepressor complex

NAC: n-acetylcysteine

NER: nucleotide excision repair

NHEJ: non homologous-end joing

PG: prostaglandins

PIP: phosphatidylinisitol

PML: promyelocytic leukemia

PPARδ: peroxisome proliferator activator receptor delta

PUFA: polyunsaturated fatty acid

RARα: retinoic receptor alpha gene

RARE: retinoic acid response element

ROS: reactive oxygen species

RXR: retinoic X receptor

SD: standard diet

SMRT: silencing mediator for retinoid or thyroid-hormone receptors

ST-HSCs: short-term hematopoietic stem cells

TRIM: tripartite motif

TX thromboxanes

WAT: white adipose tissue

WGS: whole genome sequencing

WHO: World Health Organization

Abstract

Obesity is a pathological condition characterized by an augmented presence of fat mass in the body. Obesity is known to increase the risk of many cancer types. Clinical data produced by ourselves and others have shown that the incidence of acute promyelocytic leukaemia (APL) is strongly correlated with obesity. The cytogenetic hallmark of APL is the reciprocal translocation between chromosomes 15 and 17 that fuses portions of the retinoic acid receptor α (RARα) and PML genes, resulting in the formation of the PML/RARα fusion protein. However, the molecular mechanisms explaining the effects of obesity on APL development have not been elucidated.

To recapitulate clinical observations, we developed and characterized a mouse model of diet-induced obesity using transgenic mice constitutively expressing PML/RARα in the hematopoietic system (PML/RARα KI mice) and wild type mice as a control. Mice were fed standard diet (SD) or high fat diet (HFD) (60% vs 10% of fats in the chow), and leukaemia-free survival was monitored. As expected, we observed that HFD-fed PML/RARα KI mice developed leukaemia earlier (median survival 204 vs 254 days, $p<0.001$) and with higher penetrance (100% vs 70%) than SD-fed mice.

By FACS analysis upon bone marrow (BM) subpopulations, we demonstrated that HFD increases the percentage of progenitor cells in both WT and PML/RARα KI, while concomitantly decreasing the percentage of hematopoietic stem cells (HSCs). Indeed, we demonstrated that this shift is mediated by a decrease in G0 phase in PML/RARα KI HFD-fed mice, suggesting a loss of quiescence.

We then evaluated the extent of DNA damage in hematopoietic stem cells (HSC) after four months of diet, using the comet assay. We demonstrated that that HFD-fed PML/RARα KI mice presented a 40% increase of DNA damage in HSCs as compared to SD-fed PML/RARα mice ($p<0.001$). However, this was not associated with an increased mutational load as revealed by a novel whole genome sequencing-based method. We investigated whether HFD confers a proliferative advantage to PML/RARα bone marrow using colony forming assays.

Indeed, we observed that HFD PML/RARα bone marrow has a higher clonogenicity than bone marrow from SD-fed mice.

Finally, we demonstrated that linoleic acid (LA), which is the main component of HFD increases PML/RARα enhanced self-renewal via a mechanism that may be related to PPARd activation.

Chapter 1. Introduction

1.1 Obesity and cancer

Obesity is a pathological state characterized by increased body fat mass. Nowadays, it has become a serious problem worldwide: nearly two thirds of adults in the United States are overweight or obese[1]. Likewise, in the rest of the world the percentages are rising dramatically, with projections of nearly 42% of the population being obese by 2030[2].

The parameter most widely used to identify obese individuals is the Body Mass Index (BMI), which is defined as the ratio between the weight in kilos and the square of height in meters. Based on this formula, the World Health Organization (WHO) classifies individuals in 4 different classes (table 1); with a BMI above 30 indicative of obesity[3].

BMI (Kg/m^2)	**Weight category**
<18.5	Underweight
18.5 to 24.9	Normal
25.0 to 29.9	Overweight
30.0 to 39.9	Obese
>40	Severely Obese

Table 1. BMI classification tables. On the left-hand side, the BMI values calculated as ratio between weight in kilos and height in square meters are reported, on the right-hand side - the weight category associated.

The increased prevalence of obesity can be attributed to multiple causes, like increased caloric intake, snacking patterns of eating and decreased physical activity[4,5]. Additionally, genetic factors may also contribute to obesity[6,7]. Many genes have been correlated to increased body fat mass, most notably leptin and its receptor[7]. However, in humans mutations in leptin gene and its receptor are an extreme rare cause of obesity[7]. In fact, it was reported that obesity in humans can also be due to mutations in genes implicated in

alternative pathways, like appetite regulation by central nervous system (CNS), insulin action and glucose metabolism, and lipid metabolism[8].

Clinically, obese individuals can suffer from several diseases, most notably diabetes and cardiovascular diseases, configuring what is usually referred to as metabolic syndrome[9].

Mounting evidence also correlates obesity with risk of developing cancer. Experiments in the 50's showed that a mutation in the *ob* gene (that codes in mice for leptin) correlated with increase in breast cancer risk[10], due to uncontrolled estrogen production. Ten years later, this observations was confirmed in epidemiological studies assessing the prevalence of obesity in breast cancer patients[11]. Starting from these two pivotal observations, over the past 50 years, numerous studies have established a strong correlation between obesity and risk of developing or dying of multiple tumor types such as liver, colon, ovarian and postmenopausal breast cancer[7,12–14].

Despite overwhelming epidemiological evidence, the molecular causes linking overweight/obesity and different tumors are still incompletely understood.

The obese milieu is enriched for circulating factors like hormones, cytokines and chemokines that stimulate cell proliferation. Indeed, an additional source of growth-promoting factors is the adipose tissue itself. These factors are generally known as adipokines such as adiponectin and tumor necrosis factor alpha (TNF-α). Adiponectin is secreted to signal satiety and enhances insulin sensitivity and glucose uptake[15]. In contrast to other adipokines, its expression is lowered in obese individuals[16] and inversely correlates with cancer risk[17,18]. Multiple mechanisms have been hypothesized to explain adiponectin's anticancer activity: blocking vascular endothelial growth factor A (VEGF-A)[19] in prostate cancer or mTOR signaling in colon cancer[20]. TNF-α role in cancer is quite puzzling, in fact, it was demonstrated that it may inhibit or sustain cancer growth depending on cancer type, stage and environment[21,22]. Brunn and colleagues demonstrated that *in vitro* TNF-α can reduce the mRNA levels of adiponectin, limiting its anti-cancer function[23]. However, Rubio

and colleagues have demonstrated that TNF-α reduced tumor mass by inducing tumor necrosis[24].

1.2 Epidemiological evidence in acute myeloid leukemia (AML) and acute promyelocytic leukemia (APL)

Compared to solid tumors, in haematological malignancies the correlation between risk and obesity has been less studied. Moreover, in these studies, patients were rarely stratified differentiating chronic/acute and lymphoid/myeloid leukemias[25].

The first study in which obesity was linked to acute myeloid leukemia (AML) and chronic lymphoblastic leukemia (CLL) was performed on war veterans. In this study a strong association between obesity and AML and CLL was observed[26].

Larsson and colleagues conducted a meta-analysis of cohort studies published from 1966 to July 2007[27]. The relative risk (RR) of developing disease for all subgroups (acute lymphocytic leukemia (ALL), acute myeloid leukemia (AML), chronic myeloid leukemia (CML) and chronic lymphocytic leukemia (CLL)) was statistically significantly higher in obese compared to lean subjects: 1.65 (95% CI, 1.16–2.35) for ALL, 1.65 (95% CI, 1.16–2.35) for AML, 1.25 (95% CI, 1.11-14), 1.26 (95% CI, 1.09–1.46) for CML and 1.25 (95% CI, 1.11–1.41) for CLL.

Poynter and colleagues have specifically assessed the association between obesity and AML in a retrospective case-control study. In a cohort of 422 AML patients and 1388 controls, it was shown that obesity is associated in males and females with development of the disease (OR=2.22, 95% CI 1.28-3.85 for males and OR=1.85, 95% CI 1.08-3.15 for females)[28].

A more recent meta-analysis showed that in AML a modest but significant association between obesity and disease risk is repeatedly observed[29], However, AML is increasingly understood as a disease whose natural history is strongly influenced by its underlying

biology and genetics. Consequently, obesity may influence the risk of developing only some specific AML subtypes. Thus, I will now briefly review current AML classification systems before analysing the existing evidence on the association between obesity and specific AML subtypes.

1.3 AML classifications

Acute myeloid leukemia (AML) is the most common type of acute leukemia in adults, it accounts for almost 80% of cases with acute leukemias[30]. The disease is characterized by an uncontrolled expansion of undifferentiated myeloid precursors that leads to impaired hematopoiesis. From the clinical point of view, AML patients present with anemia and thrombocytopenia. Physically, patients feel fatigue and weight loss. If uncured, this leukemia leads patients' death in few months caused by severe bleeding or infections, due to severe impairment of immune function.

AML is a very heterogeneous group of diseases; hence different classification systems have been devised. The earliest classification, still routinely used in the clinica, is the French-America-British (FAB) system, based on morphological features[31]:

More recently, the significant impact of the underlying genetic abnormalities has been recognized, prompting a new classification by the WHO based on genetic features [32,33] . In 2013, TGCA analyzed the genomes of 200 *de novo* cases of AML, using different genomic strategies e.g. whole-genome sequencing (WGS) or whole-exome sequencing (WES). It was discovered that in the analyzed patients the number of present mutations was much less compared to solid tumors, with an average of only 13 coding mutations (range 1 to 51)[34].

Acute promyelocytic leukemia (APL), which is the subject of this thesis, has distinct genetical and morphological features. This leukemia belongs to the M3 class in the FAB classification and is classified by the WHO as distinct class because of the presence of PML/RARα translocation.

From the genetic point of view, APL appears even less complex than AML. APL patients bear known translocations involving the retinoic receptor alpha gene (RARα) gene on chromosome 17. By far the most common (>99% of the cases) translocation partner is the promyelocytic leukemia (PML) gene, located on chromosome 15, resulting in the t(15;17) translocation. PML/RARα fusion mRNA was first cloned in 1991[35,36].

Historically, it was a fatal and incurable leukemia subtype. If not treated, patients within few weeks, most often of bleeding due to severe thrombocytopenia.

The introduction of all-*trans* retinoic acid (ATRA) into clinical practice in early '80s, constituted a turning point in the history of APL[37]. The molecule promotes differentiation of promyelocytes into mature granulocytes and its use is considered the paradigm of differentiation therapy. The first study in which ATRA was used in the clinics was performed in 1988[38]. In this study, 22 APL patients were treated with ATRA, and 14 of them entered complete remission (CR) after the treatment. Following this first encouraging result, other clinical trials were conducted and confirmed the efficacy of ATRA.

Arsenic trioxide, another important player in APL treatment, was first tested on humans in 1990[39]. In the first study 58 patients (11 *de novo* and 47 relapse APL) were treated with ATO. Eight out of 11 *de novo* and 40/47 relapsed patients obtained CR.

Mouse models demonstrated that combination of ATRA and ATO synergized in APL. In fact, it was demonstrated that the two molecules eradicate the disease through the degradation of PML/RARα fusion protein[40].

With advances in treatment, APL, once considered the deadliest of all leukemia types, has become the most curable. Indeed, at present, APL is characterized by CR rates of 90% and cure rates of ~80%, or even higher in low-risk patients[41].

1.4 Clinical studies demonstrating association between APL and obesity

The first study concentrating on obesity and AML subclasses was performed at the M.D Anderson Cancer Center on almost 1200 AML patients. Interestingly, only the incidence of acute promyelocytic leukemia (APL) correlated positively with obesity[42] ($p<0.0003$). This first observation was corroborated by another study in China, in which the relationship between obesity and AML subclasses was analyzed in 29 hospitals in Shanghai[43]. The risk of developing AML was inversely correlated to BMI, whilst the risk of developing APL was positively correlated. These initial observations were confirmed by other studies [13,44,45], all with very small sample sizes.

Our group independently studied the relationship between obesity and APL. In a first study on 120 APL patients[14] it was demonstrated that following ATRA and idarubicin treatment, obese patients had a higher risk of relapse than normal-weight patients (hazard ratio 2.45 95% CI, 1.00-5.99).

Subsequently, we assessed the relationship between obesity and APL risk in a large unpublished study. We first reanalyzed the data by Bhaskaran et al[13]which comprises 5,833 subjects with a diagnosis of "leukemia". This diagnosis was further classified into the following groups: "APL" (n=26), "non-APL-AML" (n=1,012), lymphoid leukemias ("LL"; n=2,823) and "other" (n=1,972). We observed that *per* each 5 kg/m^2 BMI increase, we obtained HR of 1.44 for APL (95% CI 1.0-2.08), 1.17 for non-APL-AML (95% CI 1.10-1.26), 1.04 for LL (95% CI 1.0-1.09) and 1.10 for other leukemias (95% CI 1.04-1.15). Stratifying by gender suggested a stronger effect for males in APL (HR 1.82, 95% CI 1.10-3.00 vs female (HR 1.19, 95% CI 0.67-1.98), although the sample numerosity became low (n=13 each). Together, these results imply that higher BMI is associated with increased risk of all sub-types of leukemia, particularly of APL. We then validated these results in retrospective case-control studies on cohorts obtained from Spain (PETHEMA) and Italy

(GIMEMA) and patients from the USA-based AML genome sequencing study (the AML TCGA cohort with 22 additional cases characterized at Washington University-St Louis). To generate control groups for comparison, we obtained anthropometric data from epidemiological surveys of the general population in the different countries. In all three cohorts, there was a strong evidence that the observed BMI distribution for cases within the four WHO classes was different from that expected under the null hypothesis of no association (Italy $p<0.001$, Spain $p=0.011$, USA $p<0.001$) in gender-, age- and ethnicity-(for USA) matched controls. In particular, in all three datasets, there were more APL cases than expected in the high BMI groups, and less than expected in the low BMI groups. We then analyzed the transcriptomic profile of obese APL patients from the TCGA dataset. APL was associated with increased activity of 14 and decreased activity of 47 out of 186 pathways. Intriguingly, pathways associated with the metabolism of long-chain unsaturated fatty acids (linoleic, linolenic and arachidonic acid, precursors of eicosanoids mediating inflammation-associated cancers), were among the top upregulated

These data suggest that obesity influences APL onset and eventually tumor relapse, however the mechanisms at the basis of this relationship are unknown and are the major subject of this thesis work.

1.5 Genetics and biology of APL

PML is a ubiquitously expressed nuclear protein that belongs to the TRIpartite Motif (TRIM) consisting of zinc RING finger, two alternate cysteine-histidine rich zinc binding domains, the B1 and B2 boxes, and an alpha-helical coiled-coil dimerization domain. Thanks to its conformation, PML forms particular structures in the cells known as nuclear bodies (NB)[46–48]. PML gene in humans contains nine different exons spanning 53 kb. The messenger RNA can be spliced out into seven different variants. Six of the arising proteins, called (PML I-VI), are nuclear, and, one called VIIb, is cytoplasmatic [49,50]. In NBs, PML interacts with several proteins such as p53 and pRb that exert control over major cellular processes[51]. Indeed, NBs have been implicated in controlling cell cycle, apoptosis, senescence and, in general, all processes that regulate genome stability[52,53]. PML was shown to be a potent tumor suppressor. The lack of the protein in the PML knock-out mice accelerates spontaneously or after induction with X rays the development of different types of malignancies[53–55]

Retinoic receptors (RAR) belong to the nuclear receptor family, comprising 3 members: α, β and γ. RARα and RARγ exert different function in the different phases of hematopoiesis, e.g. RARγ alone is implicated in differentiation of hematopoietic stem cell[56], while together with RARα is involved in the differentiation process of granulocytes[57]. Only RARα is crucial for APL development. RARα is a nuclear transcription factor that, in heterodimeric complex with retinoic X receptor (RXR), recognizes sequences of 6 bp (AGGTCA), separated by short spacers (1, 2 or 5bp) and named retinoic acid response elements (RARE)[58]. In the absence of its ligand, RARα is bound to RXR and the complex recruits histone deacetylase complexes (HDAC) such as nuclear receptor co-repressor complex (NCOR) and silencing mediator for retinoid or thyroid-hormone receptors (SMRT), so that transcription of downstream genes is blocked[59]. However, upon binding of its ligand, the

RARα recruits histone acetyl-transferase complexes (HAT) that ultimately leads to the transcription of downstream RARα targets[60].

The PML/RARα fusion protein works as a negative dominant protein for RARα as it has an increased binding affinity for the HDAC complexes[61], in particular SMRT [62]. Higher ligand concentrations are required to release the complex[63]. Therefore, PML/RARα and RARα compete for binding sites. Furthermore, the number of potential DNA binding sites of PML/RARα is higher than that of RARα. The protein, in fact, does not require the presence of RXR to bind DNA, is able to self-dimerize[64,65] and to bind motifs which contain longer spacer regions[66].

The molecular mechanism of PML/RARα binding on RARE is better illustrated in figure 1.

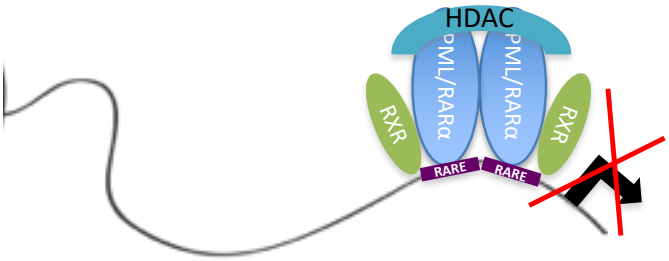

Figure 1. PML/RARα binding to RARE, modified from[67]. PML/RARα proteins (in light blue), in complex with RXR are binding retinoic acid response elements (RARE) (in violet rectangles. Upon binding, they recruit HDAC complex (in cyan) and transcription is repressed.

1.6 Cellular and mouse models to study APL

Many cellular and mouse systems to model different aspects of APL and PML/RAR biology have been developed. Our group generated a cellular model in the U937 cell line (an AML cell line) that allowed inducible PML/RARα expression, which blocked differentiation upon different stimuli[68]. In 1996, Early and colleagues cloned PML/RARα under the Cd11b promoter and observed impaired myelopoiesis following mice irradiation. After irradiation, almost 100% of WT mice survived irradiation, while almost half of the transgenic mice carrying PML/RARα mutation died of leukopenia[69]. Two years later, Altabef and colleagues infected chicken embryos with a retrovirus carrying PML/RARα oncogene and observed the onset of leukemia in 2 weeks[70].

However, none of the two systems recapitulates completely the observations in patients. In 1998, Grisolano and colleagues cloned human PML/RARα cDNA downstream of human Cathepsin G promoter (that ensures the expression only in promyelocytes and in progenitors[71]) and expressed it in transgenic mice[72]. Thirty percent of mice developed APL with clinical features compatible with those seen in patients. Low penetrance was attributed to low expression levels of the transgene. Therefore, in 2002, the same group generated a knock-in mouse model in which the cDNA was transcribed from mouse Cathepsin G promoter, increasing the expression of PML/RARα[73]. These new mice, in the C/57 background (PML/RARα KI mice) developed APL with reduced latency (between 6-19 months) and increased penetrance (60-70%) compared to the previous model.

The incomplete penetrance and relatively long latency suggest that PML/RARα mutation is insufficient to give rise to the leukemia, and that at least a second oncogenic mutation is required. Many mutations cooperate with PML/RARα to give rise to leukemia, such as internal tandem duplication in the fms-like tyrosine kinase 3 gene (FLT3 ITD)[74], or oncogenic K-*ras*[75]. Moreover, in 2011 Tim Ley's group sequenced mouse APL genomes, and they observed that PML/RARα mutation occurred with mutations in different genes

often present in human APL, such as *jak1* and lysine specific histone demethylase 6 (*kmd6a*). In particular they observed that jak1 mutation is also present in human APL[76]. More recently, in our group, Riva and colleagues sequenced the genome from 5 mouse APL and 11 human APL. They observed that in all mice 18 mutations were present in total, while in the human 73[77].

1.7 *In vivo* studies demonstrating association between obesity and APL

The availability of a mouse model able to faithfully reproduce APL prompted us to test the effect of diet-induced obesity. To this end, PML/RARα KI mice were fed ad libitum with standard diet (SD, with 10% content made of fat) or high fat diet (HFD, 60% fat). As a control, WT mice were fed with identical dietary regimens.

Weight gain was equal in both strains (Figure 2A). When mice were fed with HFD, the penetrance of the disease increased to 100% compared to 70% observed in SD. Moreover, the median survival dropped from 254 days in SD to 204 in HFD ($p<0.001$).

Taken together, these data demonstrated that mice model expressing PML/RARα could be used as a model to understand the relationship between APL onset and obesity, which is the ultimate scope of this thesis work.

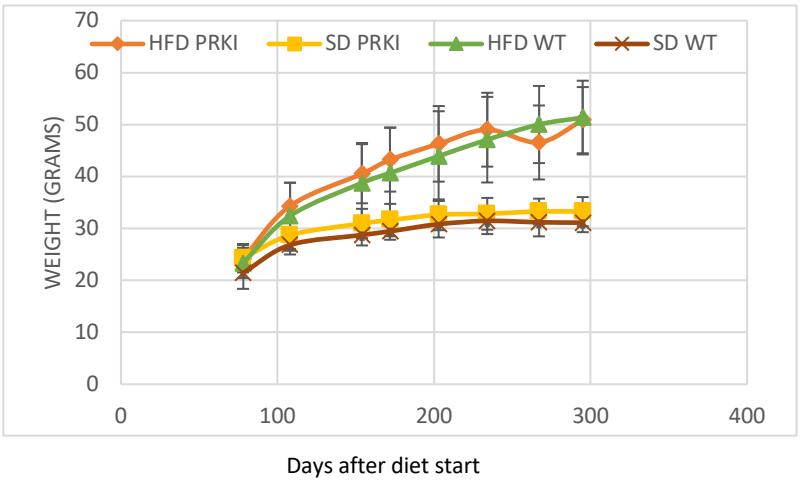

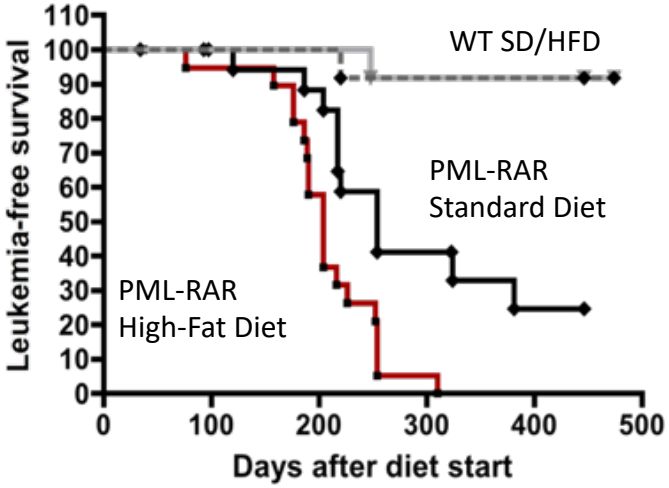

Figure 2. Obesity cooperates with PML/RARα mutation in APL development. A) Weight gain by the mice used in the experiments. On the x axis the weight is indicated in grams, on the y axis the days from diet beginning. WT SD is shown in magenta, WT HFD in green, PML/RAR KI (PRKI) SD in yellow, PML/RAR KI (PRKI) HFD in orange D **B)** Kaplan-Meier curve showing survival of 15 PML/RARα KI mice in SD (black line), 15 PML/RAR KI mice in HFD (red line), WT SD mice black dashed line and WT HFD mice grey line. Percentage of survival is shown on the y axis, while days after treatment on the x axis.

Although the association between obesity and APL development is clear in patients and in a mouse model, convincing molecular theories explaining such cooperation are missing.

Tabe and colleagues, showed that transcription of leptin overexpression is enhanced in APL cells. Moreover, when mesenchymal stem cell-derived adipocytes were co-cultured with APL cells, ATRA and doxorubicin lost their pro-apoptotic effect on APL cells[78]. However, the system used in this study does not mirror APL and our unpublished results do not support an overexpression of LepR in APL nor any correlation with obesity (not shown).

1.8 Architecture of hematopoietic system

The history of study of the hematopoietic system has had a pivotal role in the understanding of the stem cells. Blood has an extremely high regenerative potential and it is estimated that every day bone marrow (BM) produces 10^{12} cells[79] . Since the beginning of the XX century, it was postulated that hematopoietic system is organized in a hierarchical manner. The first piece of evidence for the hierarchy and, more in particular, for the existence of cells that generate other cells derived from an observation by Lorenz and colleagues in 1950[80]. They observed that following irradiation, mice were able to survive only when transplanted with donor spleen or BM. However, this first observation did not fully explain whether there was only one cell or more cells giving rise to the fully reconstituted BM. Thanks to the development of flow cytometry, surface markers were discovered and hematopoietic stem cells (HSCs) characterized[81]. HSCs are on the apex of the hematopoietic cascade and are able to generate multipotent progenitors. In turn, the progenitors divide further giving rise to more differentiated cells.

Since HSCs are extremely rare, both in mouse and in humans, the study of HSC biology has always been very difficult. Historically, HSCs to be defined must possess three different proprieties that historically were assessed only by transplantation:

a) it is capable of self-renewal. It indicates the ability of cells to divide maintaining the state of differentiation of the parent cell[82]. This propriety ensures the maintenance of the stem cell reservoir. On the contrary, differentiating potential indicates the capacity to produce mature cells upon appropriate stimuli[82]. Self-renewal and differentiation can be accomplished in a single mitosis event, in which a fate determinant is divided unequally in daughter cells giving rise to one differentiated and one stem cell (asymmetric stem cell division)[82]. To expand HSCs, a symmetric division is required, whilst to obtain committed cells, divisions with differentiation are needed[82]. Differences between symmetric and asymmetric stem cell division are illustrated in figure 3.

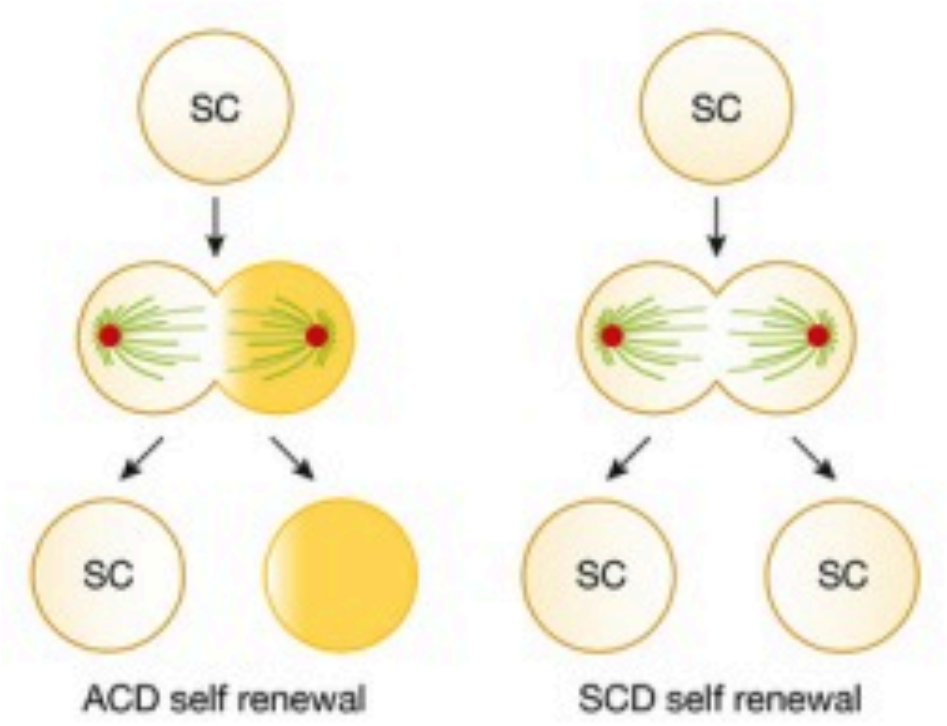

Figure 3. Asymmetric cell division and symmetric cell division modified from[82]. Schematic illustration of Asymmetric cell division (ACD) is shown on the left, in which a stem cell (SC) divides unequally into a new SC and a differentiated cell. On the right, symmetric cell division (SCD) is shown in which fate determinants are equally distributed giving rise to two identical daughter stem cells

b) it can be dormant (a property also known as quiescence);

c) can enter an actively dividing phase[83], differentiate and thus re-grow the cells forming the entire BM when recipient mice are irradiated for a long time (historically more than 12 weeks[84]). The duration of engraftment upon transplantation has allowed for the distinction between long-term reconstituting HSCs, (LT-HSC), short-term reconstituting HSCs (ST-HSCs) and multipotent progenitors (MPP).

Once HSCs divide asymmetrically they generate all of the BM cells as illustrated in the figure 4.

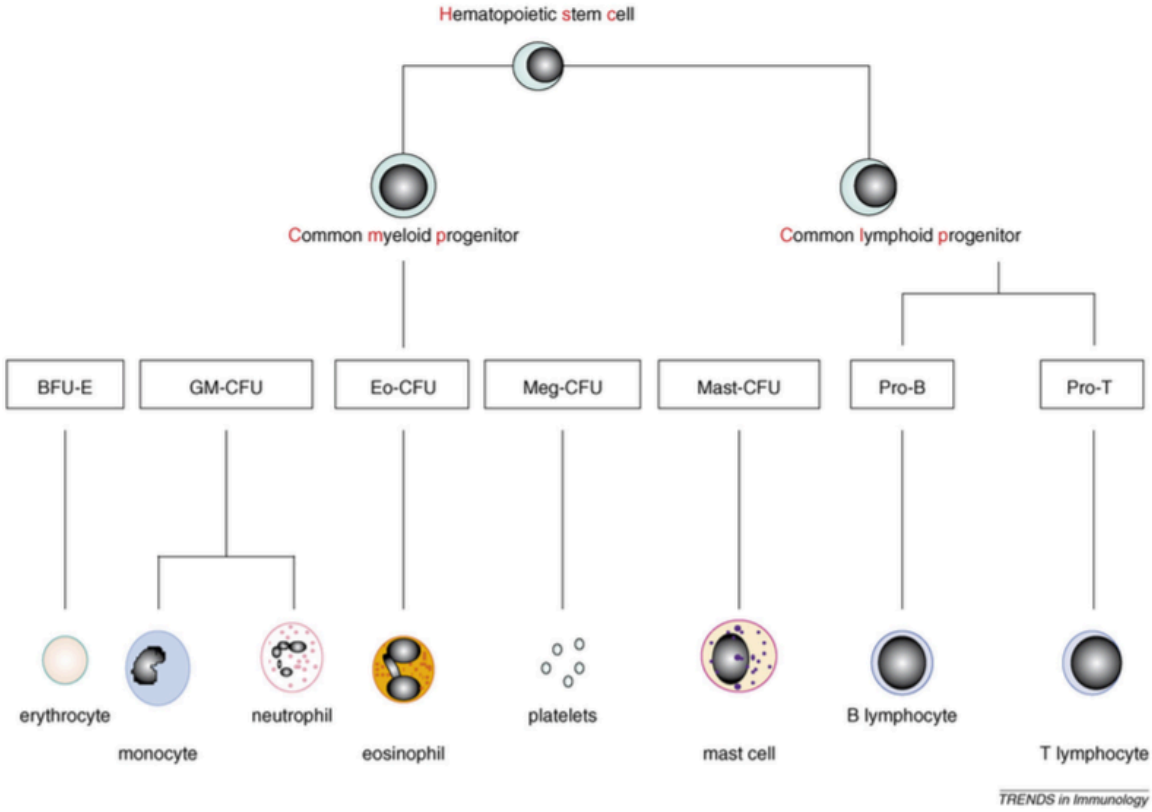

Figure 4. Schematic representation of hematopoietic system, modified from[85]. On the top are shown long-term hematopoietic stem cells (HSCs). Division of HSCs gives rise to common myeloid progenitors (CMP), and common lymphoid progenitors (CLP). CMP in turn gives rise to monocyte, erythrocyte, neutrophils, eosinophils, megakaryocytes, mast cells, while CLP to B and T lymphocytes

Differentiating cells lose self-renewal property and become more and more mature and specialized towards their ultimate function. This first model shown in figure 4 was defined as the "conventional" model. HSCs divide in a dichotomy fashion into common lymphoid and myeloid progenitors. This model was already discussed in the 80s and different observations, led researchers hypothesized a second model defined as "sequential determination model"[86,87]. This second model excludes a clear dichotomic choice of HSCs, but on the contrary supports the idea that HSCs undergo stepwise processes during maturation (Figure 5).

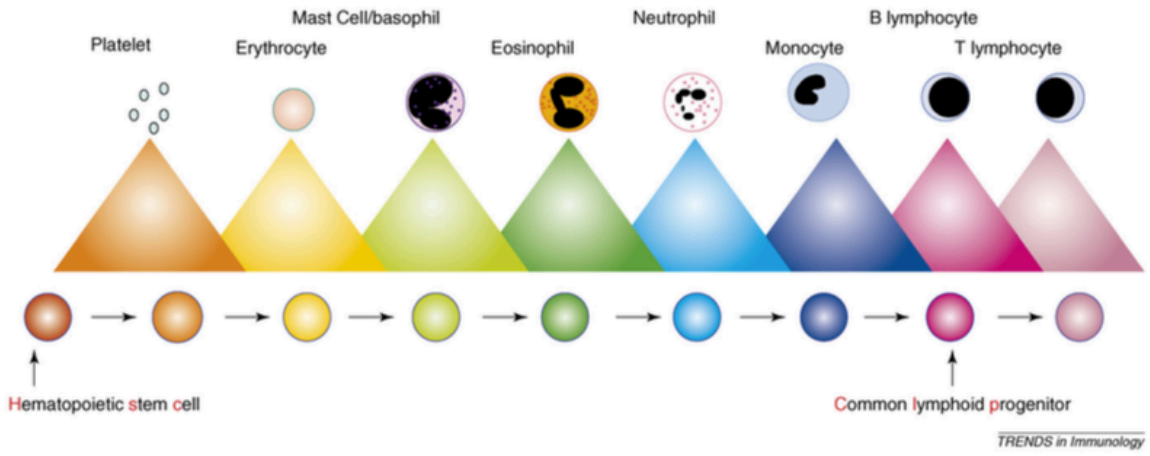

Figure 5. Sequential determination model, modified from[88]. HSCs can give rise to all cells in the BM through stepwise processes.

Indeed, more recently Camargo group has published two different papers assessing hematopoietic cascade using transposons rather than transplantation. Actually, that progenitors are the drivers of complete hematopoiesis rather than HSCs. Moreover, they also suggest that progenitors are themselves capable of self-renewal, not only HSCs[89,90].

More recently, thanks to the development and the assessment of single cell RNA-seq in the BM, a new model was proposed. Based on this new model the maturation of HSCs occurs during a continuous process. Upon commitment, HSCs give rise to unilineage-restricted cells, which will give rise to differentiated cells. However, during this phase multi and bipotent stages were not clearly found[91].

Immature multipotent cells are defined by the lack of expression of the lineage (lin) markers and are referred to as lin- cells. Moreover, they express CD117 (c-Kit) and stem cell antigen 1, also known as Sca-1[92]. A population comprising lin- cells that express c-Kit and Sca1 is known as LKS population and contains HSC, which are marked with other two surface markers known as Cd150 and Cd48[81,93]. The two markers identify clearly stem cells (HSCs) and progenitors (MPP/HPC-1 and HPC2) as reported in figure 6. Oguro and colleagues performed functional transplantation of all these subpopulations into irradiated recipient mice and reported that only HSCs are capable of fully reconstituting irradiated BM. On the other hand, MPP, HPC-1 and HPC-2 are capable of short-term reconstitution of BM. In

particular, they showed that MPPs are capable of complete but transient BM reconstitution. HPC-1 cells instead contain mostly lymphoid progenitors and myelo-erythroid progenitors, while HPC-2 possess limited reconstituting potential for lymphoid progenitors.

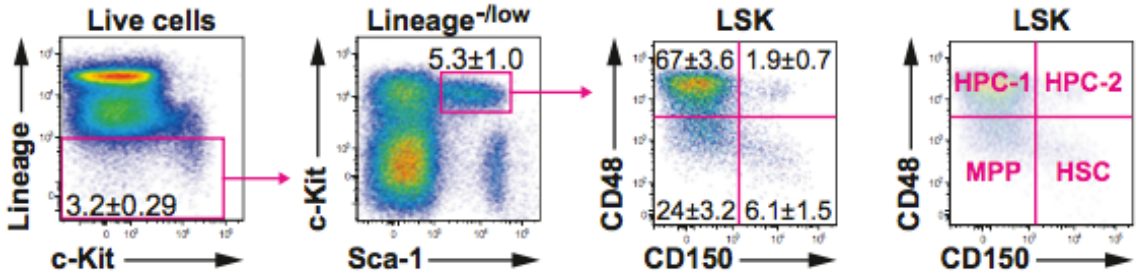

Figure 6. HSC gating strategy, modified from[81]. Representative FACS plot showing stem cell isolation (HSC). In the first panel are represented total bone marrow cells, undifferentiated cells are lineage negative (Lin-). In the second panel stem cells pool, LSK cells, are shown as c-KIT and and Sca-1 positive. In the third panel LSK are subdivided based on Cd48 and Cd150 markers in 4 quadrants, progenitors (MPP HPC1 and HPC2) and HSC. The arrows indicate the FACS parameters used to isolate the cells in each panel.

In humans, the identification of HSCs does not parallel the mouse counterpart. Many surface markers which mark HSCs in human do not identify the mouse counterpart, and vice versa. For example, CD150 marks stem cells in mice but not in humans[94]. Therefore, further markers are necessary in order to isolate HSCs in humans. The first marker that was found was CD34 which marks HSCs[95]. This marker however could not be unique, because both progenitors and HSCs are $CD34^{+}$. Therefore, in combination with CD34 also CD90 is currently used to isolate HSCs[96].

1.9 Cellular metabolism of hematopoietic stem cells

Stem cells reside in particular regions called "stem cell niches", and in recent years the role of the metabolism appears to be fundamental for the fate of self-renewal or differentiation[97,98]. HSCs reside in the bone marrow cavity in a particular region called bone marrow niche. The cavity is hyper vascularized, although oxygen concentration inside is believed to be lower than in venous blood[99]. This was attributed to the concentration of oxygen which is consumed during proliferation of HSCs[99].

Therefore, HSCs in this region must rely on anaerobic glycolysis, in order to produce ATP[100]. Similarly, using a metabolomic/proteomic approach, Takubo and colleagues have shown that HSCs generate ATP through a mechanism relying on glycolysis[101]. The authors, in fact, observed high expression of the pyruvate dehydrogenase kinase enzyme in HSCs which inhibits the pyruvate dehydrogenase enzyme responsible of the conversion of pyruvate to Acetyl-coA necessary to enter Krebs'cycle[102].

A key player in the maintenance of anaerobic metabolism in HSCs is the hypoxia inducible factor 1 alpha (HIF-1α).

The importance of HIF-1α and its fine-tuned expression in the HSCs maintenance was demonstrated in mouse models. When HIF-1α is knocked-out it leads to the impairment in HSCs quiescence, leading to their differentiation and division. On the contrary, when VHL, the E3 biding HIF-1α, was knocked-out it led to the stabilization and maintenance of HSCs quiescence impairing HSCs' capacity to repopulate the bone marrow upon transplantation[103]. Taken together, these data show the importance of the regulation of HIF-1α expression: on the one hand its expression is fundamental for the maintenance of HSCs, on the other its expression must be regulated in order not to undergo stem cell exhaustion.

Proliferation is a highly energy-consuming process. In terms of energy production, through anaerobic glycolysis two moles of ATP are obtained per one mole of glucose, instead, through the oxidative phosphorylation – 36 moles of ATP are obtained from the same

amount of glucose. Since ATP levels are much higher in progenitor cells[104] compared to progenitors, it was proposed that mitochondrial activation plays a crucial role during stem cell differentiation.

Thus, the switch from an anaerobic metabolism to OXPHOS metabolism is a fundamental step during differentiation. Together with ATP requirement, cells require also biomolecules like amino acids, lipids and nucleotides. Most of these molecules are biosynthetized *de novo* using different intermediates of TCA cycle. Mitochondria in the HSCs are smaller and less active compared to those in progenitors[101], although their number does not change[105].

Mitochondria activity in progenitors and HSCs was studied by Yu and colleagues. In a mouse model of conditional inactivation of PTPMT1 protein, a PTEN-like mitochondrial phosphatase, resulted in the lack of differentiation of HSCs and consequently in bone marrow failure[106].

1.10 Fatty acid metabolism and linoleic acid metabolism

Fatty acids play multiple essential roles in biology. Besides their activity as energy source, they are the major component of membranes and are involved in signal transduction.

The catabolism of FAs (fatty acid oxidation, FAO) occurs in the mitochondria and in the peroxisomes, depending on the length of their chain and is called, alpha in peroxisomes and beta in mitochondria. The two organelles use similar reactions to metabolize FAs, with few differences: firstly, mitochondria degrade bulk of short-, medium-, and long-chain FAs, while peroxisome degrade very long chain FAs; secondly, during the first metabolic reaction, the substrate is oxidized but the electron acceptor is different: in mitochondria FAD is reduced to FADH2, while in peroxisomes O_2 is reduced to H_2O_2. Thus, this reaction creates reactive oxygen species, which could increase DNA damage as will be illustrated in the next section.

Cells may choose between FAO and glucose consumption, and the choice between the two strategies derives from the organism status. In normal feeding conditions, cells prefer glucose metabolism and FAs are stored.

Fatty acids can be classified in saturated and mono- or poly-unsaturated. Linoleic acid, central to the present project, is a polyunsatured omega-6 fatty acid with 18 carbon atoms. It must be introduced through diet as the human organism lacks essential enzymes for its synthesis[107]. Linoleic acid (LA) can be converted by enzymatic reactions into arachidonic acid (AA, 20:4) and eicosapentaenoic acid (EPA). AA and EPA are fundamental precursor for intermediate signaling mediators like prostaglandins (PG), leukotrienes (LT), thromboxanes (TX), which are important in inflammation and as sensor molecules.

1.11 Fatty acid metabolism in stem cells

In different models, a crucial role of FAO in the regulation of stem cells was shown. For example, Knobloch and colleagues have demonstrated that in neural stem cells the impairment of FAO leads to cell death and lack of differentiation[108]. Beyaz and colleagues have shown that upon HFD intestinal stem cell (ICS) numbers are increased. The finding was corroborated *in vitro* by the demonstration that upon treatment with palmitic acid, the number of ISCs increased compared to control[98]. More recently, it was demonstrated that FAO regulates the homeostasis of ISCs[109]. They showed that upon inhibition of CPT1, the first enzyme in FAO cascade, the number of ISCs decrease dramatically.

Regarding HSCs, Ito and colleagues have shown a role of FAO regulation in the balance between symmetric/asymmetric stem cell division[97]. They demonstrated that PML regulates peroxisome proliferator activator receptor delta (PPARδ), and PPARδ in turn activates FAO. This activation influences the balance between symmetric/asymmetric stem cell division. In fact, upon PML knock-out or FAO inhibition HSCs give rise to two committed cells, while using PPARδ agonist, HSCs divide giving rise to two stem cells. More recently, it was discovered that PPARδ-FAO axis stimulates mitochondria autophagy (mitophagy) which promotes HSC self-renewal[110].

In order to understand the role of polyunsaturated FA (PUFA), and in particular of LA in HSCs, it is important to pinpoint the way LA is metabolized before going into the details of its function.

In general, LA is fundamental as it regulates the formation of messenger molecules such as prostaglandins, tromboxanes. Studies on the role of LA in HSCs have been mainly performed using PG. Porter and colleagues reported that treatment of mice with PGE2 increased the number of HSCs. This increased number of HSCs does not derive from an increase in proliferation, but instead from a fact that PGE2 inhibits their apoptosis[111]. PGE2 was demonstrated to exert effects also in other stem cells types. Yun and colleagues

demonstrated that PGE2 increases the proliferation of embryonic stem cells and mesenchymal stem cells. In that settings, a shift towards S-phase, pushing cells into proliferation caused by PGE2 was observed[112].

1.12 Fatty acid metabolism in cancer cells

Over the past 60 years, lipid metabolism in cancer has attracted a substantial amount of attention. As early as in 1950, it was observed that cancer cells synthetize de novo FA[113]. This observation is in agreement with the idea that cancer cells require lipids to store energy but also for the synthesis of membranes. One of the main observation in cancer is that the balance between the consumption of FA (FAO) and FA synthesis is shifted toward the synthesis. This leads to the accumulation of free FA in the organism that was observed in many tumor types ranging from colon and breast to brain cancer [114,115]. In particular, in 1994 FA synthase (FASN) was proposed as a diagnostic marker[116]. The upregulation of FASN was later observed in other tumor types such as prostate cancer [117]. Moreover, recent studies have shown that deletion of the short arm of chromosome 8, a common feature in breast cancer, leads to enhanced FASN activity[118].

Regarding the role of FA metabolism in the progression of cancer, several groups have demonstrated a clear correlation between FAO and cancer progression. Pandolfi group established a correlation between FAO and breast cancer progression [119] showing that PML gene stimulates activation of FAO, which in turn stimulates breast cancer growth and anoikis.

Moreover, as explained in the previous paragraph, LA metabolism can give rise to PGs that may be involved in the maintenance of HSCs. However, the same compounds may play a cancer-promoting role, as in the case of colon cancer where PGE2 triggers cell proliferation by activating the MAPK[120].

1.13 Metabolism-induced oxidative stress and DNA damage

DNA damage can be defined as alterations of the DNA structure produced by physical or chemical agents. DNA damage triggers a particular response (DNA damage response, DDR, is illustrated in figure 7). When double-stranded DNA damage is present, it is sensed by specialized sensors (DNA-damage Checkpoint 1, MDC1 and p53-binding protein 1, 53BP1) which activate the ataxia-telangiectasia mutated (ATM) kinase, that phosphorylates the H2AX histone, to form γH2AX. This in turn recruits more ATM, giving rise to a positive feedback loop increasing both ATM and γH2AX at sites of DNA damage.

In the case of single-stranded break, single-stranded DNA-binding protein replication protein A (RPA) binds the site and recruits another complex named ataxia-telengiectasia and Rad-3 related (ATR), which phosphorylates H2AX in γH2AX. However, in ATR addition signal boosters are RAD9, RAD1 and HUS1, and by topoisomerase-II-binding protein 1 (TOPBP1) and claspin.

Cells tolerate a certain threshold of DNA damage, however when this threshold is exceeded, ATR and ATM phosphorylate CHK1 and CHK2 checkpoint kinases respectively. The two proteins diffuse through nuclear pores and interact with cellular fate mediators such as p53 and CDC25 leading either to cell death or to repair of the damage.

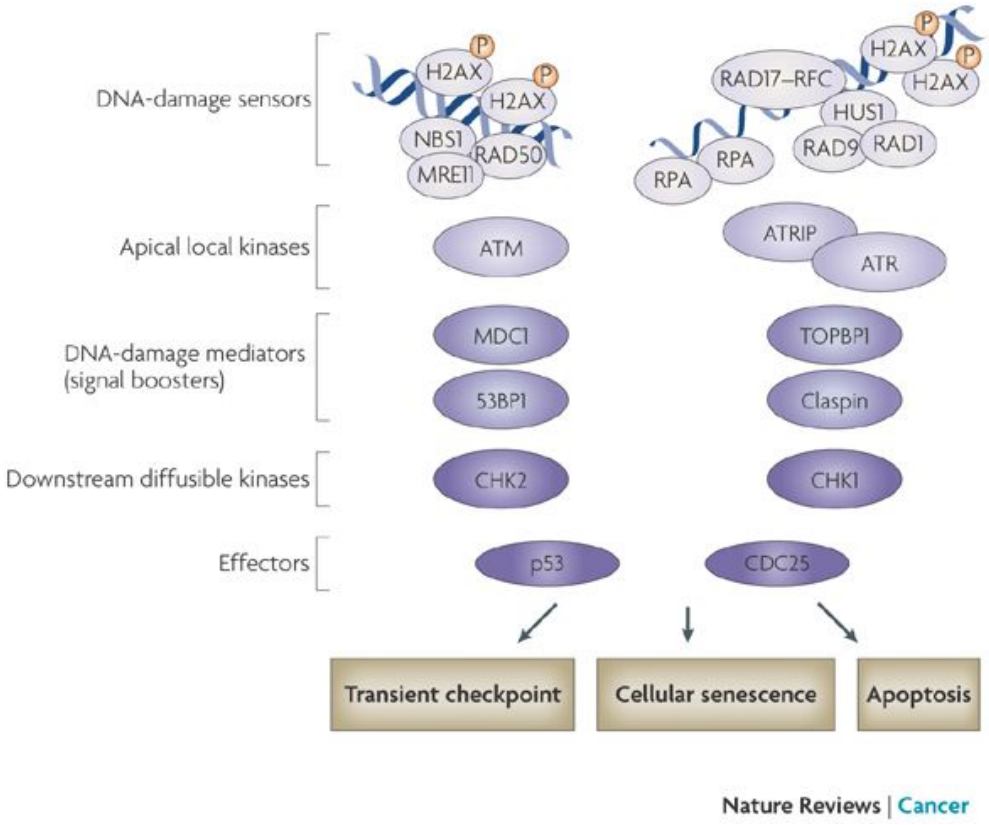

Figure 7. DDR cascade modified from[121]**.** DDR cascade is shown in this figure. On the left, double strand breaks triggering ATM response are shown, while on the left single strand breaks triggering ATR response.

The choice between the different DDR mechanisms depends on the state of the cell cycle, cell and damage type. When single- or double-stranded breaks occur in G1 phase, cells use non-homologous end-joining (NHEJ), in which broken DNA ends are bound by Ku70/80 and recruit DNA dependent protein kinase (DNA-PK) and DNA ligase XRCC4 that repair DNA breaks without keeping genetic information, possibly giving rise to genomic instability[122]. The same type of damage during S-phase is repaired by homologous direct repair (HR) which is based on the exchange of genetical information by sister chromatids, ensuring the maintenance of genetic information[122]. Missmatch repair (MRR) enzymes recognize distortion of the DNA structure (possibly loops) which may derive from wrong incorporation of bases during DNA synthesis. The key mechanism was identified clearly in prokaryotes, and it is based on the recognition of parental strand (which is methylated) from the newly synthetized strand (not methylated). When this is present, an endonuclease cuts the DNA at the site of the distortion and an endonuclease digests the mismatched

nucleotides. Finally, DNA polymerase resynthesize the strand and ligase closes the gap. In eukaryotes, the repair process works in the same manner as in prokaryotes, however, it is less clear what is the signal that activates MRR[123].

When, instead, small insertion, deletion or wrong base incorporation is present, they are repaired by nucleotide excision repair (NER), mismatch repair (MMR) and base excision repair (BER). The NER pathway is activated when cells are exposed to irradiation leading to the formation of pyrimidine dimers, which block the DNA polymerase leading to fork stall[124]. BER is mediated by DNA glycosidase and is activated when bases are oxidized, deaminated and alkylated. In this pathway, the modified base is removed, then the correct base is inserted and finally ligated[124].

The BER mechanism has great importance in the field of metabolism, because it is the primary response to ROS attack in the cells. ROS in the cells can generate more than 100 different lesions[125]. In particular, one of the most common types of DNA lesions caused by ROS oxidation is the formation of 8-oxoguanosine (8-oxoG). This type of lesion is very common due to guanosine low redox potential and when unrepaired can cause transversion from G:C to T:A. BER is the primary mechanism by which cells repair 8-oxoG and it is critical for genome maintenance[126].

Another type of lesions in which BER is crucial is the formation of 3-(2-deoxy-β-D-erythro-pentofuranosyl)pyrimido[1,2-α]purin-10(3H)-one (M1dG) adducts, which will be discussed in this thesis work. M1dG originate from condensation of guanosine with a molecule of malondialdehyde. This molecule is the final product of lipid peroxidation in the cells, which as demonstrated, is enhanced in obese patients[127]. If not repaired by BER, M1dG formation causes transversion as well from C:G to A:T[128].

1.14 Metabolism induced oxidative stress and DNA damage in stem cells

As described in the previous paragraph, metabolism *per se* has a strong role in the fate of stem cells[83]. Before going deeply in the role of metabolism in DNA damage in stem cells, it is necessary to underline key concepts regarding DNA damage and HSCs. Firstly, recent evidence shows that cells can handle DNA damage in significantly different ways. Stem cells preferentially use NHEJ[129], an error-prone repair modality, but are also able to tolerate higher amounts of DNA damage, accumulating it with aging by virtue of their long life span [130]. Furthermore, in a work from our group it was also shown that upon ionizing radiation, stem cells leave quiescence to expand progenitors[131]. This observation can be linked to another by Weissman group in which it was demonstrated that knock out of repair proteins affects self-renewal potential and leads finally to functional exhaustion[132].

In this scenario, oxidative stress induced by metabolites can play a key role. Two recent works by KJ Patel group have demonstrated that combined ablation of aldehyde-metabolizing activity and DNA damage repair leads to bone marrow failure or leukemia upon transplantation[133,134]. Indeed, aldehydes, producing in the metabolism of ethanol and other endogenous and exogenous alimentary substances, directly induce DNA damage.

1.15 Metabolism induced oxidative stress in cancer

In normal cells, the perfect balance between ROS generation and degradation is maintained by the ROS degradation machinery. These ROS are generated during the mitochondrial OXPHOS reactions and are neutralized by several proteins in the cells such as superoxide dismutase (SOD), catalases, glutathione machinery, but also cofactors such as vitamins[135]. Whenever these processes do not occur properly, ROS may undergo several reactions in the cells damaging DNA. As discussed before, ROS can lead to lipid peroxidation leading to the formation of malondialdehyde which can bind DNA forming M1dG.

However, also proteins can be attacked forming a particular adduct called 4-hydroxynonenal (4-HNE)[136]. This protein modification may alter correct protein function, leading to malignant transformation without altering DNA structure[137].

Indeed, in other different works, it was shown that ROS may modify protein structure leading to mutations which can modify specifically several pathways such as pathways controlling cell proliferation like ERK pathway. In particular, it was shown that ROS may activate different components of ERK pathway leading to its constitutive activation. For example, it was observed that nitrogen reactive species can specifically modify RAS structure leading to the formation of constitutively active form of the protein[138]. Differently, it was demonstrated in ovarian cancer that a phosphatase which acts negatively on ERK pathway can be modified by high oxygen species losing its controlling effect[139]. Therefore, treating cells with ROS scavengers, was proposed as a clinical strategy to decrease tumorigenesis, as demonstrated in breast cancer cell lines[140].

Chapter 2. Aim of the work

We and others have demonstrated that APL is associated with obesity and that this association can be reproduced using a mouse model of APL. The molecular mechanisms explaining this association are not completely elucidated.

The scope of this thesis work was to define the molecular mechanisms linking obesity to APL onset using genetic, genomic and biochemical approaches.

Chapter 3. Materials and methods

3.1 Cell lines

For the maintenance of HSCs in culture Lin^- medium was used, containing 90%RPMI (Euroclone), 10% FBS for stem cell maintenance (STEMCELL Technologies), 1% Penicillin/Streptomycin (Euroclone), 2 mM Glutamine (Euroclone), 100 μg/ml SCF (Peprotech), 10 μg/ml IL3 (Peprotech) and 10 μg/ml IL6 (Peprotech).

3.2 *In vivo* experiments

3.2.1 Mice strains

Experiments involving mice were performed according to Italian law and following an approval of the Institutional Review Board and the Italian Ministry of Health (projects 1072/15 and 967/17). PML/RARα knock-in mice were provided by T.J. Ley[73] and backcrossed in C57BL/6J background. All wild type mice used in the study were purchased from Charles River: C57BL6/Ly5.2 and C57BL6/Ly5.1. Animals were bread and housed in Specific Pathogen-Free the animal facility at the European Institute of Oncology (IEO) and Institute FIRC of Molecular Oncology (IFOM) campus. Animal received ad libitum food and drinking water, and were kept in a regimen of 12-hour light-and-darkness cycle.

3.2.2 Feeding regimens

Animals were fed with ad libitum SD or HFD (Broogarden, D12492) starting from 8-12 weeks of age. Mice were weighted at the beginning of the experiment and at the time of sacrifice.

3.2.3 Leukemia development

To monitor leukemia development, peripheral blood (PB) was taken periodically (at least 1 per month) from a small incision of the lateral caudal vein. Before the blood sampling, animals were heated up by an ultra-red light to dilate the veins. A volume of 100 μl of PB was taken from each animal and was mixed with 20 μl of 0.5M EDTA in order to prevent it from clotting. Animals were euthanized by CO_2 inhalation when signs of suffering and distress were apparent.

3.2.4 Bone marrow transplantation and competitive repopulation assay

For BM transplantation, the procedure occurred in two different stages. The night before the transplantation, recipient animals were X-ray irradiated with a lethal dose irradiation of 8.5 Gy. This procedure ensures that the recipients' BM is depleted by irradiation, and consequently that the donor cells can proliferate in the empty BM niches. Soon after irradiation, in order to avoid infection due to immune-suppression neomycin (Sigma-Aldrich) was added to drinking water at a final concentration of 1 mg/ml for two weeks following irradiation. The day after, intravenous (IV) transplantation was performed.

For the competitive BM repopulating assay, BM cells deriving from donor (Ly 45.2 allele variant) and recipient mice (Ly 45.1 allele variant) were mixed together in a 1:9 ratio. In detail, $1*10^5$ total BM cells deriving from obese/normal-weight PML/RARα mice (Ly 45.2) and $9*10^5$ total BM cells of competitor mice (Ly 45.1) were transplanted into recipient Ly45.1 mice. Cell mixture was resuspended in phosphate buffered saline (PBS) and transplanted into the lateral caudal vein. After one month, engraftment was evaluated as the ratio of Ly 45.1/ Ly 45.2 in the PB. Following the transplantation, mice were all fed SD independently of the diet that was fed to the donors.

3.2.5 N-acetylcysteine treatment

N-acetylcysteine powder (Sigma-Aldrich) was dissolved in sterile drinking water at a final concentration of 10 mg/ml. Bottles containing fresh NAC-supplemented water were changed twice a week together with food change. Animals were weighed at day 0, and every week for one month. After that mice weight, was assessed at 8 weeks, three months and at the sacrifice.

3.3 Flow cytometry

Flow cytometry is a widely used imaging technique to analyze cells based on morphological and protein expression features. Flow cytometers detect and measure fluorescence intensity. The source of fluorescence is that of a fluorescent reporter- or selection protein expressed by the cell itself upon transduction or genetic modification (such as GFP), fluorochromes conjugated to antibodies that detect antigens present in/on cells, or fluorescent molecules with affinity for a particular ligand (e.g. DNA-binding DAPI or Propidium Iodine dyes).

During FACS acquisition cells must be resuspended as a single-cell solution. When cells pass through the nozzle, the fluid sheath induces them to move from a turbulent regimen to a laminar regimen and can be scanned one by one by the laser.

The first parameter which can be evaluated by FACS analysis is the morphology of the cells. When cells are hit by the laser, light scatters in all of the directions, and detectors measure the scattering. Two physical parameters can be detected by the detectors: side scatter (SSC) and forward scatter (FSC). SSC measures the granularity of the cells, while FSC corresponds to their size. For fluorescent marker detection, the laser excites the fluorophores with specific wavelengths. If the wavelength is coherent with the excitation spectrum of the fluorophore, the electrons of the fluorophore pass from the ground state to the excited state. The electrons then fall back and return to their ground state and energy is transferred in the form of a photon with has its own wavelength, usually different from the exciting one (emission spectrum).

The wavelength produced by the emission is captured by photomultipliers which convert the signals in digital data.

In this project, FACS analysis has been performed on mouse BM in order to purify and quantify the HSC population.

3.3.1 Antibodies used

For the analyses the following fluorophore-conjugated antibodies were used:

Antibody target	Fluorophore	Producer and catalogue number
Gr-1	Pe-Cy7	Thermo-Fisher Scientific #12-9668-82
Cd3e	Pe-Cy7	Thermo-Fisher Scientific #25-0031-82
Cd45R(B220)	Pe-Cy7	Thermo-Fisher Scientific #25-0452-82
Cd11b	Pe-Cy7	Thermo-Fisher Scientific #25-0112-82
Ter-119	Pe-Cy7	Thermo-Fisher Scientific #25-5921-82
Sca-1	PerCP 5.5	Thermo-Fisher Scientific #45-5981-82
c-Kit	APC	Thermo-Fisher Scientific #17-1172-82
Cd150	PE	Thermo-Fisher Scientific #12-1502-82
Cd48	Biotin	Thermo-Fisher Scientific #13-0481-85
Streptavidin	Pacific blue	Thermo-Fisher Scientific #48-4317-82
	BV605	Beckton Dickinson #563260
Cd45.1	Fitc	Thermo-Fisher Scientific #11-0453-82
Cd45.2	PE	Thermo-Fisher Scientific #12-0454-82

Table 2. List of antibodies used in the experiments

For each experiment, cells were compared to appropriate controls such as an unstained sample, in order to check autofluorescence, a sample stained with single antibodies, in order to check the positivity for each antibody alone and set the compensation of the machine, and a sample stained with all antibodies except one (all minus one), in order to establish gating strategies.

3.3.2 Sample preparation

At sacrifice the two hind limbs of the animal were removed and put in ice-cold PBS. Under a sterile hood, tibia and the femur of the animal were cleaned off the flesh by rubbing with a gauze and put in a 60mm dish containing 5 ml of ice-cold PBS supplemented with 1% penicillin/streptomycin and 2% of FBS. BMNC were obtained by flushing the bones with PBS in a 1ml syringe. Cells were then centrifuged 1200 rpm at 4°C for five minutes. In order to remove erythrocytes cells were incubated with red cell lysis buffer (155 mM NH_4Cl, 12 mM $NaHCO_3$, 0.1 mM EDTA) for 2 minutes on ice. After incubation, cells were centrifuged again at 1200 rpm at 4°C for five minutes and cells are passed through a cell 40 μm strainer, in order to remove clumps and red cell debris. Cells were then counted following staining with Trypan-blue reagent (Sigma-Aldrich) at a dilution of 1:100.

3.3.3 HSC gating strategy/isolation

BMNC were resuspended at a final concentration of $100*10^6$/ml and antibodies mix was added. In order to isolate HSCs, SLAM isolation markers were used: Lineage antibody cocktails (Cd3e, Cd11b, Gr-1, Ter-119 and Cd45R) used at 1:100 conjugated directly with PeCy7, Sca-1 used at 1:100 conjugated directly with PerCP5.5, c-Kit used at 1:100 conjugated directly with APC, Cd150 used at 1:200 conjugated directly with PE, Cd48 conjugated with biotin used at 1:100. Staining was performed for one hour at 4°C and after that excess of antibodies was removed by centrifuging twice the cells. Finally, Pacific Blue-conjugated streptavidin as a detection reagent was used at 1:200 for one hour at 4°C. After

staining, cells were washed twice with ice-cold PBS supplemented with 2% FBS and resuspended in ice-cold PBS supplemented with 2% FBS at a final concentration of $15*10^6$/ml cells in FACS tubes, to be sorted by FACS Fusion (BD Bioscience). For HSCs isolation the following combination of markers were used $Lin^-Sca^+c\text{-}Kit^+Cd150^+Cd48^-$[93]. Cells were initially gated based on SSC-H (height) versus SSC-A (area) in order to discard cell doublets. The positive population was then gated based on the morphological parameters using FSC and SSC.

In order to distinguish various populations in the bone marrow a staining is performed with a cocktail of antibodies and cells are sequentially analyzed using a defined gating strategy. First of all, lin- negative cells are identified. Next, within the lin- population, c-Kit and Sca-1 positive cells are gated on. Finally, the expression pattern of Cd50 and Cd48 is used to distinguish HSC ($Cd150^+/Cd48^-$), MPP ($Cd150^-/Cd48^-$), HPC-1 ($Cd150^-/Cd48^+$) and HPC-2 ($Cd150^+/Cd48^+$)[81] Sorting acquisition was performed at FACS Fusion (BD Bioscience). Analysis of the FACS were performed using FlowJo X software.

3.3.4 Cell cycle

For cell cycle analysis, $5*10^6$ total BM cells stained for Lin/Sca/c-Kit/Cd150 and Cd48 were fixed for 10 minutes in 4% paraformaldehyde (PFA) on ice. After incubation cells were washed twice in ice-cold PBS. Cells then were permeabilized in 200 µl CytoFix/CytoPerm solution (BD Bioscience) for 10 minutes on ice. Cells were then resuspended in Washing buffer (BD Bioscience) and stained with FITC-conjugated KI-67 antibody (BD Bioscience) for 45 minutes on ice in the dark at a final concentration of 1:50. After staining, the excess of antibody was removed by washing cells once in Washing buffer. After wash, cells were incubated with DAPI solution (Sigma-Aldrich) resuspended at final concentration of 2 µg/ml and stained overnight at 4°C.

The following morning, FACS samples were read on FACS Celesta II (BD Bioscience) instrument. Cells were discriminated based on DAPI-H (height) versus DAPI-A (area) in

order to discriminate the cell doublets. After stem cell isolation, as shown in the previous paragraph, cell cycle was measured using KI-67 vs DAPI. Cells low for both markers are in G0 phase, cells positive for KI-67 but low for DAPI are in G1 phase, whereas double positive cells are in S/G2/M phase. Analysis of the samples was performed using FACS DIVA software (BD Bioscience).

3.3.5 Peripheral blood engraftment analysis

PB sampled from the animals was centrifuged at 1200 rpm for 5 minutes. Cell pellets were then treated thrice with red blood cell lysis buffer and every time lysis buffer was inactivated with identical volume of PBS supplemented with 2% FBS. Finally, cells were resuspended in 250 µl of FBS-supplemented PBS.

Staining was performed using an anti-Cd45.1 antibody conjugated with FITC and anti-Cd45.2 antibody conjugated with PE each one diluted 1:100. Staining was performed for 1 hour at 4°C, then excess of antibody was removed by centrifuging twice at 1200 rpm for 5 minutes. Acquisition of samples was performed on FACS Celesta II (BD Bioscience). The analysis of the results was performed using FlowJo X software.

3.5 M1dG detection

For M1dG detections, 3 WT mice kept in SD and HFD were sacrificed. BM cells were isolated as shown in the 3.3.2 section. M1dG was measured only in differentiated (Lin^+) and undifferentiated (Lin^-) BM portion due to amount of DNA required. Procedures are described in details in[141]. Briefly, genomic DNA was extracted from cellular pellet. DNA was then fragmented into single nucleotides and M1dG nucleotides were detected via chromatography.

3.6 Alkaline Comet assay

Alkaline Comet assay is a technique that is widely used in order to detect DNA damage. This technique compared to neutral comet assay offers the advantage of discriminating both single stranded breaks (SSB) and double stranded breaks (DSB). In this technique cells are blocked in agarose matrix and put on a microscopy slide. After cell lysis, naked DNA is subjected to an electrophoretic run. After the run, DNA is stained and thus, it is possible to follow the path of electrophoresis of DNA in the agarose matrix. DNA migration in this case is proportional to the extent of DNA damage: the more serious the DNA damage, the more apparent the migration of DNA. Therefore, this technique can be used as a qualitative and quantitative instrument to detect DNA damage. For this experiment, HSC after sorting were resuspended in PBS+2%FBS and kept at 4°C just before the assay. Cells were pelleted and resuspended in a mix containing 9 volumes of 37°C melted agarose and 1 volume of room temperature PBS. Cells were directly spotted on comet slide and comet assay was performed following manufacturer's instructions (Trevigen). After comet assay cells were stained using Syber-Gold dye (Thermo-Fisher Scientific) resuspended 1:10000 in cold PBS. Cells were stained for 10 minutes at room temperature and the excess of Syber-Gold was removed by two washes in water. Comets were observed with fluorescent microscope using Alexa-488 filter, using Leica X software. Analysis of comets were performed using Autocomet, a

manual plugin for ImageJ, following online instructions. For quantifications, percentage of DNA in the tails was used as parameters. These parameter is an index of the integrity of DNA: the longer are the tails, the higher is the extent of DNA damage.

3.7 Mutation analysis

Mutation analysis was performed using an optimized strategy that is based on the expansion of a single stem cell in culture giving rise to a colony. After four months of diets (SD and HFD), WT mice and PML/RARα KI mice were sacrificed. Total BM was isolated and SLAM isolation markers were used in order to identify HSC ($Lin^-Sca^+c\text{-}Kit^+Cd150^+Cd48^-$). Single cells were sorted into 96-wells plates containing Lin^- maintaining medium: 90% RPMI (Euroclone), 10% FBS for stem cell maintenance (STEMCELL Technologies), 1% Glutamine (Euroclone), 100 μg/ml SCF (Peprotech), 10 μg/ml IL3 (Peprotech) and 10 μg/ml IL6 (Peprotech), 1% Penicillin/Streptomycin (Euroclone). After two weeks of culture, colonies were observed using light-contrast inverted microscope (Leica) and five random colonies were picked. Genomic DNA was extracted using DNA micro Kit (Qiagen) including a step of RNase A treatment at 42°C for 10 minutes prior to the proteinase K treatment, in order to remove proteins and RNA contaminants. Quantification of genomic DNA was performed using Qubit Analyzer (Thermo Fisher Scientific) and only DNA the total amount of which was higher than 150 ng was sequenced. As a healthy tissue control, also genomic DNA from the tail was extracted using DNA mini Kit (Qiagen).

Libraries were obtained as shown by Kozarewa and colleagues[142]. After library preparation, 100 base paired-end sequencing was performed using Hiseq 2000 genome analyzer in accordance with the Illumina Genome Analyzer operating manual. After library preparation, DNA has been sequenced on 2 lanes of Illumina HiSeq2000 analyzer in paired-end mode with 100 bp read length. Average sequence coverage was 30x for the colonies and the tails. Short insert paired-end reads were aligned to the mouse reference genome (mm10) using Burrows-Wheeler Aligner (BWA)[143] and duplicated reads were removed using MarkDuplicates from Picard tools [http://broadinstitute.github.io/picard/].

To enumerate mutations, we propose to call variants in comparison to the germline DNA obtained from the same animal's tail using two different algorithms: CaVEMan[144](Cancer Variants Through Expectation Maximization) and Shearwater[145].

CaVEMan is part of an integrated bioinformatics analysis pipeline developed at the Wellcome Trust Sanger Institute as part of their Cancer Genome Project (CGP). It has been used on a number of projects as part of the International Cancer Genome Consortium (ICGC).

In detail, CaVEMan applies an expectation maximisation algorithm to call single nucleotide substitutions. Through comparison of reads from both tumour (data from the single stem cell expanded) and normal (the tail of the corresponding mouse) with the reference genome, CaVEMan calculates a probability for each possible genotype per base. In order to provide more accurate estimates of sequence error rates within the algorithm, thus aids identification of true variants, variables such as base quality, read position, lane, and read orientation are incorporated into the calculations.

Shearwater is an approach for detecting clonal and subclonal variants; it exploits the power of a large sample set for precisely defining the local error rates and which uses prior information to call variants with high specificity and sensitivity. More in detail, Shearwater is built over a probabilistic framework that offers the flexibility to account for prior information, which turns to be useful for modeling the error distribution. The hypothesis is based on the observation that sequencing artifacts are recurrent on specific loci. The larger is the sample cohort, the better a background error distribution on each locus can be defined, above which true variants can be called.

3.8 Colony forming assay

Colony forming assay allows the quantification of clonogenicity of HSCs. In this assay, total BM or stem cell subpopulations are plated in methylcellulose medium. After a short period (normally between 6-10 days) colonies appearing on the plates are counted on a phase contrast microscope (Evos Thermo-Fisher Scientific). A colony by definition derives from a single cell. After the count, colonies were disaggregated and cells were re-plated at the same cell density in methylcellulose. The procedure is repeated for multiple passages or until no colonies are present on the plates. Total BM cells were plated in MethoCult M3434 (STEMCELL Technologies), a semisolid medium containing cytokines supporting the proliferation of stem/progenitor cells. The number of colonies mirror indirectly the number of pre-existing stem cells.

3.8.1 Colony forming assay following SD or HFD

To evaluate whether the diet could contribute to the increase of stem cells, we sacrificed 4 mice per conditions: diet (HFD and SD) and genotype (WT and PML/RARα KI). BMNCs were plated directly in methylcellulose at a final concentration of $1*10^4$ per plate. After 6 days, colonies were counted on a phase contrast microscope (Evos Thermo-Fisher Scientific). After counting methylcellulose was dissolved in fresh medium, colonies disaggregated and cells counted and plated again at the same cell density. After another week colonies were counted again.

3.8.2 Colony forming assay for FA screening

For FA screening experiment, one PML/RARα mouse was sacrificed and processed as described in the 3.3.2 section. Cells were counted and plated in methylcellulose at a cell density of $1*10^4$ in duplicate. Oleic Acid (Sigma-Aldrich) at a final concentration of 3.2 mM, Linoleic acid (Sigma-Aldrich) at a final concentration of 5 mM, and Arachidonic Acid (Sigma-Aldrich) at a final concentration of 5 μM were added to the methylcellulose. N.B.

We have demonstrated that high concentration of Arachidonic Acid is toxic for the cells. Ethanol and BSA were used as controls as carrier of FAs.

3.8.3 Colony forming assay upon linoleic acid signalling inhibitor treatment

For FAs/drug treatment experiments bone marrow cells deriving from 6-month old mice were plated at $1*10^4$. FAs were used at a concentration which is present in obese mice as is shown in[146]: palmitate was used at a final concentration of 11.5 μM (we have demonstrated that higher concentration of palmitate is toxic for the cells), linoleic acid at 5mM. Drugs instead were used as reported in literature[147,148]: GSK 3787 (Abcam) at a final concentration of 10 μM, and Zileuton (Sigma-Aldrich) at 10 μM.

3.8.4 Colony forming assay upon NAC treatment

For NAC experiments, four 12-week old PML/RARα KI mice were sacrificed and BM cells isolated as shown. Cells were plated in MethoCult M3434 at a final concentration of $1*10^4$ and Linoleic Acid was used at a final concentration of 5mM. NAC (Sigma-Aldrich) was dissolved in sterile water and used at a final concentration of 1.5 mM as reported in the literature[149].

3.9 CFSE proliferation assay

Carboxyfluorescein succinimidyl ester (CFSE) is a dye widely used to monitor cell proliferation. CFSE is a small molecule that enters passively into the cells and covalently couples to intracellular structures. It possesses an emission spectrum similar to Alexa-488 in FACS analysis. Given the progressive halving of CFSE fluorescence within daughter cells after each cell division, it can be used to mark non-dividing cells. We used CFSE to track cell division, in order to identify whether cells underwent symmetric/asymmetric cell divisions upon BSA or Linoleic acid treatment.

Total BM cells were stained with CellTrace Proliferation Kit (Invitrogen) following manufacturer's protocol. Briefly, $10*10^6$ total BM cells were pelleted and resuspended in 1 ml PBS. Two µl of CFSE dye were added to the cell suspension and incubated 10 minutes at 37°C in the dark. After incubation, cells were washed twice in PBS to remove the excess of dye and the fluorescence was immediately measured on FACS Celesta II.

One week later, colonies were disaggregated and cells were pelleted at 1200 rpm and washed twice with PBS in order to remove medium. Cells were then resuspended in 200 µl of PBS and acquired on FACS Celesta II. Analysis were performed with FlowJO X software.

3.10 Live cell imaging

For live cell imaging experiments, total BM cells were stained with LSK/Cd48/Cd150 antibodies in order to isolate HSCs. One-hundred cells were then plated in MethoCult M3434 in the presence of BSA or 5 mM linoleic acid in 6 wells to perform live cell imaging with Olympus Scan R microscope, using ScanR software.

Cells were incubated in a humidified incubator in the presence of 5% CO_2 in order to sustain cell growth and each well was divided in 169 fields. For each field the microscope took 5 planes for each time point which was every 6 hours for 7 days.

After taking all the images, ScanR software was used to reconstruct the cell divisions. Finally, FiJi software (ImageJ), was used to isolate cells at 1,2,4,8,16 and complete colonies.

3.11 Statistical analysis

For comet assay, values were converted into arcsin for statistical analysis, the value of percentage was converted using the following formula:

Arcsin (square root (Percentage/100)), Student's t test was performed on converted values, and since variables do not follow a normal distribution, the Mann Whitney U test was performed. For all other experiments two-tailed Student's t-test was performed. Graphs were plotted using GraphPad Prism Software.

Chapter 4. Results

4.1 HFD is associated with increased DNA damage in HSCs

The simplest way of explaining the cooperation between obesity and PML/RARα is a classic genetic model, in which HFD behaves as a carcinogen, inducing DNA mutations. Indeed, an increase of DNA adducts deriving from metabolism was shown to augment mutation rate ultimately leading to leukemia or bone marrow failure [133,134]. Thus, we set up a series of experiments to evaluate if HFD induces adduct-mediated DNA damage and if this is fixed in mutations. We reasoned that prolonged low-level oxidative damage may be at play, so we focused on cells with prolonged life span, ie stem and progenitor cells. We started by analyzing whether HFD cause increased DNA damage by alkaline comet assay performed on HSC, progenitors and differentiated cells isolated by FACS from the BM of HFD- or SD-fed mice [150]. We used HSCs isolated from an aged-matched, UV-treated (500 uJ) mouse as a positive control.

DNA damage is quantified as percentage of DNA in the tails, arcsin-transformed for statistical reasons (see methods for a discussion on the arcsin conversion) (Figure 7A). In HSC, HFD increased DNA damage both in WT (0.67 vs 0.76, $p<0.0001$) and in PML/RARα KI background (0.61 vs 0.85, $p<0.0001$). To better quantify the difference, each mean value was normalized to its own SD control. Applying this transformation, the extent of DNA damage appeared higher in PML/RARα (40%) than in WT (15%). These data points towards the existence of a cooperating mechanism between the diet and the genotype (fig. 7B).

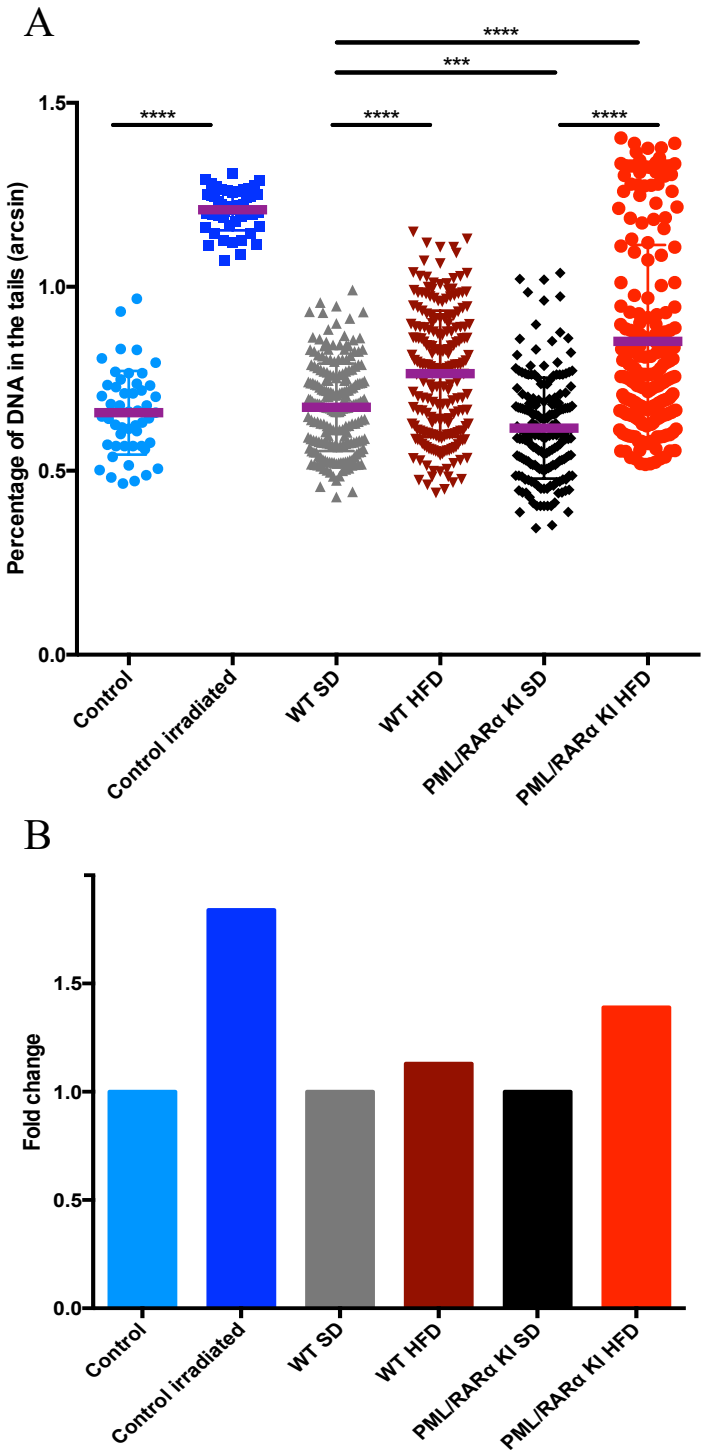

Figure 7. Obesity increases the DNA damage in HSC of PML/RARα KI mice. A) Quantification of comet assay on HSC expressed as arcsin of percentage of DNA in the tails. The statistical analysis for was performed on at least 50 events for any of the 7 mice per experimental group, whilst the analysis on control not irradiated or irradiated animals was done on one mouse each. Light-blue dots represent control, blue squares irradiated control, grey triangles WT mice in SD, reverse dark red triangles WT HFD, black rhombuses PML/RARα KI mice in SD and red dots PML/RARα KI HFD. Purple lines indicate the average DNA damage. B) Quantification of the extent of DNA damage after normalization to SD. Light blue bar indicates the control, blue bar the control irradiated, grey WT SD, dark red WT HFD, black PML/RARα Ki SD and red PML/RARα KI HFD. ****p<0.001

We then asked whether the damage occurs preferentially in HSCs or ubiquitously in the entire BM in the PML/RARα KI background. DNA damage was also significantly increased in progenitor and differentiated cell fractions upon HFD but comparatively lower than in HSC (30% higher than SD in progenitors, 9% in differentiated cells) (Figure 8A/B).
Thus, DNA damage is progressively resolved as cells differentiate.

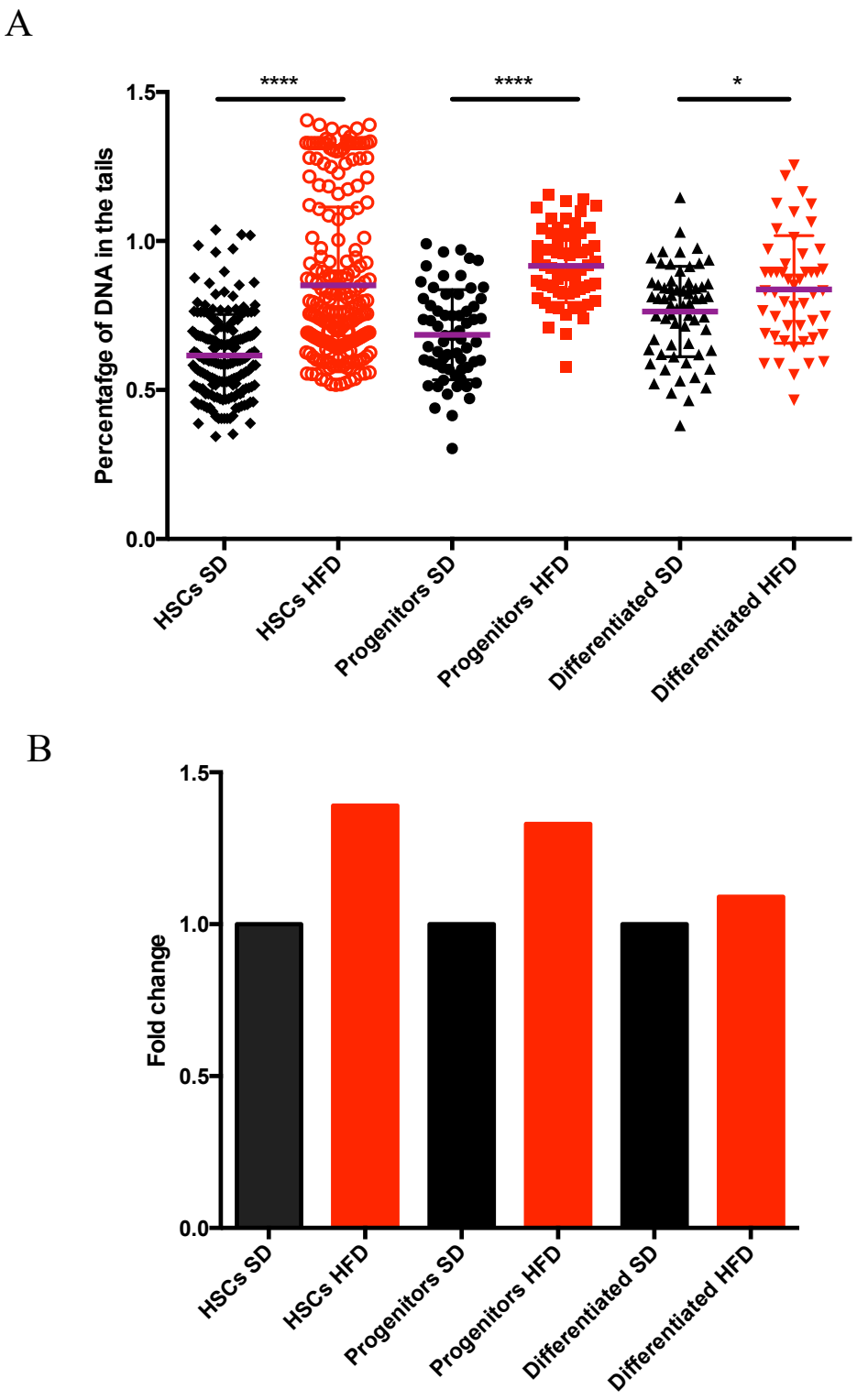

Figure 8. Differentiated cells display less DNA damage. Quantification of DNA damage in HSCs, progenitors and differentiated cells deriving from PML/RARα KI mice kept in SD and HFD. Black rhombuses indicate the HSCs od mice in SD, red empty dots HSCs of mice in HFD, black dots the progenitors of mice in SD, red squares the progenitors cells of mice in HFD, black triangles the differentiated cells of mice in SD and red reverse triangles the differentiated cells of mice in HFD. D) quantification of DNA damage in progenitors and differentiated cells normalizing to their own controls. black bars progenitors and differentiated in SD, red bars progenitor and differentiated in HFD. ****$p<0.001$, *$p>0.05$

4.2 HFD increases fatty acid-derived genotoxic aldehydes in hematopoietic stem and progenitor cells

Oxidative attack on long-chain FA by ROS generates malondialdehyde [151], a highly reactive molecule that produces M1dG (pyrimido[1,2-*a*]purin-10(*3H*)-one) DNA adduct, which we measured in bone marrow (Lin+ and Lin- cells) from long-lived (2yr old) WT mice subjected to SD or HFD. It was not possible to separately analyze Lin- subpopulations as the technique employed requires amounts of DNA not obtainable from such rare cells. M1dG levels are plotted as number of nucleotides carrying the adduct per 10^7 nucleotides (Figure 9). No difference in M1dG amount in DNA deriving from Lin^+ cells was shown for mice kept on the two diets (31 vs 24 per 10^7 nucleotides, $p>0.05$). However, a strong difference in the amount of the adducts was observed in the Lin^- cells (7.5 in SD vs 99 in HFD per 10^7 nucleotides, $p<0.001$). These results show that HFD induces an accumulation of genotoxic DNA adducts, and this occurs preferentially in undifferentiated BM cells.

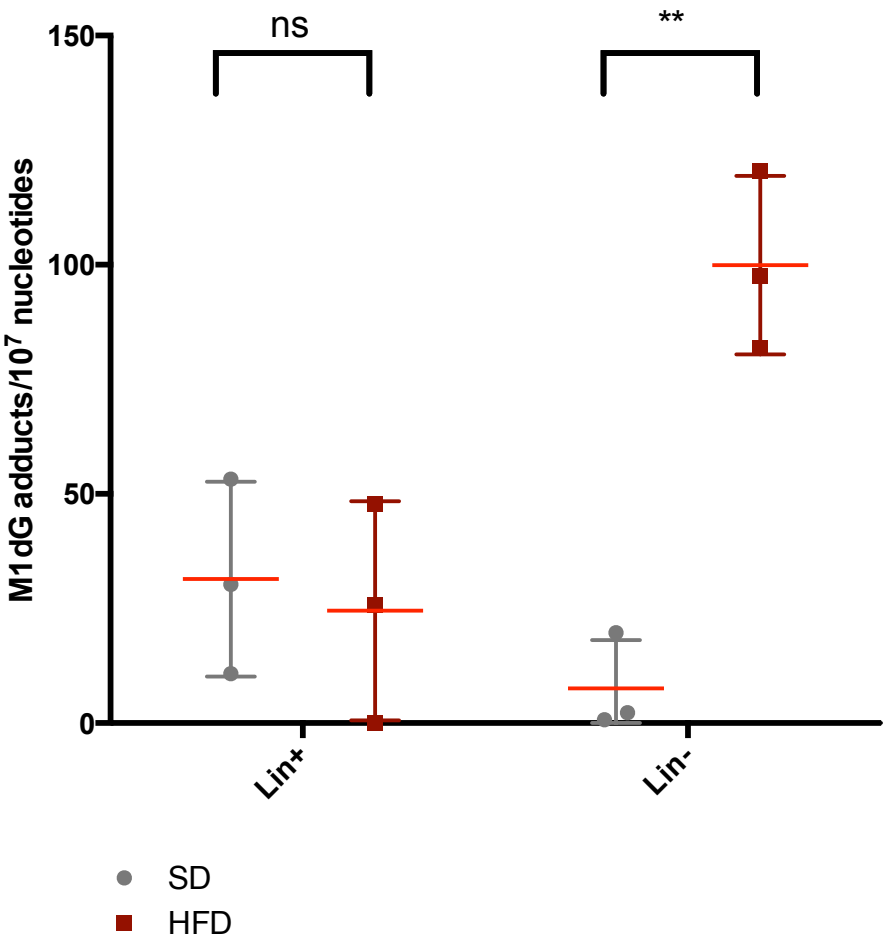

Figure 9. M1dG adducts are increased in Lin- cells of HFD treated mice. Quantification of M1dG adducts per 10^7single nucleotides analyzed in Lin- cells (on the right) and Lin+ cells (on the left) of mice fed with HFD. Greyd dots represent 3 mice in SD, while red squares represent 3 mice in HFD. **p<0.01

4.3 Antioxidant supplementation decreases HFD-associated DNA damage

We then evaluated if the observed DNA damage was due to HFD-induced oxidative stress by measuring the effect of a ROS scavenger. We kept PML/RARα KI mice for four months on SD or HFD, with or without n-Acetylcysteine (NAC), a well-known antioxidant which is orally bioavailable. and well-tolerated and can be administered in drinking water [152].

First, we monitored weight gain for four months to examine the hitherto unknown effect of NAC on mice weight (Figure 10). We did not detect any statistically relevant weight alterations in SD nor HFD upon NAC addition.

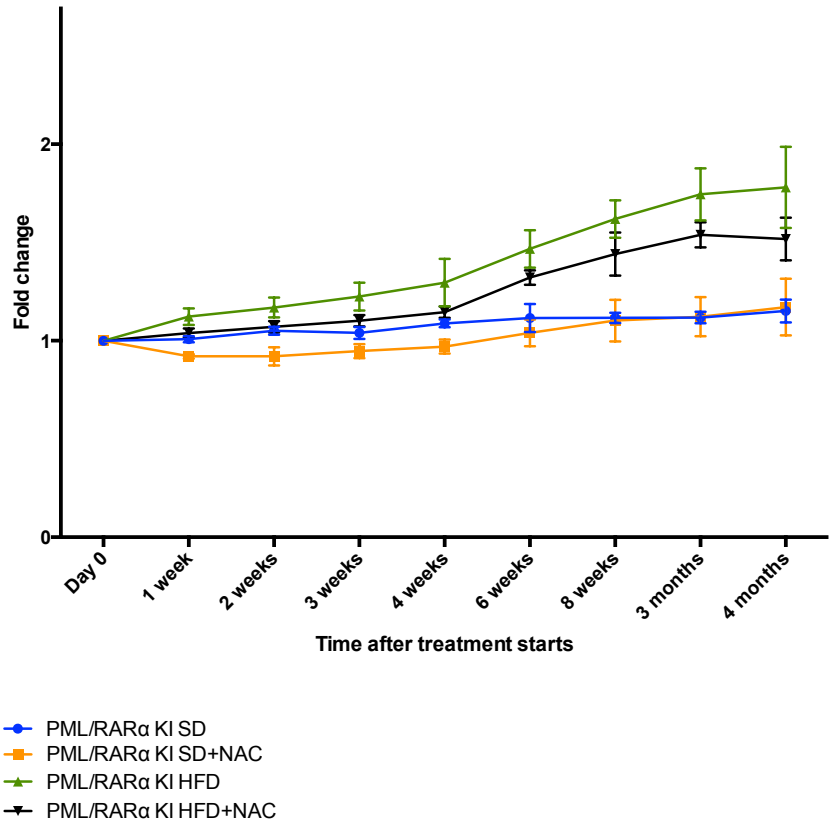

Figure 10. Fold change of weight using NAC antioxidant. Fold change of weight of mice kept on SD or HFD and NAC measured in grams is plotted as a curve for four months. Blue curve represents PML/RARα KI mice in SD, orange PML/RARα KI mice in SD and NAC, green curve PML/RARα KI mice in HFD, black curve PML/RARα KI mice in HFD and NAC.

We then measured whether HFD and NAC treatment resulted in modulation of ROS content in HSCs by measuring the binding of the ROS-sensitive 2'-7'-dichlorodhydrofluorescein diacetate (DCDFA) dye by flow cytometry. HFD resulted in ROS level elevation, which was abrogated or even reduced below baseline levels by NAC treatment (Figure 11). However, the variability within each group was high, such that differences are not statistically significant and results should be considered preliminary.

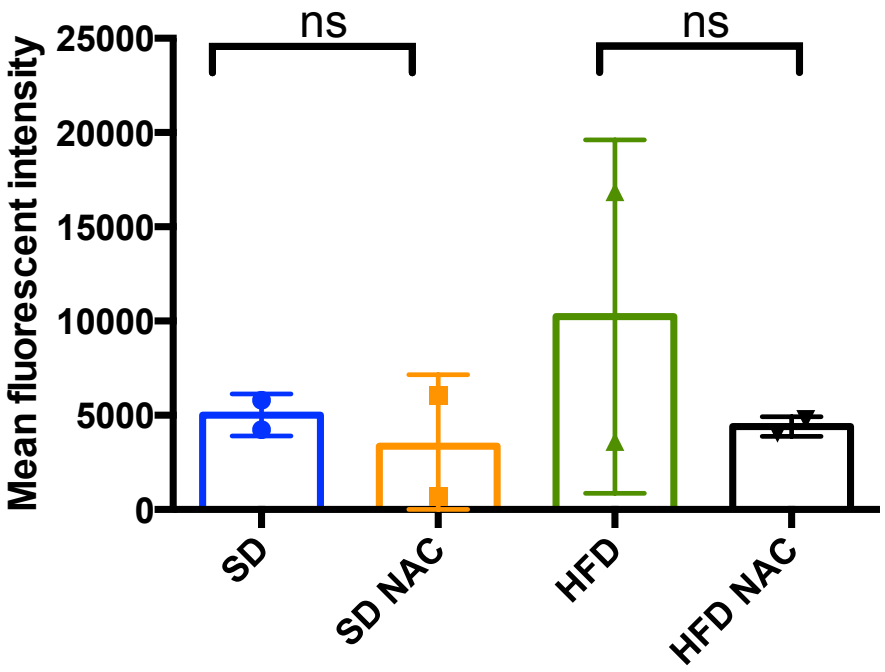

Figure 11. ROS decrease with NAC treatment. DCFDA expression was monitored in HSCs in two mice per condition. Mean fluorescent intensity is reported on y axis.

Finally, we evaluated DNA damage in HSCs by alkaline comet assay. The amount of DNA damage in HSCs did not change upon NAC treatment in mice fed SD. However, there was a 30% decrease in HSCs deriving from HFD-fed and NAC-treated mice compared to HFD alone (Figure 12). The decrease was so pronounced that the levels of DNA damage in HFD-fed NAC-treated mice were comparable to those encountered in animals kept on SD regardless of NAC treatment.

All together, these results suggest that HFD increases DNA damage through ROS production elevation. Elevated ROS may directly cause the formation of DNA adducts (M1dG) through lipid peroxidation.

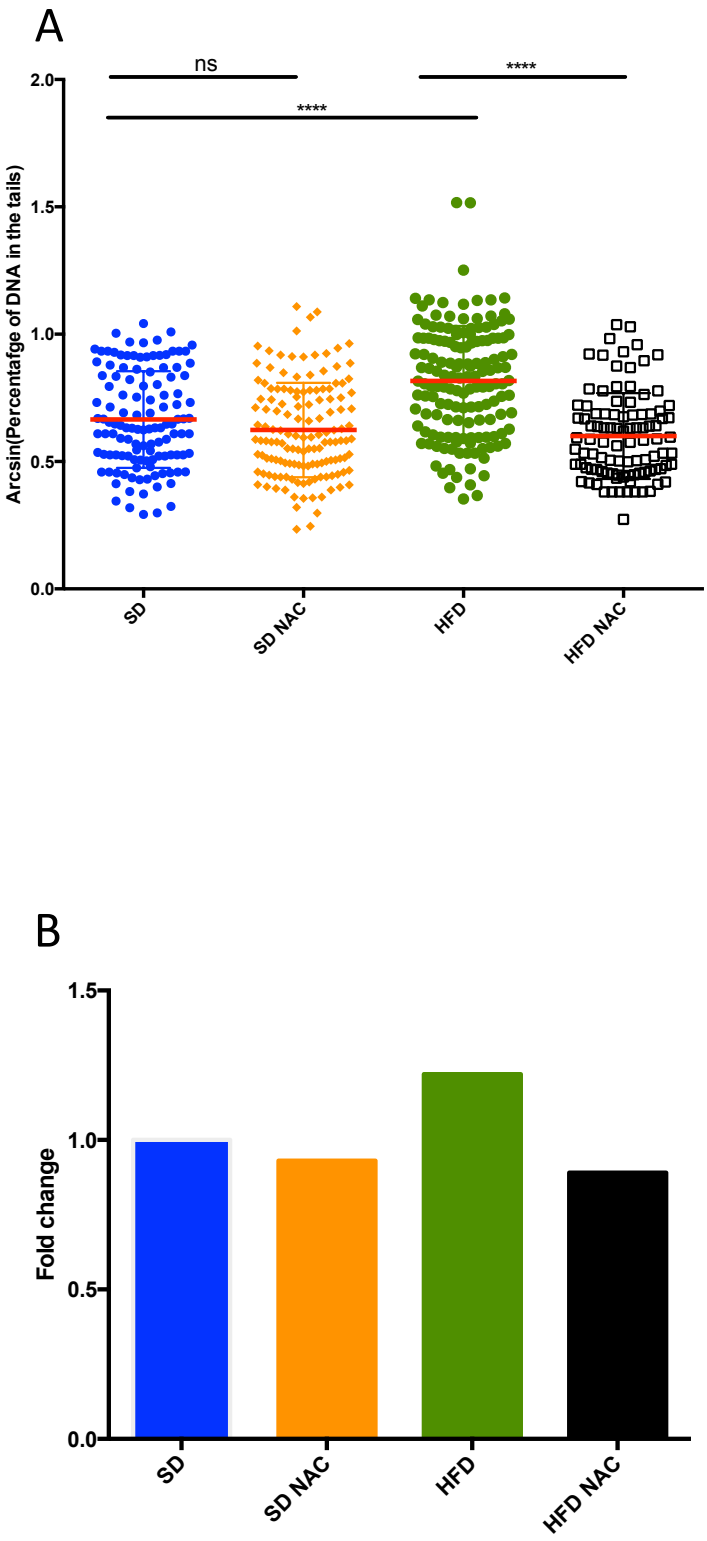

Figure 12. DNA damage decreases using antioxidant agent. A) Comet quantification expressed as arcsin(sqr root(percentage of DNA damage)) in 4 mice per experimental condition. Blue dots are PML/RARα KI in SD, orange rhombuses PML/RARα KI SD+NAC, green dots PML/RARα KI HFD and black squared PML/RARα KI HFD+NAC. Red line indicates average B) fold change variation using PML/RARα KI SD as 1. Blue bar is PML/RARα KI SD, orange PML/RARα KI SD+NAC, green PML/RARα KI HFD and black PML/RARα KI is HFD+NAC. $p<0.0001$ ****

4.4 HFD does not increase frequency of mutations in pre-leukemic HSC as revealed by Whole Genome Sequencing of HSC-derived clonal colonies

We then tested if the increase in DNA damage translates into a higher number of mutations in HSCs. Hence, we developed a novel technique for physiologically amplifying individual HSC genomes, exploiting their ability to generate colonies in culture. HSCs from PML/RARα mice kept on HFD or SD for 4 months were single-cell sorted into 96-wells plates and allowed to proliferate for 2 weeks. No substantial differences in terms of colony formation efficiency were noticed among groups (Figure 13). Genome amplification obtained through cell proliferation exploits the physiological proof-reading machinery, circumventing the problem of elevated polymerase-associated error introduction *in vitro* of whole genome amplification [153].

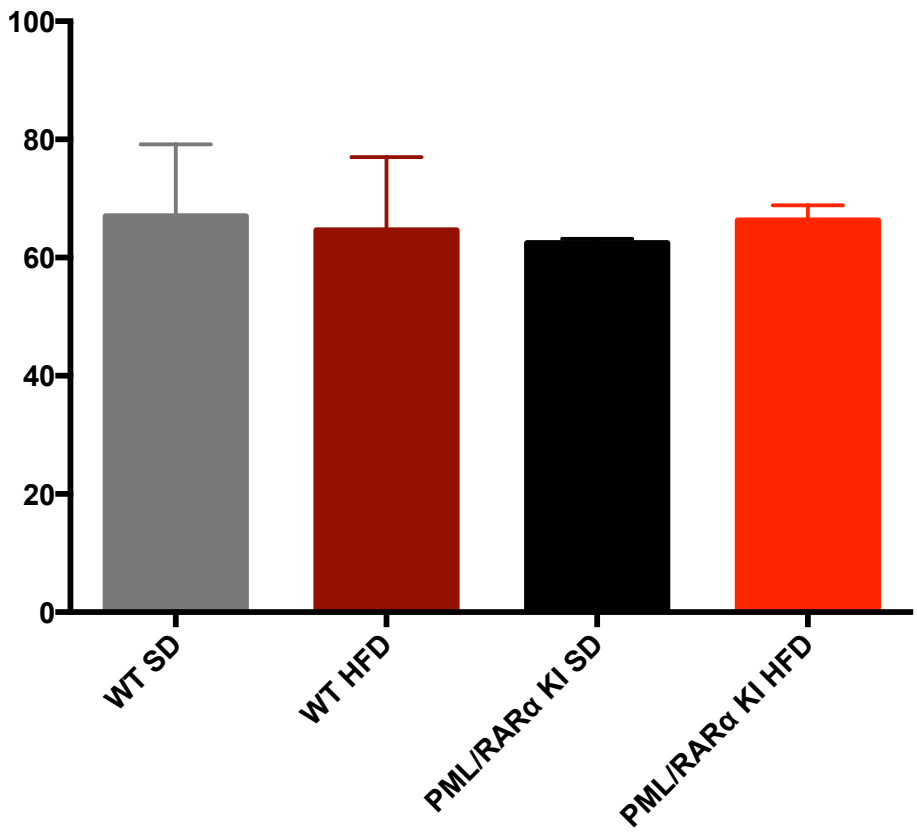

Figure 13. Diet nor genotype influence the growth of colonies. Number of wells containing colonies were represented in the graph. Grey bar represents WT SD, dark red bar WT HFD, black bar PML/RARα KI SD and red bar PML/RARα KI HFD. 3 mice were analyzed per each experimental group.

For each experimental condition, five colonies each from two individual mice were randomly picked and genomic DNA was extracted and subjected to Whole Genome Sequencing. As internal germline reference, genomic DNA extracted from the animal tail was also sequenced.

Sequencing data were subjected to different analytical pipelines: CavEMAn[154] and Shearwater [155]. A significant difference between the two algorithms is that the former utilizes a matched reference to call variants (the matched tail DNA, in this case), and as such is prone to systematic error if a tail is sequenced to significantly different coverage than other tails. CavEMan variant calling pipeline includes a post-processing level able to translate a pool of raw variants in a set of high-confidence somatic mutations; its filters allow specificity to be set as high as desired to reduce the likelihood of detection of false positives in WGS data.

Additionally, CavEMan was recently used in the identification of physiological mosaicism during embryonic development[144]. On the other hand, Shearwater is less prone to the bias of germline coverage. Indeed, the latter method is less prone to such a bias since it uses a pool of multiple WT references to call variants. Given the shortage of WT WGS available, the reference pool includes all the samples (minus the analyzed one) in any experiment, and thus only enumerates variants that are not in common between samples and mice. Results of the mutation analysis using the two different algorithms are shown in figure 14A (CaVEMan) and 14B (Shearwater). As expected, the two algorithms gave different results. Firstly, the total number of mutations differed by about an order of magnitude (max 200 vs 60). Although CaVEMan showed a moderate diet-associated difference, this was not confirmed with Shearwater.

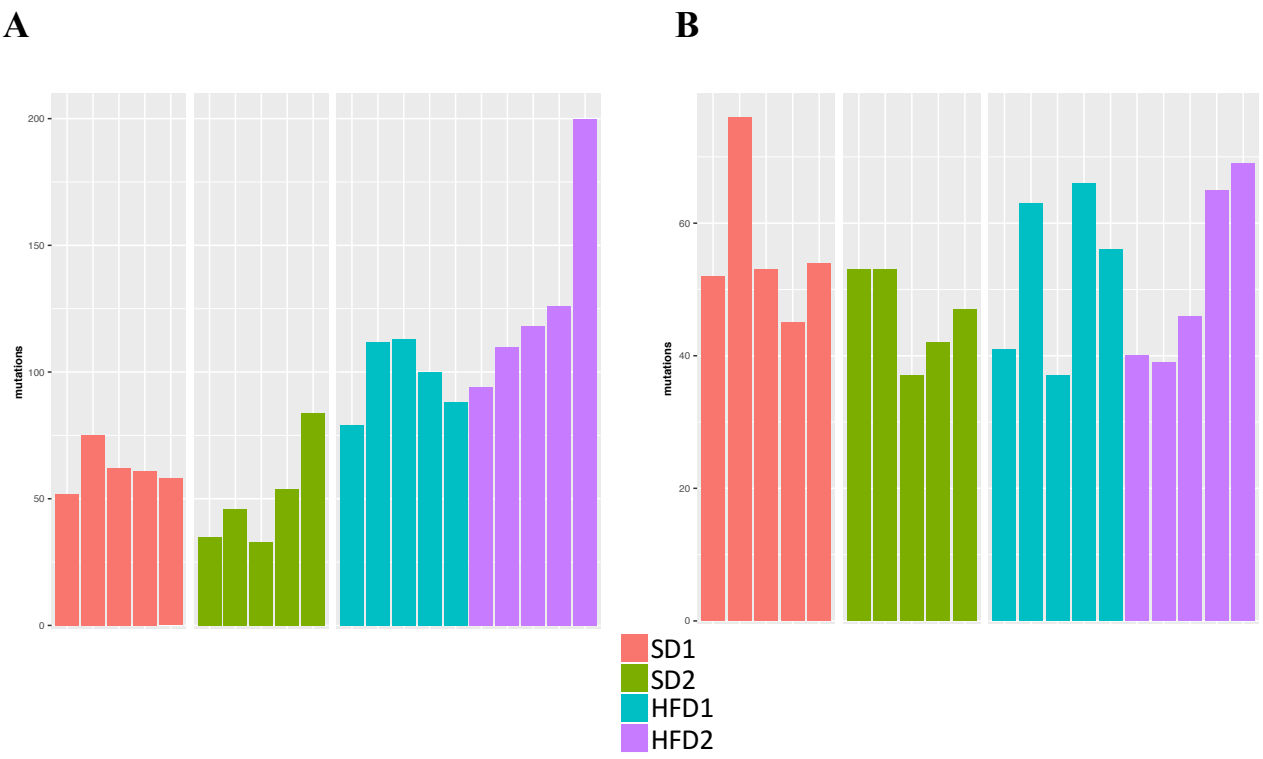

Figure 14. Analysis of point mutations in PML/RARα KI mice. In these two graphs are shown the results of mutations using CaVEMan (A) and Shearwater (B). Each colour corresponds to a single mouse. For each mice are 5 independent colonies were analysed which are shown by each bar; on y axis are reported the total number of mutations.

Despite differences in mutation numbers, both strategies strongly suggested that DNA damage does not translate into mutations.

In addition to point mutations, we also analyzed the insertions and deletions in the genome, using Pindel algorithm, considering variant allele frequencies above 0.3% [156]. Similarly, to point mutations, we could not detect any difference between the two dietary regimens (Figure 15) in acquisition of insertions and deletions.

Figure 15. Analysis of deletions/insertions of PML/RARα KI mice. In the histrograms are shown the different colonies from 2 SD and 2 HFD PML/RARα KI mice. Blue bars indicate the number of insertions counted for each colony, while red bars the number of deletions.

Finally, we analyzed the amount of structural mutations, by counting the number of chromosomal translocations. For this purpose, breakpoint via assembly algorithm (BRASS) was used to detect structural variations. Only in SD2 mouse less structural variations were counted compared to other mice (Figure 16).

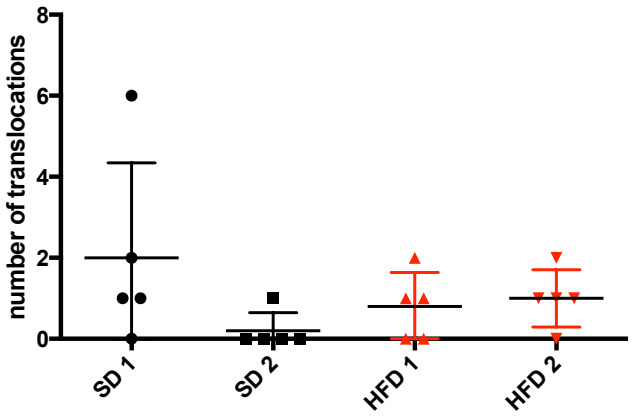

Figure 16. Analysis of deletions/insertions of PML/RARα KI mice. Black dots and squares indicate the number of rearrangements in SD colonies, red triangles in HFD colonies.

4.5 HFD increases self-renewal of PML/RARα KI bone marrow cells

The lack of a significant HFD-associated increase in DNA mutations, prompted us to investigate alternative mechanisms. PML/RARα is known to enhance self-renewal and inhibit differentiation of myeloid-committed progenitors[68,157], so we investigated if HFD impacts stem cell properties. We performed serial replating colony forming assays in methylcellulose. In this assay bone marrow cells are plated in semisolid medium with cytokines allowing hematopoietic differentiation; the number of colonies reflects the number of stem-progenitor cells and the ability to maintain colony-forming activity upon serial passaging is considered a mirror of self-renewal.

Whereas the assay performed on BM from WT mice revealed a reduction in colony-forming ability that was unaffected by diet, as expected[158], BM from HFD-fed PML/RARα KI were able to maintain self-renewal upon serial replating, statistically significant from the second passage (on average 129 colonies in SD vs 276 in HFD, $p<0.0001$, figure 17).

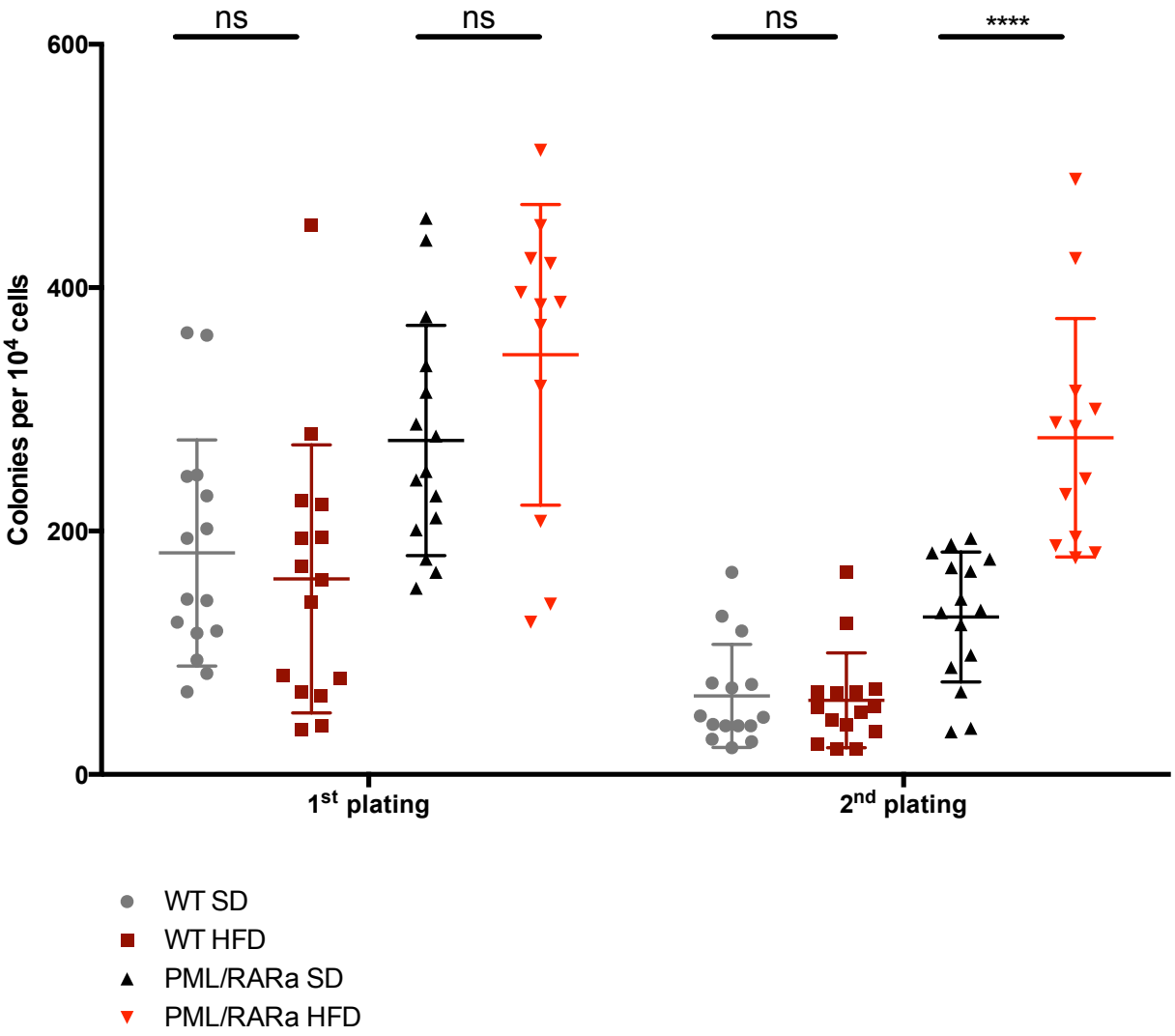

Figure 17. PML/RARα KI BM kept in HFD shows increased clonogenicity. Total BM cells were plated at 10^4 cells/plate; after one week the resulting colonies were counted and the cell suspension replated at the same density. Four mice were used per condition and each condition was plated in triplicate. Grey dots is WT SD, dark red squares WT HFD, black triangles PML SD and reverse red triangles PML HFD. **p<0.001.

4.6 *In vitro* fatty acid screening suggests that unsaturated fatty acids enhance self-renewal

We then tried to understand if a specific component of HFD could recapitulate HFD-induced enhanced self-renewal in PML/RARα KI BM. As HFD mainly differs in its content of fatty acids, we measured the effect if adding different FAs to semisolid medium and measured colony forming activity of bone marrow from SD mice We included a monounsaturated FA (3.2 mM oleic acid), and two polyunsaturated FA (PUFA): linoleic Acid (LA, 5 mM), the main unsaturated component of HFD used in the experiments and arachidonic acid (5 μM). The latter derives from linoleic acid and is a known mediator of general inflammation potentially involved in obesity-induced inflammation[159]. Arachidonic acid had to be used at lower concentrations since initial experiments showed direct cytotoxicity on bone marrow cells at higher concentrations.

In cells treated with control vehicle (BSA or ethanol) the expected decrease in colony formation was seen at the second passage (Figure 18). Instead, increased colony formation was observed upon oleic acid (100 vs 300 $p=0.05$) and even more strongly increase upon linoleic acid (100 vs 446, $p<0.001$) addition.

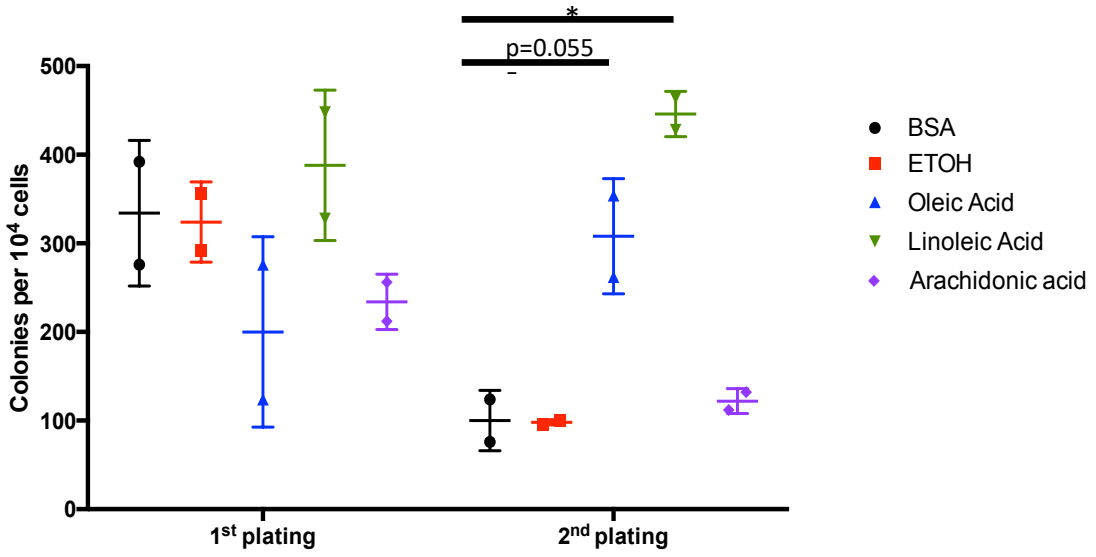

Figure 18. Linoleic increases clonogenicity. Colonies count per 10^4 total bone marrow cells plated. Experiment was carried out in duplicate. Black dots represent control with BSA, red squares ET-OH, blue triangle Oleic acid, reverse green triangles linoleic acid and violet rhombus arachidonic acid

A role for linoleic acid is consistent with the observed upregulation of linoleic acid-metabolizing genes in promyelocyitic vs non-promyelocytic leukemias observed in the TCGA (see intorduction). Thus, we decided to focus on the effects of LA only. LA had no effect on WT BM. Importantly, adding LA with either a lipoxygenase inhibitor (Zileuton, (1 µM) or PPARδ inhibitor (GSK3787, 1 µM) completely abrogated LA-enhanced self-renewal. This suggests that LA may mediate its activity through a direct action on PPARδ through the generation of endogenous PPARδ agonists. (Figures 19/20)

.

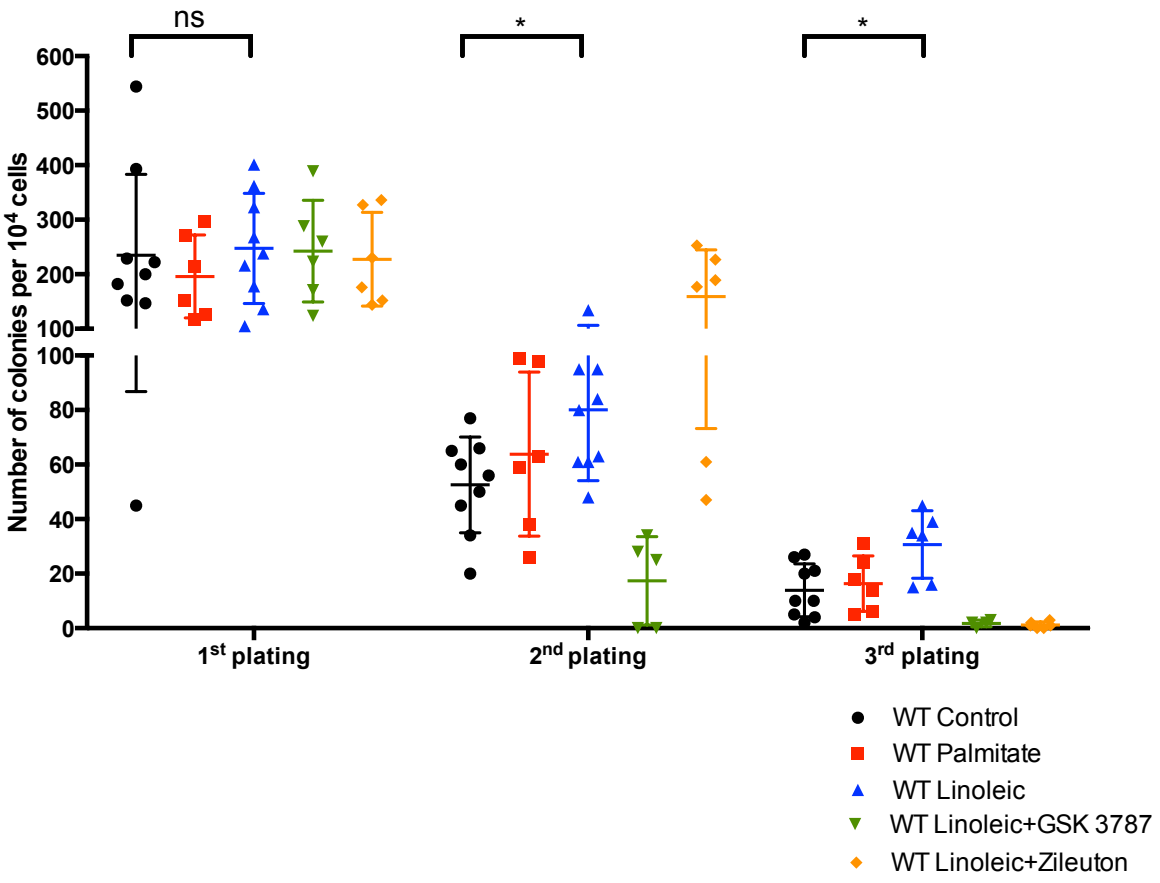

Figure 19. Linoleic acid induces slight increase of colonies in WT mice. Colonies obtained from 10^4 cells plated for 3 WT mice are represented. For control, linoleic experiment was carried out in triplicate, while for palmitic, linoleic+GSK3787 and linoleic+Zileuton in duplicate. Week 1,2,3 indicate three serial platings. Black dots indicate WT control, red square WT treated with 11.5 µM palmitic acid, blue triangles WT treated with 3 mM linoleic acid, green reverse triangles WT treated with linoleic acid and GSK3787, and orange rhombus. *$p<0.05$

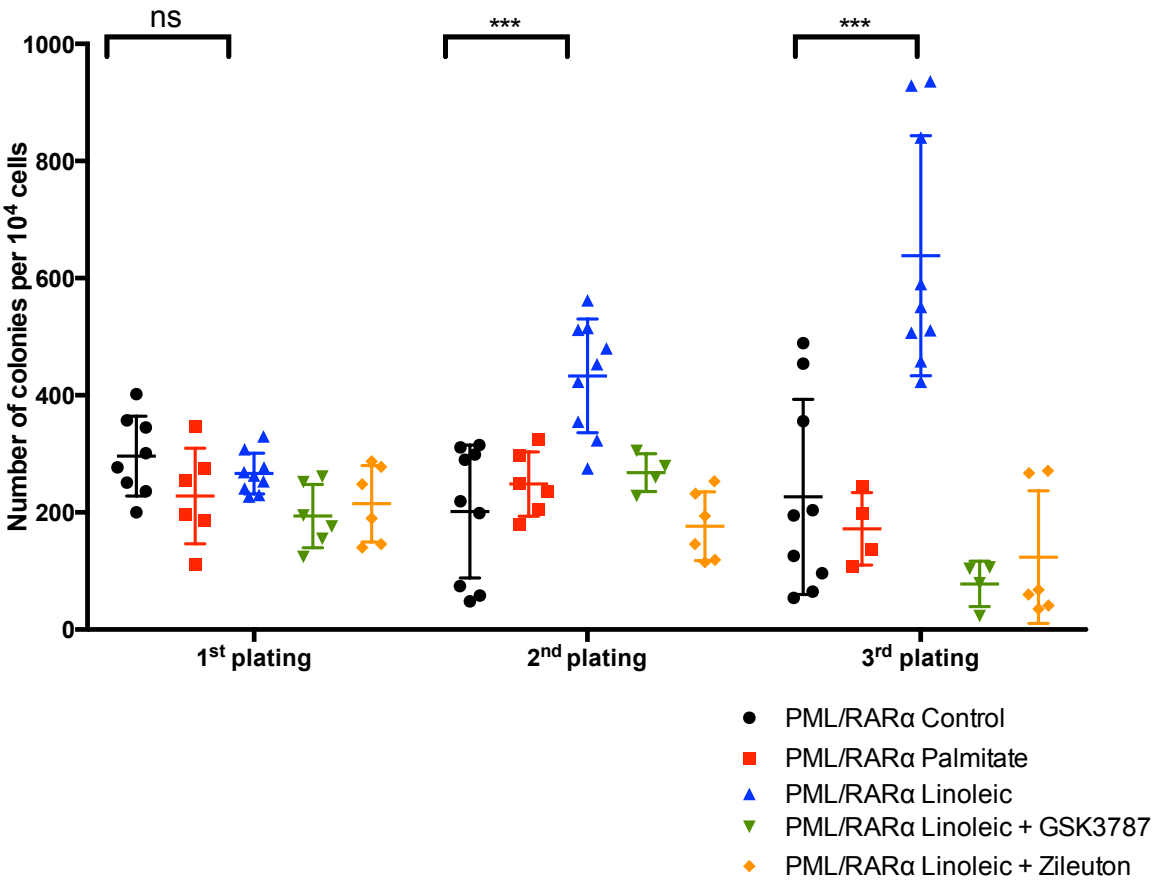

Figure 20. Linoleic acid enhances colony formation of BM cells from PML/RARα KI mice. Colonies obtained for 10^4 cells plated for three PML/RARα KI mice are represented. For control, linoleic experiment was carried out in triplicate, while for palmitate, linoleic+GSK3787 and linoleic+Zileuton in duplicate. Black dots indicate PML/RARα KI control, red square PML/RARα KI treated with 11.5 μM palmitic acid, blue triangles PML/RARα KI treated with 5 mM linoleic acid, green reverse triangles PML/RARα KI treated with linoleic acid and GSK3787, and orange rhombus PML/RARα KI with Linoleic and Zileuton ***$p<0.01$.

We then checked if LA is required continuously for enhanced self-renewal. We performed an experiment in which LA was either removed or maintained after the first replating (Figure 21).

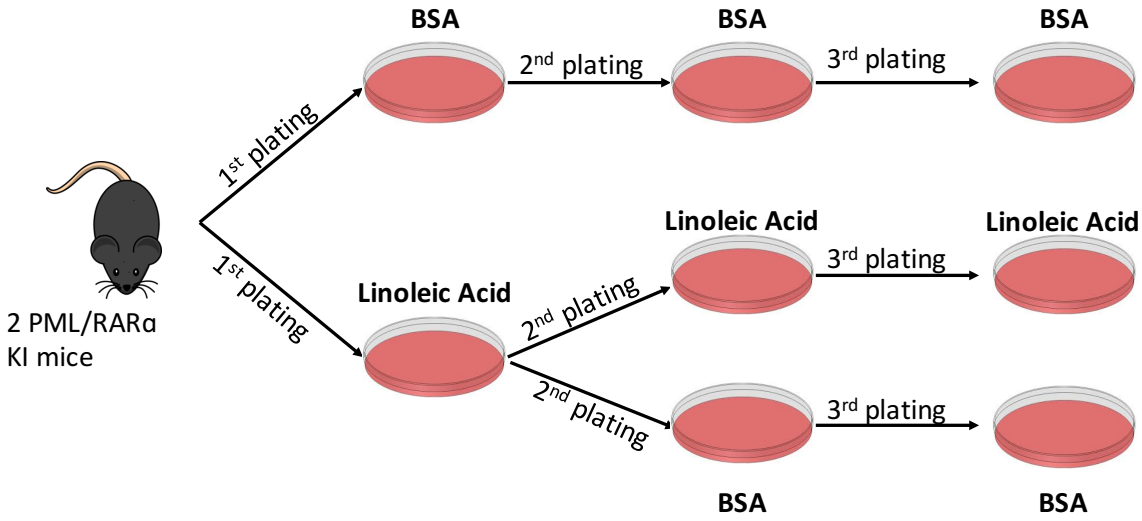

Figure 21. Experimental design. Cells from PML/RARα mice were plated in medium supplemented with BSA or Linoleic acid (First plating). Subsequently, cells grown in linoleic acid-supplemented medium were plated either with linoleic or with BSA (Second plating). The same media were used for the third plating.

We confirmed enhanced clonogenicity upon linoleic acid treatment compared to BSA-treated sample (134 vs 475, $p<0.0001$) (Figure 22). At the second passage, elimination of LA did not result in decreased colony formation (475 vs 479, $p>0.05$)., suggesting that the prior exposure was sufficient to enhance self-renewal. However, this was only maintained for one passage, since at the subsequent passage colony formation efficiency dropped significantly

These data demonstrate that linoleic acid is responsible of enhanced clonogenicity and that it must be present continuously in order to maintain its effect.

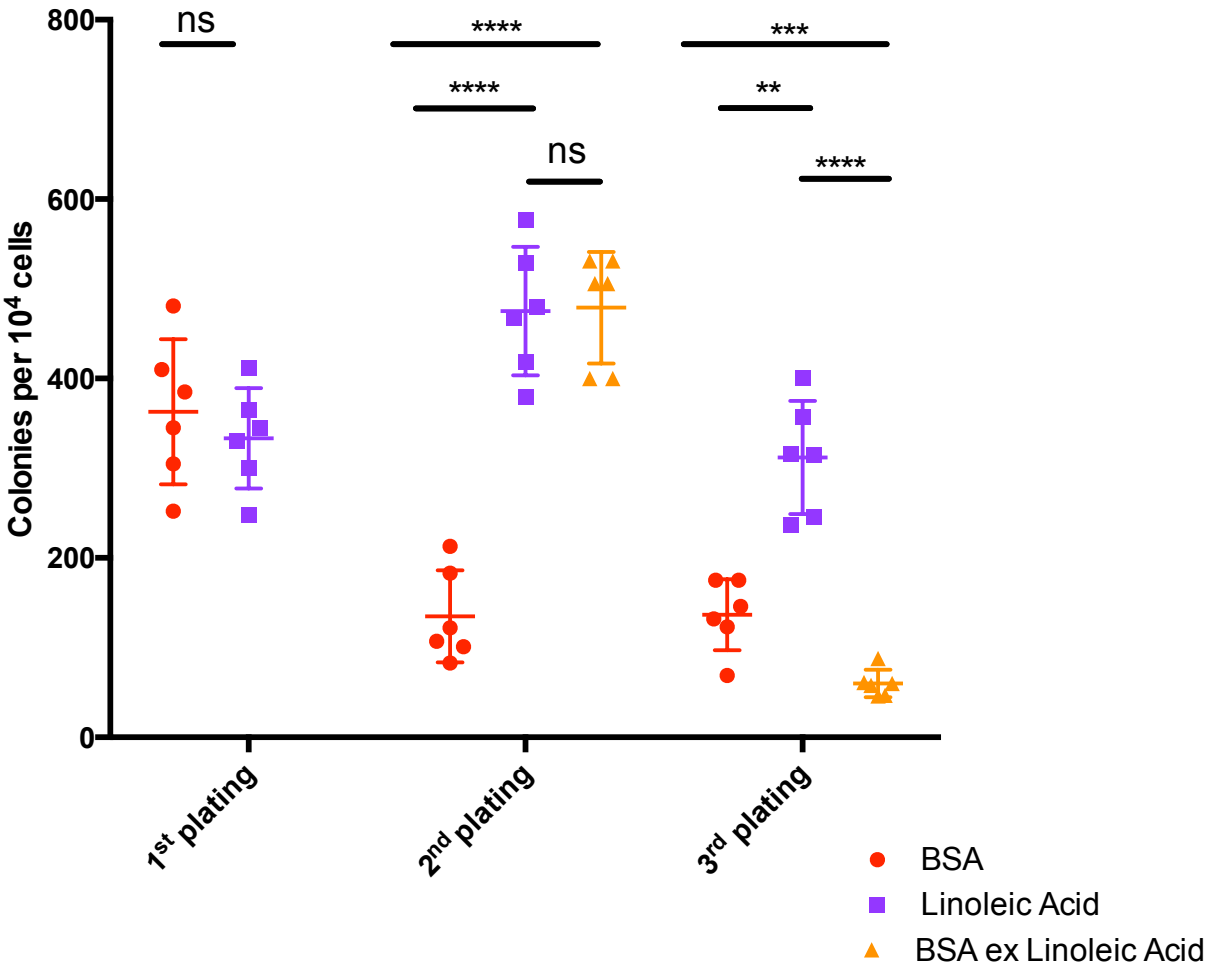

Figure 22. Cells require linoleic acid to maintain their clonogenic potential. Colonies number for 10^4 total bone marrow cells. Red dots indicate cells treated with BSA, violet square cells treated with 5 mM linoleic acid, orange triangles cells treated with BSA after initial treatment with Linoleic Acid.

4.7 Linoleic acid-enhanced self-renewal is not due to increased symmetric stem cell division

We then asked whether LA-enhanced self-renewal is due to an increased frequency of symmetric stem cell divisions. Since in the hematopoietic system stem cells are characterized by metabolic and proliferative quiescence[83], the balance between symmetric and asymmetric stem cell divisions could be measured by quantitating the proliferative history upon plating. A symmetric division of a stem cell could result in either two quiescent or two proliferative daughter cells; an asymmetric division would result in one quiescent and one proliferative. However, the balance between these two proliferative modes has not been specifically assessed in conditions used for vitro colony forming assay. Therefore, we measured the cell division rates using carboxyfluorescein succinimidyl ester (CFSE) incorporation assay and stem cell live imaging.

CFSE is a cell permeable dye incorporated by cells and diluted upon division, allowing to track proliferative history by flow cytometry. In particular, quiescent or slowly dividing cells maintain high levels of CFSE staining, whereas fast cycling cells lose it. Our measurements suggest that all cells divide actively at least 12 times (beyond which individual CFSE peaks are not distinguishable,) in both treatments (Figure 23)

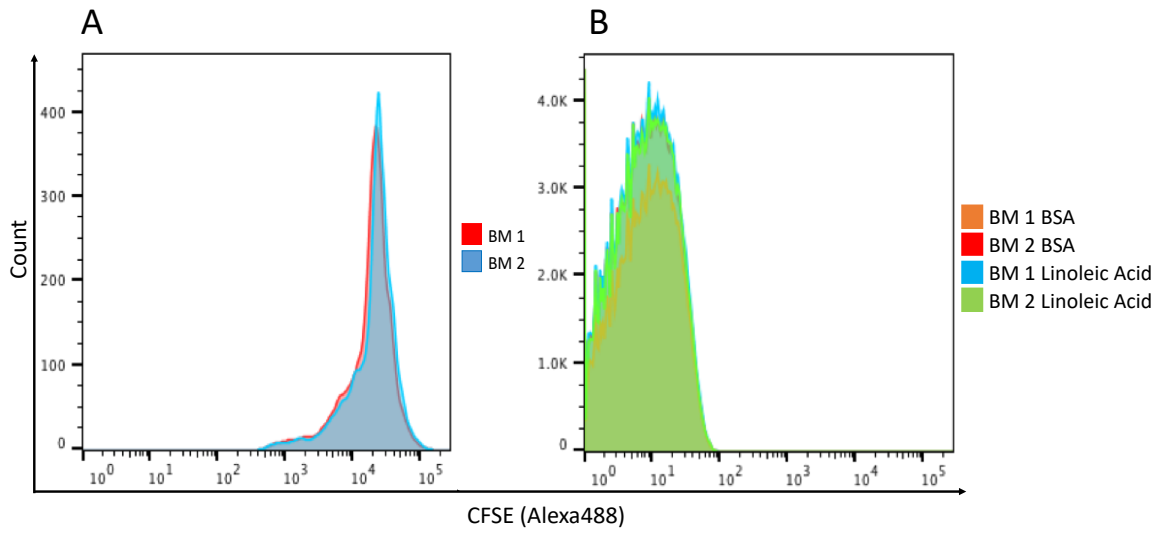

Figure 23. Linoleic and BSA treated cells do no retain CFSE. A) Histogram showing BM cells positivity for CFSE. Light blue and red curve represent two independent mice. B) Histogram showing BM cells retention of CFSE after one week. Orange and red curve represent the cells treated with BSA, while green and light blue the cells treated with linoleic acid.

We cannot completely rule out that asymmetric stem cell division occurs after 12 stem cell divisions. However, if we mathematically model this hypothesis we can easily conclude that this is an extremely unlikely scenario: if symmetric stem cell division occurred 12 times prior to the first asymmetric division, then either all the first 12 divisions were symmetric and gave rise to 2^{12} stem cells, which would give rise to the same number of colonies in the subsequent passage, or the first division would have given rise to two non-self-renewing proliferating cells, which would exhaust the colony-forming potential. This is likely to happen in the absence of LA, but cannot happen in LA-treated cells which maintain self-renewal upon serial replating.

To further confirm this observation, we performed live cell imaging to directly track stem cell division. For this purpose, stem cells were plated in methylcellulose in the presence of BSA or linoleic acid. We followed cell divisions for the first four passages and counted how many cells were there at the end of every passage. If cells divide asymmetrically cells follow 2^n exponential growth, so that four divisions result in 16 cells. If cells divide asymmetrically, upon completion of a cell division, one cell enters quiescence. Thus, they would not follow 2^n exponential growth, meaning that after four division there will be less than 16 cells. Upon

both BSA and linoleic acid treatment, we counted 16 cells after four passages, meaning that all cells undergo equally timed symmetric cell divisions (Figure 24).

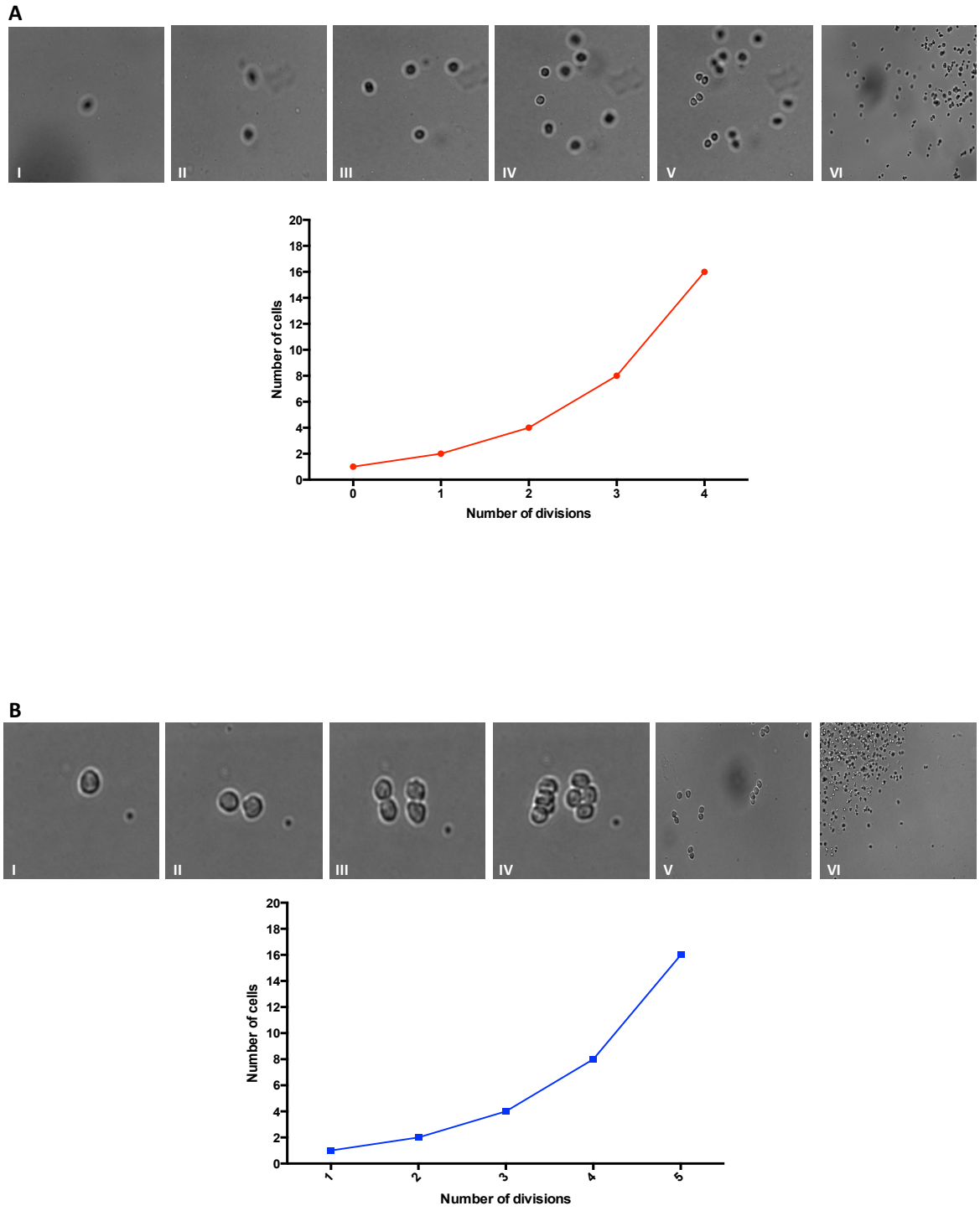

Figure 24. Linoleic does not induce symmetric HSC division. A) Live cell imaging of BSA treated HSCs. In the images are reported: I one cell; II two cells, III four cells; IV eight cells; V sixteen cells; VI entire colony. The graph reported the number of cells counted in four different fields; B) Live cell imaging of Linoleic Acid treated HSC. In the images are reported: I one cell; II two cells, III four cells; IV eight cells; V sixteen cells; VI entire colony. The graph reports the number of cells counted in four different fields.

4.8 HFD induces HSC exit from quiescence and expansion of the progenitor pool

To prove that HFD enhances self-renewal also *in vivo*, we measured the effect of diet on the number and percentage of HSC and progenitors

An optimized flow cytometry protocol was used for the identification of progenitors and HSCs (See Introduction and Methods sections; fig.6). The proportion of Lin^- uncommitted cells in the total BM ranged from 10-20%. LSK population, that includes HSCs, comprised about 0.2% of the total BM population. HSCs are the 0.02% of total bone marrow cells, while 0.18 cells are progenitors divided in HPC-1, HPC-2 and MPP (Figure 25).

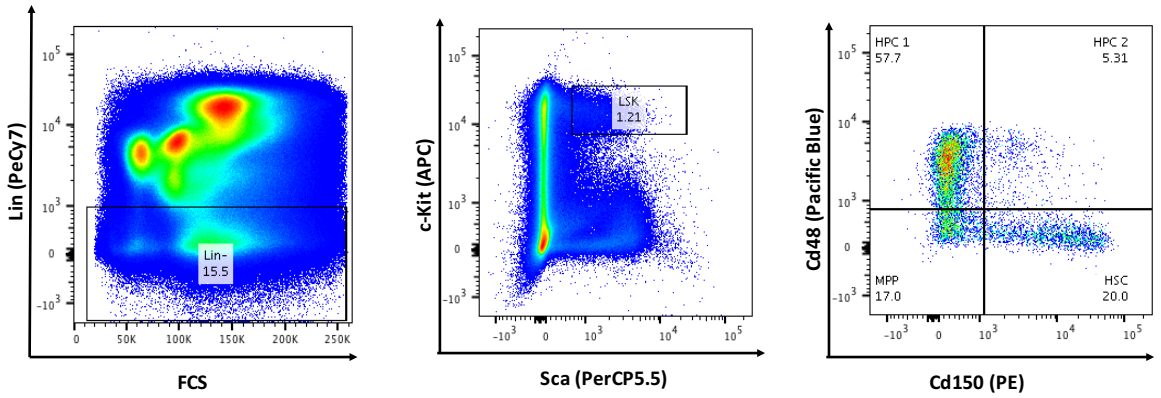

Figure 25. Representative result of FACS quantification of various populations in the BM. The arrows indicate the FACS parameters used to isolate the cells in each panel, and for each target the fluorophore conjugated is given in parentheses. Percentages are referred to the parental cells.

For the purpose of this analysis, HPC1, HPC 2 and MPPs were grouped into a single category denominated "progenitors". For both WT and PML/RARα KI mice, HFD caused an increase in progenitor numbers in agreement with previous observations[152] (78% vs 85% in WT, $p<0.01$ and 73% vs 82% in PML/RARα $p<0.01$). In particular, HFD increased the percentage of HPC1/2 subpopulations. Moreover, we also observed a marked reduction in HSCs in WT and most markedly in PML/RARα KI mice (21% vs 14% in WT $p<0.01$ and 26% vs 17%, $p<0.01$ in PML/RARα KI) (Figure 26).

A

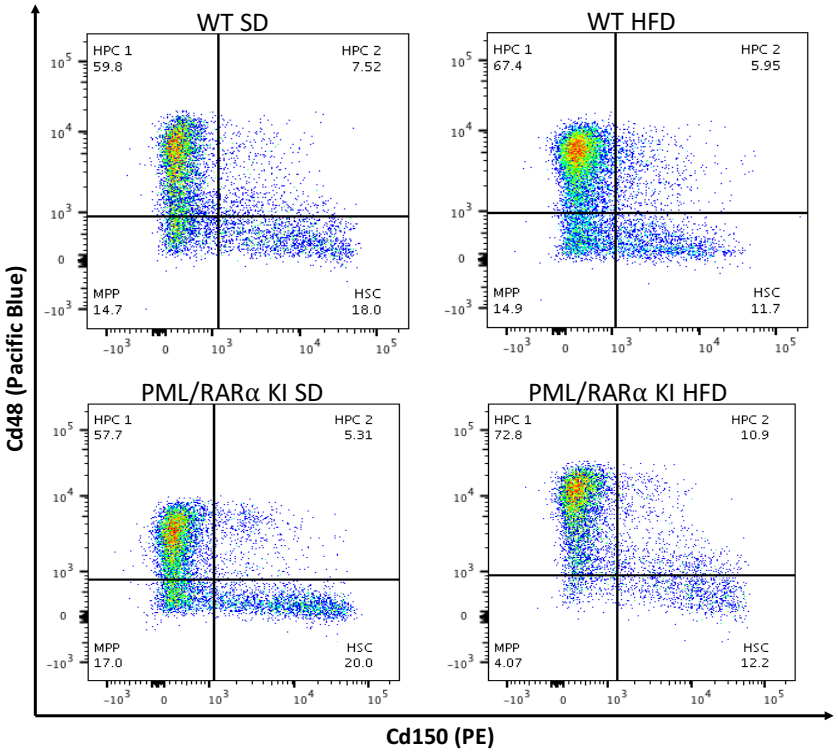

B

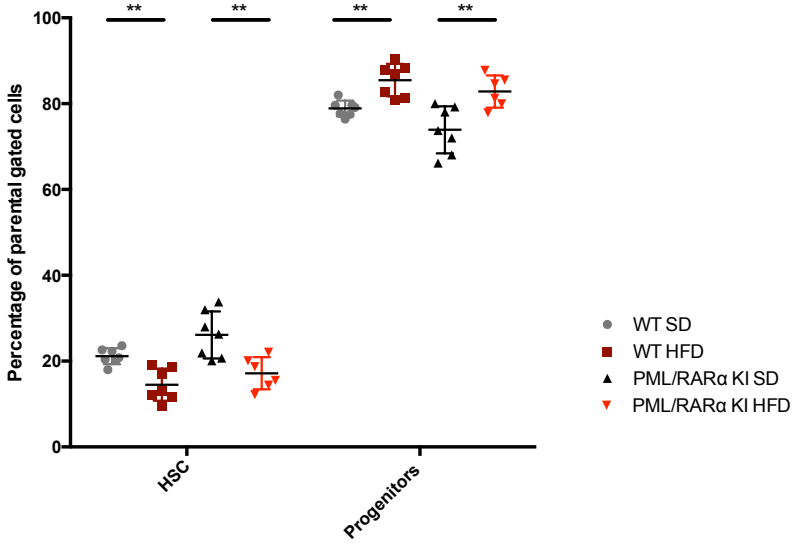

Figure 26. Obesity reduces HSC and increases progenitor numbers. A) HSCs, HCP1/2 and MPP cells from a representative mouse per experimental branch (WT SD, WT HFD, PML/RARα KI SD and PML/RARα KI HFD) are shown as FACS plots.5 The fluorophore of each antibody is indicated in parentheses. B) Statistical analysis for the four cohorts. Grey dots represent WT in SD, dark red squares WT in HFD, black triangles PML/RARα KI in SD and reverse red triangles PML/RARα KI in HFD. For each condition 8 mice are represented. SD is represented with bars. **p<0.01.

Given that HFD decreases the percentage of HSCs and increases the percentage of progenitors, we wondered whether HFD would alter the balance in HSC cell cycle progression as assessed by DAPI staining. Ki67 staining was used to discriminate between G0 (Ki67-) and G1 (Ki67+). HFD was associated with a shift in cell cycle distribution towards increased proliferation in both genotypes, with more frequent cells in S/G2/M phases (5% vs 22% in WT, $p>0.05$ and 23.1% vs 42.85% in PML/RARα KI, $p<0.05$) and fewer in G0 and G1, although these changes were only statistically significant in the PML/RAR***α*** Ki background (Figure 27). Progenitors, instead, did not show any significant alteration in cell cycle distribution (data not shown).

In conclusion, HFD induces HSC exit from quiescence and an increased pool of committed progenitors, more strongly in PML/RARα KI than in WT mice.

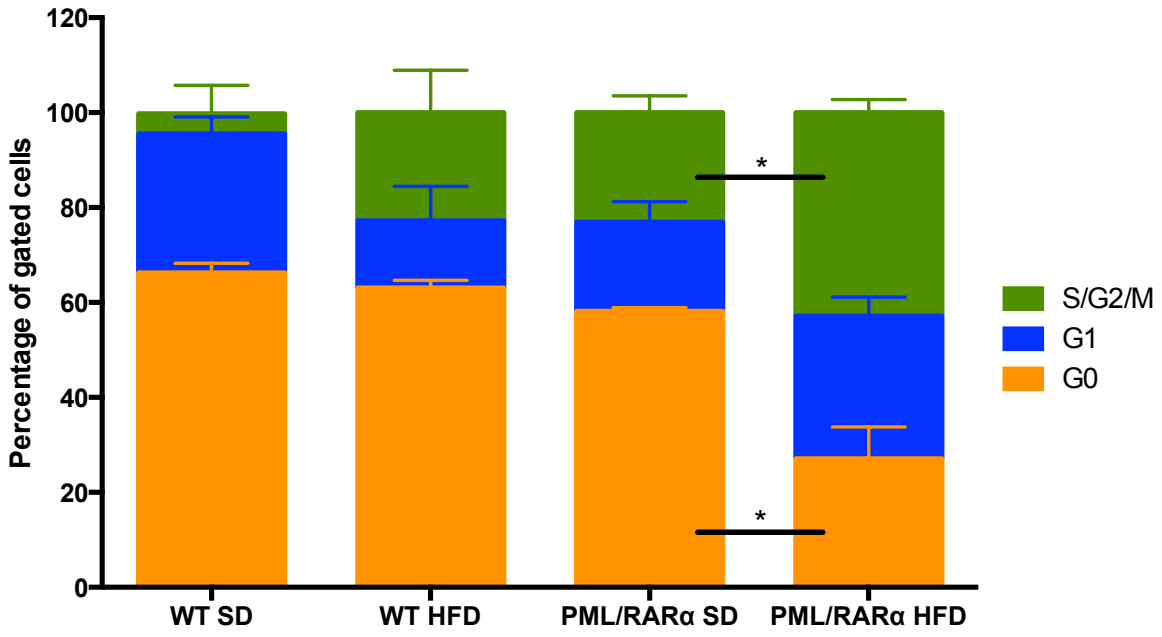

Figure 27. Obesity alters cell cycle progression in PML/RARα obese mice. Stacked columns showing percentages of cells in the G0, G1, S/G2/M phases of the cell cycle in WT SD, WT HFD, PML/RARα KI SD and PML/RARα KI HFD mice (n=2 per experimental class) are shown. G0 phase is shown as orange bar, G1 phase in blue bar, S/G2/M phase in green bar. SD are shown for each stack. *$p<0.05$.

4.9 HFD enhances *in vivo* self-renewal of PML/RARa KI HSC

To assess if the HFD enhances HSC self-renewal also *in vivo*, we performed competitive bone marrow transplantation in syngeneic mice. In this assay, BM cells deriving from SD and HFD-fed PML/RARα KI mice (Cd45.2 allele variant) were mixed in 1:9 ratio with recipient BM cells (Cd45.1 allele variant) and transplanted into irradiated Cd45.1 recipient mice. The engraftment was assessed at 1 month post-transplant in the PB by measuring the percentages of the two allelic variants by FACS. Prior to the transplantation, the actual ratio was verified (Figure 28).

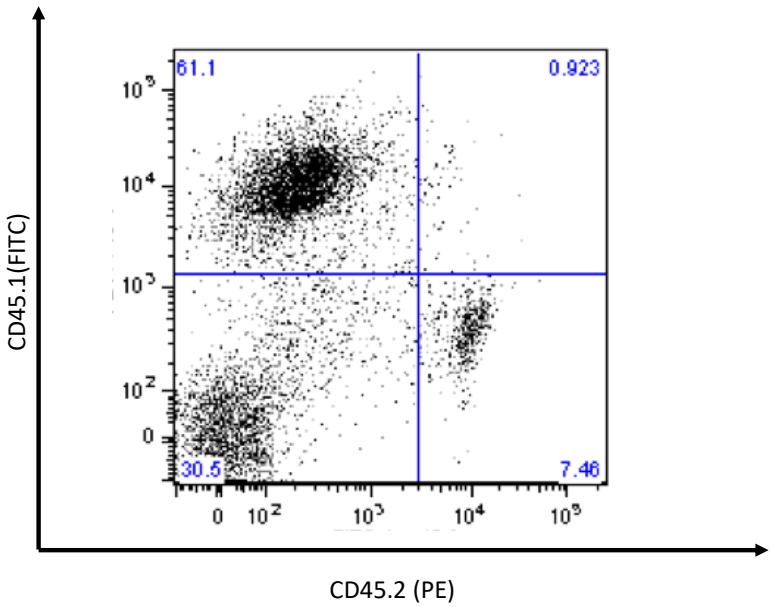

Figure 28. Transplantation is performed at the 1:9 ratio. Example of a FACS plot of BM cells to be transplanted. The percentage of carrier cells marked with anti-Cd45.1 was 9 times higher than that of donor cells marked with anti-Cd45.2 antibody. The fluorophore conjugated to the specific antibody is indicated in parentheses.

Six individual recipient mice per diet type were analyzed. The percentage of engrafted Cd45.2 cells was higher for cells deriving from HFD-fed compared to SD-fed animals. A representative example is shown in Figure 29A. The average percentage of engrafted Cd45.2 cells in peripheral was 7.5% from SD-fed donors versus 18.7% from HFD-fed donors ($p<0.001$, Figure 29B).

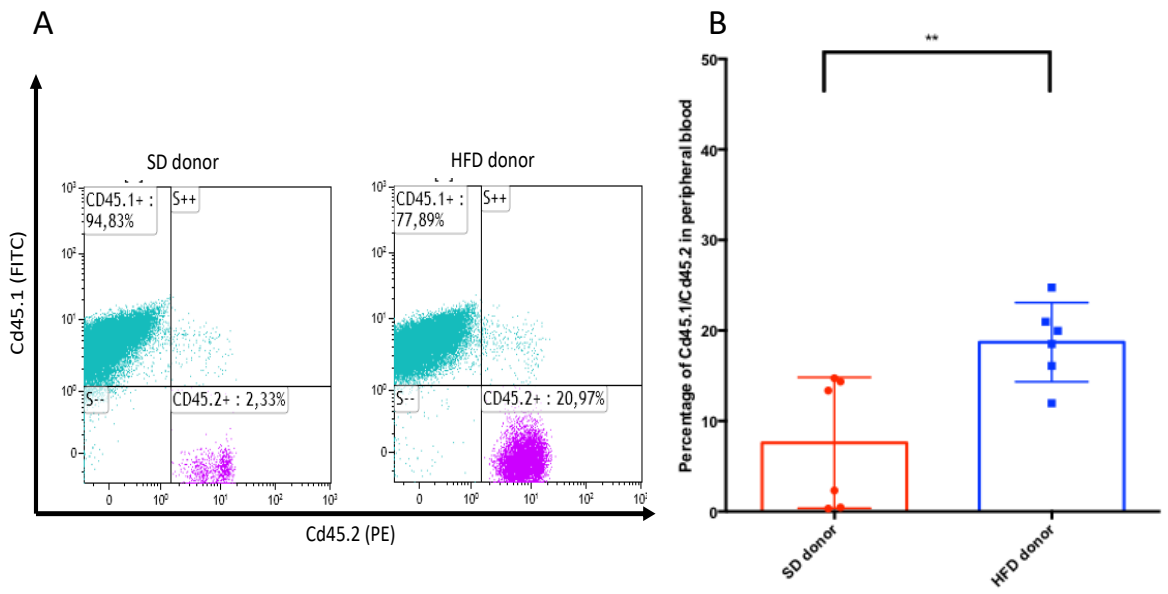

Figure 29. Engraftment of SD-fed and HFD-fed mice derived BM cells in PB. A) FACS plot of a representative mouse per condition deriving from SD-fed and HFD-fed donor. In light blue Cd45.1 are shown, in violet Cd45.2. B) 6 mouse per experimental branch are shown. Red bar represents Cd45.2 percentage in the PB from SD-derived mice, while blue bar in HFD derived mice. ** $p<0.001$

These results, together with data obtained from *ex vivo* experiments clearly show that BM cells derived from HFD-fed mice possess a higher self-renewal ability both *in vivo* and *in vitro*.

4.10 Antioxidant treatment enhances self-renewal per se but does not revert HFD-associated changes (preliminary)

Having demonstrated that HFD is associated with both increased ROS-dependent DNA damage and increased self-renewal of hematopoietic stem cells, we wished to assess if the two observations are related, in other words if ROS-dependent DNA damage is the cause of enhanced self-renewal. Therefore, we assessed the effect of NAC on self-renewal. If the above hypothesis is true, then NAC treatment should abolish LA- (in vitro) or HFD- (in vivo) enhanced self-renewal. These results are currently being replicated and should be considered preliminary.

We isolated BM cells from four 12-week old PML/RARα KI mice and plated them in methylcellulose with BSA or linoleic acid alone or either one with NAC (at a final concentration of 1.5mM). For technical reasons (the only available mice were younger than usual, so the efficiency of colony formation was higher than expected, preventing adequate counting) we could only perform this first experiment for a single plating. This proved sufficient to observe an increased clonogenicity upon linoleic acid treatment compared to BSA. Strikingly, we saw that NAC treatment alone enhances self-renewal in control-treated samples, as we saw a rise from of colony number 104 to 171 ($p<0.01$) (Figure 30), but it had no effect on LA-treated cells.

In vivo, we measured the percentage of HSC and progenitors in PML/RARa Ki mice fed SD or HFD, with or without NAC in drinking water, after 4 months of treatment.

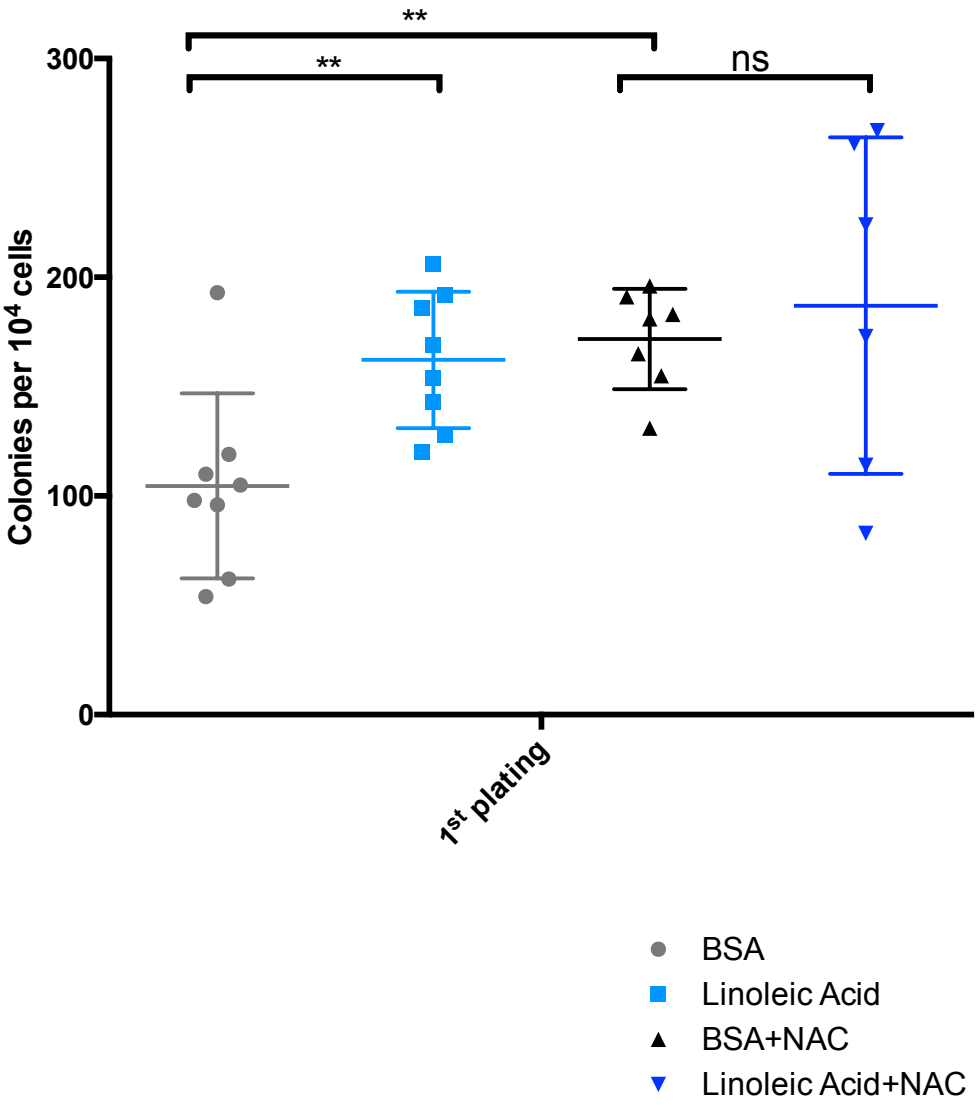

Figure 30. NAC treatment enhances self-renewal. Colony number after one week of plating with BSA/5mM linoleic acid and 1.5mM NAC. Dark red dots are BSA treated samples, light blue squares Linoleic treated samples, red triangles BSA+NAC and reverse blue triangles LA+NAC. Four mice were used in the experiment and each condition was plated in duplicate. $p<0.01$**

Again, NAC treatment leads to a decrease in HSCs and an increase in progenitors in both HFD and SD (Figure 31).

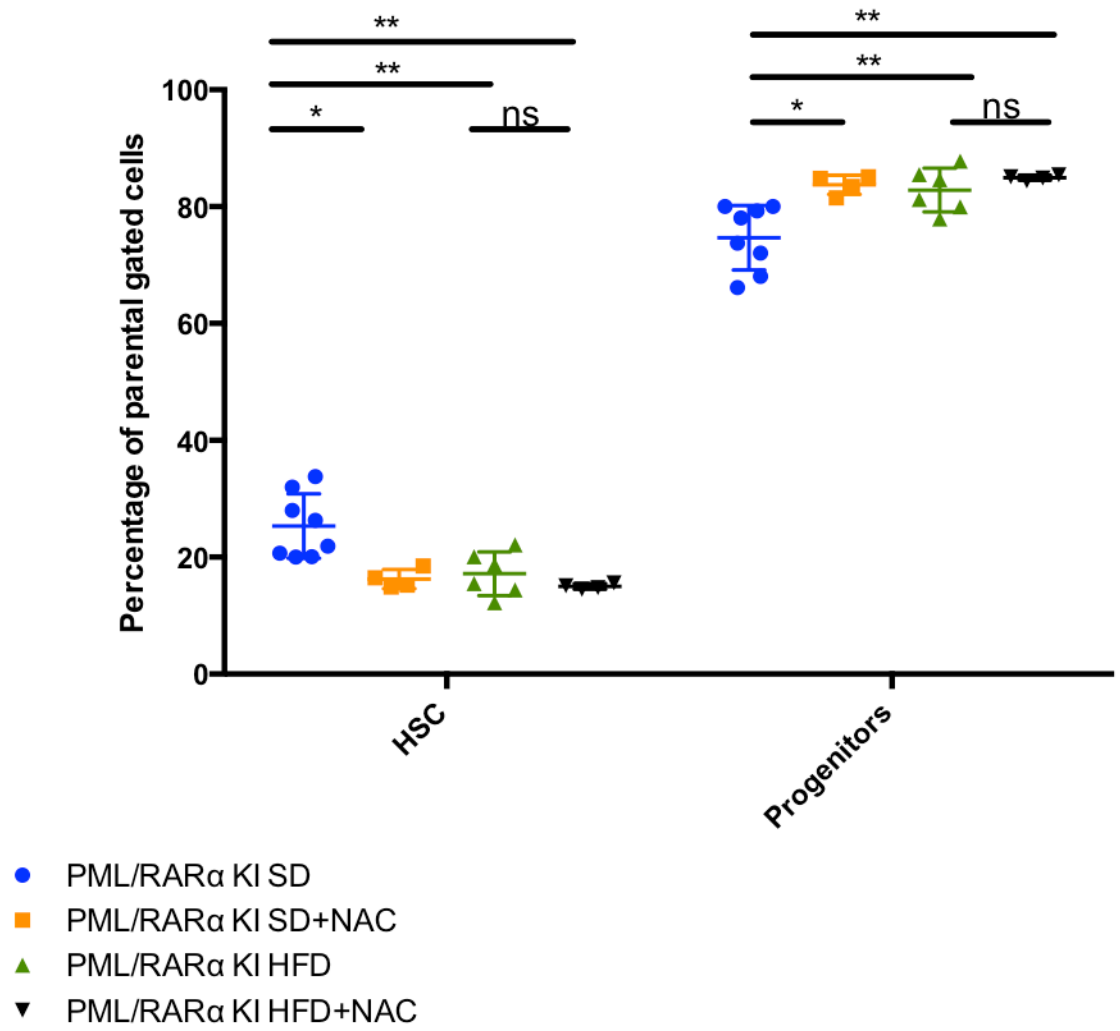

Figure 31. NAC decreases HSC and increases progenitors. Percentage of HSCs and of progenitors are shown in this graph. Blue dot is PML in SD, orange squares PML SD+NAC, green triangles PML in HFD and reverse black triangles PML in HFD+NAC. *p<0.05, **p<0.

Although preliminary, these results suggest that ROS-dependent DNA damage is not the cause for enhanced stem and progenitor self-renewal.

Chapter 5. Discussion and conclusions

The final goal of this project was to understand how obesity accelerates the development of leukemia in a mouse model of APL. Firstly, it must be pinpointed that the mouse model we have currently used perfectly recapitulates the physiology of obesity in humans[160], although we did not consider the sugar uptake that could lead to insulin resistance and finally to cancer[161].

The simplest theoretical model to explain the association between obesity and APL is a genetic model in which HFD behaves as a classic carcinogenic, generating DNA mutations through the induction of DNA damage. A similar model has been proposed in a different context by the Patel lab, who showed that endogenously generated aldehydes lead to leukemia or bone marrow failure, when physiological DNA repair mechanisms are genetically ablated[133,134]. Coherently with this model, in our system we observed accumulation of malondialdehyde-derived DNA adducts (M1dG) and DNA damage in hematopoietic cells from HFD-fed mice. Furthermore, the more differentiated the cells, the lesser the extent of DNA damage detected, supporting the idea that quiescent HSCs tolerate more DNA damage compared to differentiated cells, but repair damage before entering cell cycle[130,150]. Most of the DNA damage repair systems are error-prone and are considered to be the molecular mechanism through which mutations are fixed into the genome[162]. However, the colony WGS experiments performed here suggest that no significant increase in background mutation rate occurs in HSCs. Thus, the accumulated DNA damage may not be fixed into mutations and a purely genetic model does not seem tenable (Figure 32A). It must be underlined that we performed WGS only on 5 colonies deriving from 2 mice that could underestimate the mutation levels. Moreover, the final results of the competitive transplantation experiment of SD- and HFD-fed PML/RARα mice will be important: if recipient mice transplanted with PML/RARα KI BM from HFD-fed mice die sooner of leukemia than those transplanted with BM taken from SD-fed ones, it is highly possible that mutations arising before transplantation may have accelerated leukemia development.

The lack of mutations deriving from DNA damage in PML/RARα KI mice fed HFD, urged an investigation into alternative explanation potentially responsible for the increase in leukemogenesis. One such possibility is the acquisition of self-renewal, a typical property of stem cells, by progenitor cells thus hugely extending the pool of cells that may undergo malignant transformation. This hypothesis seems appealing, as it was shown that both HSCs and progenitors can become leukemia-initiating cells[163]. Indeed, APL originates from myeloid-committed progenitors, at least in mouse models[73]. Thus, long-term expansion of myeloid-committed progenitors in an APL-prone genetic context (provided by PML/RARα) may result in an expansion of the pool of potential APL-initiating cells (Figure 32B). Importantly, progenitor expansion per se seems not to be specific for PML/RARα, as we observed similar imbalances in WT HFD-fed mice. However, only PML/RARα progenitors derived from HFD or in the presence of linoleic acid were able to maintain colony forming activity over several passages. Thus, the transition from stem cell to progenitor in the obese or obese-mimicking environment is not accompanied by loss of self-renewal in the PML/RARα context.

The molecular cause of progenitor expansion, and whether it is sufficient to explain increased leukemogenesis is not entirely certain. Indeed, prior data from our group[131] showed that radiation-induced DNA damage induces cell cycle entry of quiescent stem cells. One would imagine that DNA damage caused by the HFD metabolites is less severe, albeit chronic, compared to irradiation. Whether such levels of DNA damage can influence cell cycle entry has not been hitherto studied. However, our data suggest that this is not the case, since treating HFD-fed mice with antioxidants (NAC) abolished DNA damage but not progenitor expansion (Figure 33C). Furthermore, HFD-treated BM was more efficient at reconstituting secondary recipients, unlike irradiated BM[152]. In fact, our data show that self-renewal is enhanced by ROS decrease (as in NAC-treated mice).

The fact that linoleic acid, a single component of HFD, can induce enhanced self-renewal *in vitro* similarly to HFD itself suggests a more reductionist model in which linoleic acid itself,

and possibly other polyunsaturated FA, can directly modulate self-renewal in the presence of PML/RARα.

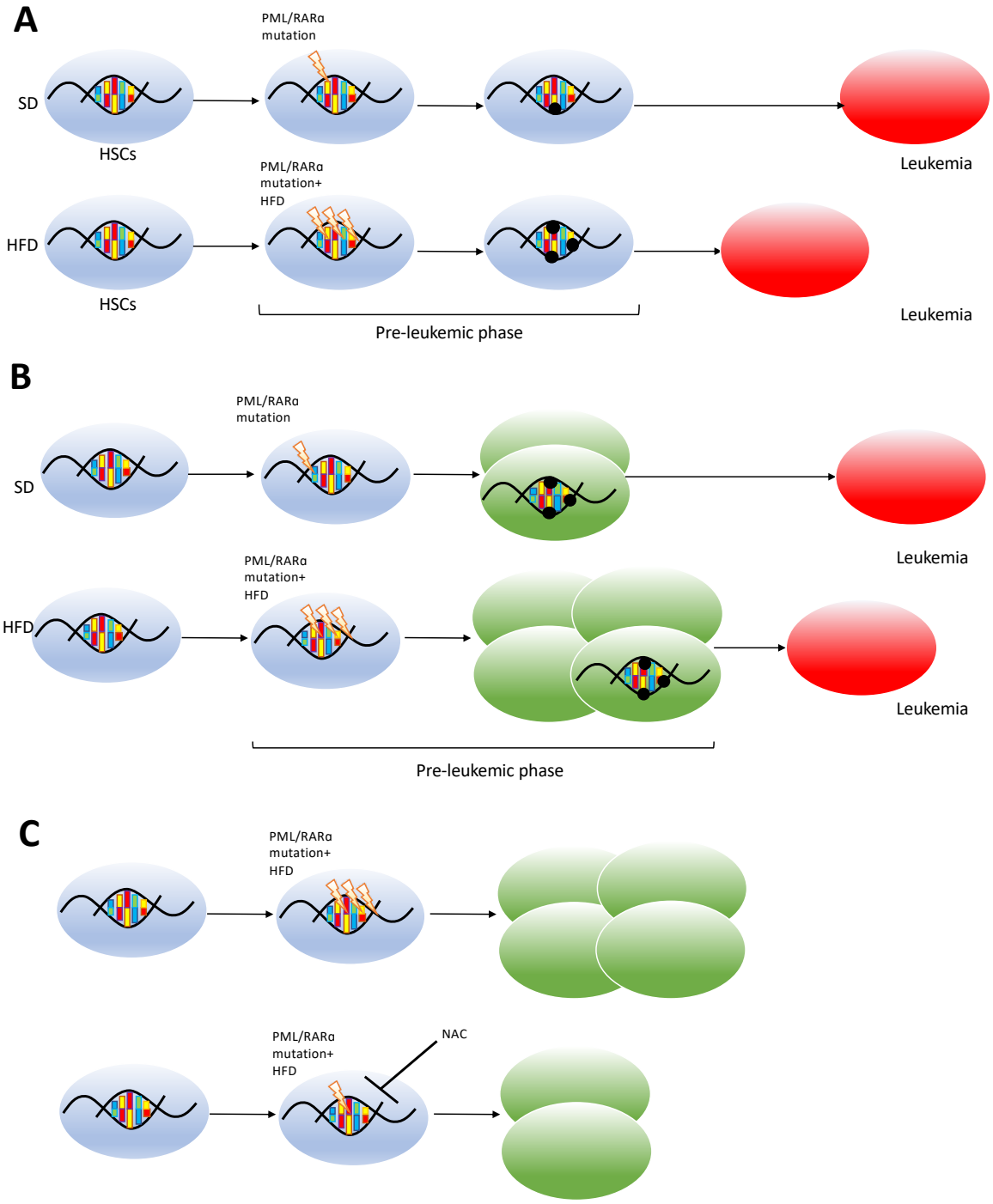

Figure 32. Molecular models to explain how obesity accelerates APL. A) First model in which HFD works as carcinogen is represented. DNA damage in SD is mediated only by the presence of PML/RARα oncogene, while in HFD-fed mice it originates from a combination of HFD-deriving metabolites and the oncogene. DNA damage is then translated into mutations, and this explains leukemia anticipation; B) Second model in which HFD increases self-renewal. In this second model DNA damage increases the self-renewal ability, increasing in HFD the pool of cells which potentially could have the second hit and give rise to leukemia; C) Third model in which it is shown that self-renewal can be blocked decreasing DNA damage.

Our data are in agreement with the work of Beyaz and colleagues that have shown that HFD increases the stemness potential of intestinal stem cells and highlighted the role played by PPARδ[98]. Current study extends their work to hematopoiesis, a different hierarchical system, and identifies linoleic acid as a suitable mediator for the effect of HFD. Although the molecular mechanism of this effect remains still poorly understood, we provide evidence for the involvement of the lipoxygenase pathway and PPARδ. PPARδ is known to functionally interact with PML to regulate FAO and HSC fate. Whether PPARδ also interacts functionally with PML/RARα, and what is the molecular basis of such an interaction, constitute as yet unexplored questions onto which this work has started to shed some light. LA-derived metabolites (which require lipoxygenase activity[164]) can act as PPAR activators, although most evidence has been gathered for the structurally related PPARγ.

The presence of PML/RARα imposes a differentiation block at the promyelocyte stage through transcriptional deregulation mediated by interaction of PML/RARα with epigenetic modifiers and transcription factors. Importantly, RARα, PML/RARα and PPAR factors all require interaction with RXR for their transcriptional activity, so that RXR-mediated molecular interactions may be the key to the mechanism under investigation. Based on our data, we can speculate that upon interaction with LA-derived PPARδ activators, PML/RARα-imposed differentiation block becomes more effective, to a degree able to trigger the leukemic phenotype. Key to this mechanism may be the interaction with different chromatin modifiers of PML/RARα and PPARδ. Future experiments should aim at characterizing diet-associated differences in epigenetic features and PML/RARα and PPARδ interaction complexes. These experiments may reveal novel strategies for therapeutic targeting.

An important consequence of this model is that the interaction between HFD and PML/RARα may be reversible, so that dietary modifications aimed at reducing polyunsaturated fat levels may have a therapeutic or preventive effect. We have extensively

explored these hypotheses in a parallel work, not shown here, in which we show that caloric restriction in mice, i.e. polyunsaturated FA intake limitation, does, in fact, lead to a delayed leukemia onset and prolonged survival when used therapeutically.

References

1. Ogden, C. L., Carroll, M. D., Kit, B. K. & Flegal, K. M. Prevalence of childhood and adult obesity in the United States, 2011-2012. *Jama* **311,** 806–814 (2014).
2. Finkelstein, E. A. *et al.* Obesity and severe obesity forecasts through 2030. *Am. J. Prev. Med.* **42,** 563–570 (2012).
3. Bray, G. A. Classification and evaluation of the obesities. *Med. Clin. North Am.* **73,** 161–184 (1989).
4. Cameron, A. J. *et al.* Overweight and obesity in Australia: the 1999-2000 Australian diabetes, obesity and lifestyle study (AusDiab). *Med. J. Aust.* **178,** 427–432 (2003).
5. Swinburn, B., Sacks, G. & Ravussin, E. Increased food energy supply is more than sufficient to explain the US epidemic of obesity. *Am. J. Clin. Nutr.* **90,** 1453–1456 (2009).
6. Coady, S. A. *et al.* Genetic variability of adult body mass index: a longitudinal assessment in Framingham families. *Obesity* **10,** 675–681 (2002).
7. Calle, E. E. & Thun, M. J. Obesity and cancer. *Oncogene* **23,** 6365 (2004).
8. Porte, D., Baskin, D. G. & Schwartz, M. W. Insulin signaling in the central nervous system: a critical role in metabolic homeostasis and disease from C. elegans to humans. *Diabetes* **54,** 1264–1276 (2005).
9. Lovren, F., Teoh, H. & Verma, S. Obesity and atherosclerosis: mechanistic insights. *Can. J. Cardiol.* **31,** 177–183 (2015).
10. Waxler, S. H., Tabar, P. & Melcher, L. R. Obesity and the time of appearance of spontaneous mammary carcinoma in C3H mice. *Cancer Res.* **13,** 276–278 (1953).
11. De Waard, F., Halewijn, E. A. B. & Huizinga, J. The bimodal age distribution of patients with mammary carcinoma. Evidence for the existence of 2 types of human breast cancer. *Cancer* **17,** 141–151 (1964).
12. Renehan, A. G., Tyson, M., Egger, M., Heller, R. F. & Zwahlen, M. Body-mass index and incidence of cancer: a systematic review and meta-analysis of prospective

observational studies. *Lancet* **371,** 569–578 (2008).

13. Bhaskaran, K., Forbes, H. J., Douglas, I., Leon, D. A. & Smeeth, L. Representativeness and optimal use of body mass index (BMI) in the UK Clinical Practice Research Datalink (CPRD). *BMJ Open* **3,** e003389 (2013).
14. Breccia, M. *et al.* Increased BMI correlates with higher risk of disease relapse and differentiation syndrome in patients with acute promyelocytic leukemia treated with the AIDA protocols. *Blood* **119,** 49–54 (2012).
15. Soliman, P. T. *et al.* Association between adiponectin, insulin resistance, and endometrial cancer. *Cancer* **106,** 2376–2381 (2006).
16. Dalamaga, M., Diakopoulos, K. N. & Mantzoros, C. S. The role of adiponectin in cancer: a review of current evidence. *Endocr. Rev.* **33,** 547–594 (2012).
17. Miyoshi, Y. *et al.* Association of serum adiponectin levels with breast cancer risk. *Clin. cancer Res.* **9,** 5699–5704 (2003).
18. Goktas, S. *et al.* Prostate cancer and adiponectin. *Urology* **65,** 1168–1172 (2005).
19. Gao, Q., Zheng, J., Yao, X. & Peng, B. Adiponectin inhibits VEGF-A in prostate cancer cells. *Tumor Biol.* **36,** 4287–4292 (2015).
20. Sugiyama, M. *et al.* Adiponectin inhibits colorectal cancer cell growth through the AMPK/mTOR pathway. *Int. J. Oncol.* **34,** 339–344 (2009).
21. Chung, T. D. *et al.* Tumor necrosis factor-alpha-based gene therapy enhances radiation cytotoxicity in human prostate cancer. *Cancer Gene Ther.* **5,** 344–349 (1998).
22. Sethi, G., Sung, B. & Aggarwal, B. B. TNF: a master switch for inflammation to cancer. *Front Biosci* **13,** 5094–5107 (2008).
23. Bruun, J. M., Roeske-Nielsen, A., Richelsen, B., Fredman, P. & Buschard, K. Sulfatide increases adiponectin and decreases TNF-α, IL-6, and IL-8 in human adipose tissue in vitro. *Mol. Cell. Endocrinol.* **263,** 142–148 (2007).
24. Rubio, M. F. *et al.* TNF-α enhances estrogen-induced cell proliferation of estrogen-dependent breast tumor cells through a complex containing nuclear factor-kappa B.

Oncogene **25,** 1367 (2006).

25. Lichtman, M. A. Obesity and the risk for a hematological malignancy: leukemia, lymphoma, or myeloma. *Oncologist* **15,** 1083–1101 (2010).
26. Samanic, C. *et al.* Obesity and cancer risk among white and black United States veterans. *Cancer Causes Control* **15,** 35–44 (2004).
27. Larsson, S. C. & Wolk, A. Overweight and obesity and incidence of leukemia: A meta-analysis of cohort studies. *Int. J. cancer* **122,** 1418–1421 (2008).
28. Poynter, J. N. *et al.* Obesity over the life course and risk of acute myeloid leukemia and myelodysplastic syndromes. *Cancer Epidemiol.* **40,** 134–140 (2016).
29. Castillo, J. J. *et al.* Obesity but not overweight increases the incidence and mortality of leukemia in adults: a meta-analysis of prospective cohort studies. *Leuk. Res.* **36,** 868–875 (2012).
30. Yamamoto, J. F. & Goodman, M. T. Patterns of leukemia incidence in the United States by subtype and demographic characteristics, 1997–2002. *Cancer Causes Control* **19,** 379–390 (2008).
31. Bennett, J. M. *et al.* Proposals for the classification of the acute leukaemias French-American-British (FAB) Co-operative Group. *Br. J. Haematol.* **33,** 451–458 (1976).
32. Vardiman, J. W. *et al.* The 2008 revision of the World Health Organization (WHO) classification of myeloid neoplasms and acute leukemia: rationale and important changes. *Blood* **114,** 937–951 (2009).
33. Arber, D. A. *et al.* The 2016 revision to the World Health Organization (WHO) classification of myeloid neoplasms and acute leukemia. *Blood* blood-2016 (2016).
34. Network, C. G. A. R. Genomic and epigenomic landscapes of adult de novo acute myeloid leukemia. *N. Engl. J. Med.* **368,** 2059–2074 (2013).
35. DETHE, H., Lavau, C. & Marchio, A. The PML/RARa fusion mRNA generated by the t (15, 17) translocation encodes a functionally altered retinoic acid receptor. *Cell* **66,** 675–684 (1991).
36. Kakizuka, A. *et al.* Chromosomal translocation t (15; 17) in human acute

promyelocytic leukemia fuses RARα with a novel putative transcription factor, PML. *Cell* **66,** 663–674 (1991).

37. Wang, Z.-Y. & Chen, Z. Acute promyelocytic leukemia: from highly fatal to highly curable. *Blood* **111,** 2505–2515 (2008).

38. Castaigne, S. *et al.* All-trans retinoic acid as a differentiation therapy for acute promyelocytic leukemia. I. Clinical results [see comments]. *Blood* **76,** 1704–1709 (1990).

39. Niu, C. *et al.* Studies on treatment of acute promyelocytic leukemia with arsenic trioxide: remission induction, follow-up, and molecular monitoring in 11 newly diagnosed and 47 relapsed acute promyelocytic leukemia patients. *Blood* **94,** 3315–3324 (1999).

40. Giannì, M. *et al.* Combined arsenic and retinoic acid treatment enhances differentiation and apoptosis in arsenic-resistant NB4 cells. *Blood* **91,** 4300–4310 (1998).

41. Coombs, C. C., Tavakkoli, M. & Tallman, M. S. Acute promyelocytic leukemia: where did we start, where are we now, and the future. *Blood Cancer J.* **5,** e304 (2015).

42. Estey, E. *et al.* Association between increased body mass index and a diagnosis of acute promyelocytic leukemia in patients with acute myeloid leukemia. *Leuk.* **11,** (1997).

43. Wong, O., Harris, F., Armstrong, T. W. & Hua, F. A hospital-based case-control study of acute myeloid leukemia in Shanghai: analysis of environmental and occupational risk factors by subtypes of the WHO classification. *Chem. Biol. Interact.* **184,** 112–128 (2010).

44. Tedesco, J., Qualtieri, J., Head, D., Savani, B. N. & Reddy, N. High prevalence of obesity in acute promyelocytic leukemia (APL): implications for differentiating agents in APL and metabolic syndrome. *Ther. Adv. Hematol.* **2,** 141–145 (2011).

45. Castillo, J. J. *et al.* Relationship between obesity and clinical outcome in adults with

acute myeloid leukemia: A pooled analysis from four CALGB (alliance) clinical trials. *Am. J. Hematol.* **91,** 199–204 (2016).

46. Reymond, A. *et al.* The tripartite motif family identifies cell compartments. *EMBO J.* **20,** 2140–2151 (2001).

47. Pearson, M. & Pelicci, P. G. PML interaction with p53 and its role in apoptosis and replicative senescence. *Oncogene* **20,** 7250 (2001).

48. Mazza, M. & Pelicci, P. G. Is PML a tumor suppressor? *Front. Oncol.* **3,** 174 (2013).

49. Jensen, K., Shiels, C. & Freemont, P. S. PML protein isoforms and the RBCC/TRIM motif. *Oncogene* **20,** 7223 (2001).

50. Nisole, S., Maroui, M. A., Mascle, X., Aubry, M. & Chelbi-Alix, M. K. Differential roles of PML isoforms. *Front. Oncol.* **3,** 125 (2013).

51. Alcalay, M. *et al.* The promyelocytic leukemia gene product (PML) forms stable complexes with the retinoblastoma protein. *Mol. Cell. Biol.* **18,** 1084–1093 (1998).

52. Lin, H.-K., Bergmann, S. & Pandolfi, P. P. Cytoplasmic PML function in TGF-β signalling. *Nature* **431,** 205 (2004).

53. Bernardi, R. & Pandolfi, P. P. Structure, dynamics and functions of promyelocytic leukaemia nuclear bodies. *Nat. Rev. Mol. cell Biol.* **8,** 1006 (2007).

54. Rego, E. M. *et al.* Role of promyelocytic leukemia (PML) protein in tumor suppression. *J. Exp. Med.* **193,** 521–530 (2001).

55. Wang, Z.-G. *et al.* PML is essential for multiple apoptotic pathways. *Nat. Genet.* **20,** 266 (1998).

56. Purton, L. E. *et al.* RARγ is critical for maintaining a balance between hematopoietic stem cell self-renewal and differentiation. *J. Exp. Med.* **203,** 1283–1293 (2006).

57. Labrecque, J. *et al.* Impaired granulocytic differentiation in vitro in hematopoietic cells lacking retinoic acid receptors α1 and γ. *Blood* **92,** 607–615 (1998).

58. del Mar Vivanco-Ruiz, M., Tiollais, P., Stunnenberg, H. & Dejean, A. Identification

of a retinoic acid responsive element in the retinoic acid receptor & beta; gene. *Nature* **343,** 177 (1990).

59. Drumea, K., Yang, Z. & Rosmarin, A. Retinoic acid signaling in myelopoiesis. *Curr. Opin. Hematol.* **15,** 37–41 (2008).

60. Cairns, B. R. Emerging roles for chromatin remodeling in cancer biology. *Trends Cell Biol.* **11,** S15–S21 (2001).

61. Minucci, S. *et al.* Oligomerization of RAR and AML1 transcription factors as a novel mechanism of oncogenic activation. *Mol. Cell* **5,** 811–820 (2000).

62. Zhou, J., Pérès, L., Honoré, N., Nasr, R. & Zhu, J. Dimerization-induced corepressor binding and relaxed DNA-binding specificity are critical for PML/RARA-induced immortalization. *Proc. Natl. Acad. Sci.* **103,** 9238–9243 (2006).

63. Perrotta, S. *et al.* Vitamin A and infancy. Biochemical, functional, and clinical aspects. *Vitam. Horm.* **66,** 457–591 (2003).

64. Perez, A. *et al.* PMLRAR homodimers: distinct DNA binding properties and heteromeric interactions with RXR. *EMBO J.* **12,** 3171–3182 (1993).

65. Jansen, J. H. *et al.* Multimeric complexes of the PML-retinoic acid receptor alpha fusion protein in acute promyelocytic leukemia cells and interference with retinoid and peroxisome-proliferator signaling pathways. *Proc. Natl. Acad. Sci.* **92,** 7401–7405 (1995).

66. Kamashev, D. & Vitoux, D. PML–RARA-RXR oligomers mediate retinoid and rexinoid/cAMP cross-talk in acute promyelocytic leukemia cell differentiation. *J. Exp. Med.* **199,** 1163–1174 (2004).

67. Gruszka, A. M. & Alcalay, M. PML/RARα Fusion Gene and Response to Retinoic Acid and Arsenic Trioxide Treatment. in *Handbook of Therapeutic Biomarkers in Cancer* (Pan Stanford Publishing Pte. Ltd., 2013).

68. Grignani, F. *et al.* The acute promyelocytic leukemia-specific PML-RARα fusion protein inhibits differentiation and promotes survival of myeloid precursor cells.

Cell **74,** 423–431 (1993).

69. Early, E. *et al.* Transgenic expression of PML/RARalpha impairs myelopoiesis. *Proc. Natl. Acad. Sci.* **93,** 7900–7904 (1996).

70. Altabef, M. *et al.* A retrovirus carrying the promyelocyte-retinoic acid receptor PML-RARalpha fusion gene transforms haematopoietic progenitors in vitro and induces acute leukaemias. *EMBO J.* **15,** 2707–2716 (1996).

71. Wartman, L. D. *et al.* Expression and function of PML-RARA in the hematopoietic progenitor cells of Ctsg-PML-RARA mice. *PLoS One* **7,** e46529 (2012).

72. Grisolano, J. L., Wesselschmidt, R. L., Pelicci, P. G. & Ley, T. J. Altered myeloid development and acute leukemia in transgenic mice expressing PML-RARα under control of cathepsin G regulatory sequences. *Blood* **89,** 376–387 (1997).

73. Westervelt, P. *et al.* High-penetrance mouse model of acute promyelocytic leukemia with very low levels of PML-RARα expression. *Blood* **102,** 1857–1865 (2003).

74. Kelly, L. M. *et al.* PML/RARα and FLT3-ITD induce an APL-like disease in a mouse model. *Proc. Natl. Acad. Sci.* **99,** 8283–8288 (2002).

75. Chan, I. T. *et al.* Oncogenic K-ras cooperates with PML-RARα to induce an acute promyelocytic leukemia-like disease. *Blood* **108,** 1708–1715 (2006).

76. Wartman, L. D. *et al.* Sequencing a mouse acute promyelocytic leukemia genome reveals genetic events relevant for disease progression. *J. Clin. Invest.* **121,** 1445–1455 (2011).

77. Riva, L. *et al.* Acute promyelocytic leukemias share cooperative mutations with other myeloid-leukemia subgroups. *Blood Cancer J.* **3,** e147 (2013).

78. Tabe, Y. *et al.* PML-RARα is associated with leptin-receptor induction: the role of mesenchymal stem cell–derived adipocytes in APL cell survival. *Blood* **103,** 1815–1822 (2004).

79. Shaz, B. H. & Hillyer, C. D. *Transfusion medicine and hemostasis: clinical and laboratory aspects*. (Newnes, 2013).

80. Lorenz, E., Uphoff, D., Reid, T. R. & Shelton, E. Modification of irradiation injury

in mice and guinea pigs by bone marrow injections. *J. Natl. Cancer Inst.* **12,** 197–201 (1951).

81. Oguro, H., Ding, L. & Morrison, S. J. SLAM family markers resolve functionally distinct subpopulations of hematopoietic stem cells and multipotent progenitors. *Cell Stem Cell* **13,** 102–116 (2013).

82. Santoro, A., Vlachou, T., Carminati, M., Pelicci, P. G. & Mapelli, M. Molecular mechanisms of asymmetric divisions in mammary stem cells. *EMBO Rep.* **17,** 1700–1720 (2016).

83. Cabezas-Wallscheid, N. *et al.* Vitamin A-retinoic acid signaling regulates hematopoietic stem cell dormancy. *Cell* **169,** 807–823 (2017).

84. Benveniste, P. *et al.* Intermediate-term hematopoietic stem cells with extended but time-limited reconstitution potential. *Cell Stem Cell* **6,** 48–58 (2010).

85. Brown, G., Hughes, P. J., Michell, R. H., Rolink, A. G. & Ceredig, R. The sequential determination model of hematopoiesis. *Trends Immunol.* **28,** 442–448 (2007).

86. Brown, G., Bunce, C. M. & Guy, G. R. Sequential determination of lineage potentials during haemopoiesis. *Br. J. Cancer* **52,** 681 (1985).

87. Brown, G., Bunce, C. M., Lord, J. M. & McConnell, F. M. The development of cell lineages: a sequential model. *Differentiation* **39,** 83–89 (1988).

88. Brown, G., Hughes, P. J., Michell, R. H., Rolink, A. G. & Ceredig, R. The sequential determination model of hematopoiesis. *Trends Immunol.* **28,** 442–448 (2007).

89. Sun, J. *et al.* Clonal dynamics of native haematopoiesis. *Nature* **514,** 322 (2014).

90. Rodriguez-Fraticelli, A. E. *et al.* Clonal analysis of lineage fate in native haematopoiesis. *Nature* **553,** 212 (2018).

91. Laurenti, E. & Göttgens, B. From haematopoietic stem cells to complex differentiation landscapes. *Nature* **553,** 418 (2018).

92. Morrison, S. J. & Weissman, I. L. The long-term repopulating subset of

hematopoietic stem cells is deterministic and isolatable by phenotype. *Immunity* **1,** 661–673 (1994).

93. Kiel, M. J. *et al.* SLAM family receptors distinguish hematopoietic stem and progenitor cells and reveal endothelial niches for stem cells. *Cell* **121,** 1109–1121 (2005).

94. Larochelle, A. *et al.* Human and rhesus macaque hematopoietic stem cells cannot be purified based only upon SLAM family markers. *Blood* blood-2009 (2010).

95. Sidney, L. E., Branch, M. J., Dunphy, S. E., Dua, H. S. & Hopkinson, A. Concise review: evidence for CD34 as a common marker for diverse progenitors. *Stem Cells* **32,** 1380–1389 (2014).

96. Murray, L. *et al.* Enrichment of human hematopoietic stem cell activity in the CD34+ Thy-1+ Lin-subpopulation from mobilized peripheral blood. *Blood* **85,** 368–378 (1995).

97. Ito, K. *et al.* A PML-PPAR-[delta] pathway for fatty acid oxidation regulates hematopoietic stem cell maintenance. *Nat. Med.* **18,** 1350–1358 (2012).

98. Beyaz, S. *et al.* High fat diet enhances stemness and tumorigenicity of intestinal progenitors. *Nature* **531,** 53 (2016).

99. Ito, K. & Suda, T. Metabolic requirements for the maintenance of self-renewing stem cells. *Nat. Rev. Mol. cell Biol.* **15,** 243–256 (2014).

100. Simsek, T. *et al.* The distinct metabolic profile of hematopoietic stem cells reflects their location in a hypoxic niche. *Cell Stem Cell* **7,** 380–390 (2010).

101. Takubo, K. *et al.* Regulation of glycolysis by Pdk functions as a metabolic checkpoint for cell cycle quiescence in hematopoietic stem cells. *Cell Stem Cell* **12,** 49–61 (2013).

102. Wu, P. Regulation of the activity of the pyruvate dehydrogenase complex. *Adv. Enzyme Regul.* **42,** 249 (2002).

103. Takubo, K. *et al.* Regulation of the HIF-1α level is essential for hematopoietic stem cells. *Cell Stem Cell* **7,** 391–402 (2010).

104. Inoue, S.-I. *et al.* Mitochondrial respiration defects modulate differentiation but not proliferation of hematopoietic stem and progenitor cells. *FEBS Lett.* **584,** 3402–3409 (2010).

105. Norddahl, G. L. *et al.* Accumulating mitochondrial DNA mutations drive premature hematopoietic aging phenotypes distinct from physiological stem cell aging. *Cell Stem Cell* **8,** 499–510 (2011).

106. Yu, W.-M. *et al.* Metabolic regulation by the mitochondrial phosphatase PTPMT1 is required for hematopoietic stem cell differentiation. *Cell Stem Cell* **12,** 62–74 (2013).

107. Kang, J. X. The omega-6/omega-3 fatty acid ratio in chronic diseases: animal models and molecular aspects. in *Healthy Agriculture, Healthy Nutrition, Healthy People* **102,** 22–29 (Karger Publishers, 2011).

108. Knobloch, M. *et al.* A fatty acid oxidation-dependent metabolic shift regulates adult neural stem cell activity. *Cell Rep.* **20,** 2144–2155 (2017).

109. Mihaylova, M. M. *et al.* Fasting activates fatty acid oxidation to enhance intestinal stem cell function during homeostasis and aging. *Cell Stem Cell* **22,** 769–778 (2018).

110. Ito, K. *et al.* Self-renewal of a purified Tie2+ hematopoietic stem cell population relies on mitochondrial clearance. *Science (80-.).* **354,** 1156–1160 (2016).

111. Porter, R. L. *et al.* Prostaglandin E2 increases hematopoietic stem cell survival and accelerates hematopoietic recovery after radiation injury. *Stem Cells* **31,** 372–383 (2013).

112. Yun, S. P., Lee, M. Y., Ryu, J. M. & Han, H. J. Interaction between PGE2 and EGF receptor through MAPKs in mouse embryonic stem cell proliferation. *Cell. Mol. life Sci.* **66,** 1603–1616 (2009).

113. Medes, G., Thomas, A. & Weinhouse, S. Metabolism of neoplastic tissue. IV. A study of lipid synthesis in neoplastic tissue slices in vitro. *Cancer Res.* **13,** 27–29 (1953).

114. Tirinato, L. *et al.* Lipid droplets: a new player in colorectal cancer stem cells unveiled by spectroscopic imaging. *Stem Cells* **33,** 35–44 (2015).

115. Tirinato, L. *et al.* An overview of lipid droplets in cancer and cancer stem cells. *Stem Cells Int.* **2017,** (2017).

116. Kuhajda, F. P. *et al.* Fatty acid synthesis: a potential selective target for antineoplastic therapy. *Proc. Natl. Acad. Sci.* **91,** 6379–6383 (1994).

117. Swinnen, J. V *et al.* Selective activation of the fatty acid synthesis pathway in human prostate cancer. *Int. J. cancer* **88,** 176–179 (2000).

118. Cai, Y. *et al.* Loss of chromosome 8p governs tumor progression and drug response by altering lipid metabolism. *Cancer Cell* **29,** 751–766 (2016).

119. Carracedo, A. *et al.* A metabolic prosurvival role for PML in breast cancer. *J. Clin. Invest.* **122,** 3088–3100 (2012).

120. Castellone, M. D., Teramoto, H., Williams, B. O., Druey, K. M. & Gutkind, J. S. Prostaglandin E2 promotes colon cancer cell growth through a Gs-axin-ß-catenin signaling axis. *Science (80-.).* **310,** 1504–1510 (2005).

121. di Fagagna, F. d'Adda. Living on a break: cellular senescence as a DNA-damage response. *Nat. Rev. Cancer* **8,** 512 (2008).

122. Takata, M. *et al.* Homologous recombination and non-homologous end-joining pathways of DNA double-strand break repair have overlapping roles in the maintenance of chromosomal integrity in vertebrate cells. *EMBO J.* **17,** 5497–5508 (1998).

123. Modrich, P. Mechanisms in eukaryotic mismatch repair. *J. Biol. Chem.* (2006).

124. Sinha, R. P. & Häder, D.-P. UV-induced DNA damage and repair: a review. *Photochem. Photobiol. Sci.* **1,** 225–236 (2002).

125. Maynard, S., Schurman, S. H., Harboe, C., de Souza-Pinto, N. C. & Bohr, V. A. Base excision repair of oxidative DNA damage and association with cancer and aging. *Carcinogenesis* **30,** 2–10 (2008).

126. Fortini, P. *et al.* 8-Oxoguanine DNA damage: at the crossroad of alternative repair

pathways. *Mutat. Res. Mol. Mech. Mutagen.* **531,** 127–139 (2003).

127. Yesilbursa, D. *et al.* Lipid peroxides in obese patients and effects of weight loss with orlistat on lipid peroxides levels. *Int. J. Obes.* **29,** 142 (2005).

128. Marnett, L. J. Lipid peroxidation—DNA damage by malondialdehyde. *Mutat. Res. Mol. Mech. Mutagen.* **424,** 83–95 (1999).

129. Mohrin, M. *et al.* Hematopoietic stem cell quiescence promotes error-prone DNA repair and mutagenesis. *Cell Stem Cell* **7,** 174–185 (2010).

130. Beerman, I., Seita, J., Inlay, M. A., Weissman, I. L. & Rossi, D. J. Quiescent hematopoietic stem cells accumulate DNA damage during aging that is repaired upon entry into cell cycle. *Cell Stem Cell* **15,** 37–50 (2014).

131. Insinga, A. *et al.* DNA damage in stem cells activates p21, inhibits p53, and induces symmetric self-renewing divisions. *Proc. Natl. Acad. Sci.* **110,** 3931–3936 (2013).

132. Rossi, D. J. *et al.* Deficiencies in DNA damage repair limit the function of haematopoietic stem cells with age. *Nature* **447,** 725 (2007).

133. Garaycoechea, J. I. *et al.* Genotoxic consequences of endogenous aldehydes on mouse haematopoietic stem cell function. *Nature* **489,** 571 (2012).

134. Garaycoechea, J. I. *et al.* Alcohol and endogenous aldehydes damage chromosomes and mutate stem cells. *Nature* **553,** 171 (2018).

135. Hayes, J. D. & Pulford, D. J. The glut athione S-transferase supergene family: regulation of GST and the contribution of the lsoenzymes to cancer chemoprotection and drug resistance part I. *Crit. Rev. Biochem. Mol. Biol.* **30,** 445–520 (1995).

136. Houglum, K., Filip, M., Witztum, J. L. & Chojkier, M. Malondialdehyde and 4-hydroxynonenal protein adducts in plasma and liver of rats with iron overload. *J. Clin. Invest.* **86,** 1991–1998 (1990).

137. Gasparovic, A. C., Milkovic, L., Sunjic, S. B. & Zarkovic, N. Cancer growth regulation by 4-hydroxynonenal. *Free Radic. Biol. Med.* **111,** 226–234 (2017).

138. Lander, H. M. *et al.* A molecular redox switch on p21ras structural basis for the nitric oxide-p21ras interaction. *J. Biol. Chem.* **272,** 4323–4326 (1997).

139. Chan, D. W. *et al.* Loss of MKP3 mediated by oxidative stress enhances tumorigenicity and chemoresistance of ovarian cancer cells. *Carcinogenesis* **29,** 1742–1750 (2008).

140. Zhou, J., Chen, Y., Lang, J.-Y., Lu, J.-J. & Ding, J. Salvicine inactivates β1 integrin and inhibits adhesion of MDA-MB-435 cells to fibronectin via reactive oxygen species signaling. *Mol. Cancer Res.* **6,** 194–204 (2008).

141. Wauchope, O. R. *et al.* Nuclear oxidation of a major peroxidation DNA adduct, M1dG, in the genome. *Chem. Res. Toxicol.* **28,** 2334–2342 (2015).

142. Kozarewa, I. *et al.* Amplification-free Illumina sequencing-library preparation facilitates improved mapping and assembly of (G+C)-biased genomes. *Nat. Methods* **6,** 291–295 (2009).

143. Li, H. & Durbin, R. Fast and accurate short read alignment with Burrows–Wheeler transform. *bioinformatics* **25,** 1754–1760 (2009).

144. Behjati, S. *et al.* Genome sequencing of normal cells reveals developmental lineages and mutational processes. *Nature* **513,** 422 (2014).

145. Gerstung, M., Papaemmanuil, E. & Campbell, P. J. Subclonal variant calling with multiple samples and prior knowledge. *Bioinformatics* **30,** 1198–1204 (2014).

146. Eisinger, K. *et al.* Lipidomic analysis of serum from high fat diet induced obese mice. *Int. J. Mol. Sci.* **15,** 2991–3002 (2014).

147. Lu, P. *et al.* Mechanism-based inhibition of human liver microsomal cytochrome P450 1A2 by zileuton, a 5-lipoxygenase inhibitor. *Drug Metab. Dispos.* **31,** 1352–1360 (2003).

148. Shearer, B. G. *et al.* Identification and characterization of 4-Chloro-N-(2-{[5-trifluoromethyl)-2-pyridyl] sulfonyl} ethyl) benzamide (GSK3787), a selective and irreversible peroxisome proliferator-activated receptor δ (PPARδ) antagonist. *J. Med. Chem.* **53,** 1857–1861 (2010).

149. Maillet, A., Yadav, S., Loo, Y. L., Sachaphibulkij, K. & Pervaiz, S. A novel Osmium-based compound targets the mitochondria and triggers ROS-dependent

apoptosis in colon carcinoma. *Cell Death Dis.* **4,** e653 (2013).

150. Li, T., Zhou, Z.-W., Ju, Z. & Wang, Z.-Q. DNA damage response in hematopoietic stem cell ageing. *Genomics. Proteomics Bioinformatics* **14,** 147–154 (2016).

151. Del Rio, D., Stewart, A. J. & Pellegrini, N. A review of recent studies on malondialdehyde as toxic molecule and biological marker of oxidative stress. *Nutr. Metab. Cardiovasc. Dis.* **15,** 316–328 (2005).

152. Lee, J.-M. *et al.* Obesity alters the long-term fitness of the hematopoietic stem cell compartment through modulation of Gfi1 expression. *J. Exp. Med.* **215,** 627–644 (2018).

153. Chapman, A. R. *et al.* Single cell transcriptome amplification with MALBAC. *PLoS One* **10,** e0120889 (2015).

154. Stephens, P. J. *et al.* The landscape of cancer genes and mutational processes in breast cancer. *Nature* **486,** 400–404 (2012).

155. Gerstung, M., Papaemmanuil, E. & Campbell, P. J. Subclonal variant calling with multiple samples and prior knowledge. *Bioinformatics* **30,** 1198–204 (2014).

156. Ye, K., Schulz, M. H., Long, Q., Apweiler, R. & Ning, Z. Pindel: a pattern growth approach to detect break points of large deletions and medium sized insertions from paired-end short reads. *Bioinformatics* **25,** 2865–2871 (2009).

157. Welch, J. S., Yuan, W. & Ley, T. J. PML-RARA can increase hematopoietic self-renewal without causing a myeloproliferative disease in mice. *J. Clin. Invest.* **121,** 1636–1645 (2011).

158. Zhang, Y. *et al.* AML1-ETO mediates hematopoietic self-renewal and leukemogenesis through a COX/β-catenin signaling pathway. *Blood* blood-2012 (2013).

159. Samuelsson, B. Arachidonic acid metabolism: role in inflammation. *Z. Rheumatol.* **50,** 3–6 (1991).

160. Nascimento-Sales, M. *et al.* Is the FVB/N mouse strain truly resistant to diet-induced obesity? *Physiol. Rep.* **5,** (2017).

161. Olefsky, J. M. The insulin receptor: its role in insulin resistance of obesity and diabetes. *Diabetes* **25,** 1154–1161 (1976).

162. Rodgers, K. & McVey, M. Error-prone repair of DNA double-strand breaks. *J. Cell. Physiol.* **231,** 15–24 (2016).

163. Wojiski, S. *et al.* PML–RARα initiates leukemia by conferring properties of self-renewal to committed promyelocytic progenitors. *Leukemia* **23,** 1462 (2009).

164. Garssen, G. J., Vliegenthart, J. F. G. & Boldingh, J. An anaerobic reaction between lipoxygenase, linoleic acid and its hydroperoxides. *Biochem. J.* **122,** 327–332 (1971).

Appendix

Relevant pubblication

Tumour-derived PGD2 and NKp30-B7H6 engagement drives an immunosuppressive ILC2-MDSC axis.

Trabanelli S, Chevalier MF, Martinez-Usatorre A, Gomez-Cadena A, Salomé B, Lecciso M, Salvestrini V, Verdeil G, Racle J, Papayannidis C, Morita H, Pizzitola I, Grandclément C, Bohner P, Bruni E, Girotra M, Pallavi R, Falvo P, Leibundgut EO, Baerlocher GM, Carlo-Stella C, Taurino D, Santoro A, Spinelli O, Rambaldi A, Giarin E, Basso G, Tresoldi C, Ciceri F, Gfeller D, Akdis CA, Mazzarella L, Minucci S, Pelicci PG, Marcenaro E, McKenzie ANJ, Vanhecke D, Coukos G, Mavilio D, Curti A, Derré L, Jandus C.

Nat. Commun. 2017

Abstract

Group 2 innate lymphoid cells (ILC2s) are involved in human diseases, such as allergy, atopic dermatitis and nasal polyposis, but their function in human cancer remains unclear. Here we show that, in acute promyelocytic leukaemia (APL), ILC2s are increased and hyper-activated through the interaction of CRTH2 and NKp30 with elevated tumor-derived PGD2 and B7H6, respectively. ILC2s, in turn, activate monocytic myeloid-derived suppressor cells (M-MDSCs) via IL-13 secretion. Upon treating APL with all-trans retinoic acid and achieving complete remission, the levels of PGD2, NKp30, ILC2s, IL-13 and M-MDSCs are restored. Similarly, disruption of this tumor immunosuppressive axis by specifically blocking PGD2, IL-13 and NKp30 partially restores ILC2 and M-MDSC levels and results in

increased survival. Thus, using APL as a model, we uncover a tolerogenic pathway that may represent a relevant immunosuppressive, therapeutic targetable, mechanism operating in various human tumor types, as supported by our observations in prostate cancer.Group 2 innate lymphoid cells (ILC2s) modulate inflammatory and allergic responses, but their function in cancer immunity is still unclear. Here the authors show that, in acute promyelocytic leukaemia, tumor-activated ILC2s secrete IL-13 to induce myeloid-derived suppressor cells and support tumor growth.

Congress abstracts

1. Inhibition of the Histone Demethylase LSD1 Combined with Caloric Restriction or IGF1/Insulin Inhibition Leads to Durable Responses in a Preclinical Model of Acute Myeloid Leukemia

Luca Mazzarella, Tiphanie Durfort, Rani Pallavi, Elena Mylonas, Paolo Falvo, Anna Giulia Sanarico, Massimo Stendardo, Luciano Giaco', Anna Russo, Lucilla Luzi, Massimiliano Mazza, Giulia De Conti, Paola Vianello, Pier Luigi Rossi, Elena Ceccacci, Mohamed Elgendy, Marco Giorgio, Ciro Mercurio, Saverio Minucci and Pier Giuseppe Pelicci

American Society of Hematology (ASH) 5-7 December 2015, Orlando (FL)

Abstract

Introduction. There is increasing interest in therapeutic modulation of metabolic pathways in cancer. Tumor cells preferentially use aerobic glycolysis to meet their energetic demands. However, glycolysis inhibition alone is unable to bring durable responses because of limited therapeutic index and because of previously underappreciated metabolic adaptability in tumor cells, which can switch to alternative substrate usage when specific nutrients are limiting. The molecular basis of metabolic adaptation is poorly understood. Recently, the histone demethylase LSD1 (Lysine-Specific Demethylase 1) has been implicated in the control of oxidative phosphorylation (OXPHOS) in adipocytes through its interaction with NRF1 (Nuclear Respiratory Factor 1), a master regulator of metabolic gene transcription (1). We hypothesized that LSD1 could regulate metabolic adaptability and be a therapeutic target upon metabolic modulation through Caloric Restriction (CR) in Acute Myeloid Leukaemia (AML) and specifically in APL (Acute Promyelocytic Leukaemia), which we showed to be sensitive to body fatness in the clinic (2).

Methods. APLs were generated in mice expressing the PML-RARa fusion under the control of the Cathepsin G promoter (3). Primary leukemias were transplanted into recipients

subjected to 30% CR or Standard Diet (SD). We scored the effect of CR alone or in combination with the LSD1 inhibitor IEO368 (4) on mouse survival, Leukemia Initiating Cell (LIC) frequency and epigenomic, transcriptomic and metabolic parameters.

Results. Compared to SD controls, CR-fed recipients experienced an initial dramatic decrease in the total leukemic burden accompanied by cell cycle slowdown ("adaptation phase"); this was followed by a delayed disease progression that brought animals to death ("terminal phase") (median survival 91 vs 51 days, p=0.038). Limiting-dilution transplantation of CR-conditioned leukemias revealed increased frequency of LICs (estimated frequency 1/3064 cells in SD vs 1/947 in CR, p=0.003) and increased aggressiveness (median survival reduced to 49 vs 70.5 days with 5000 cells injected, p<0.0001). Thus, CR limits the expansion of leukemic cells but enriches for cells with increased ability to regrow.RNAseq of leukemic cells purified during the terminal phase (but not earlier) showed that a dramatic transcriptional reprogramming in CR, characterized by upregulation of genes controlling OXPHOS, Krebs cycle and nucleotide and protein biosynthesis, and downregulation of insulin signaling and glucose transporters. Flow cytometry with Mitotracker Red confirmed increased mitochondrial activity. Thus, leukemic cells exposed to CR put in place adaptive transcriptional changes to allow survival in a nutrient/growth factor deprived environment.To investigate the basis of these transcriptional changes, we revised ChIPseq analysis of LSD1 binding in human APL cell lines and found a significant enrichment for i) NRF1 consensus binding motif and ii) promoters of genes encoding for OXPHOS and Krebs cycle enzymes. NRF1 binding to OXPHOS/Krebs enzymes was confirmed on mouse leukemias by ChIPseq. These data suggested that the CR-induced adaptive changes could be mediated by LSD1/NRF1.Strikingly, co-treatment of leukemic mice with CR and our LSD1 inhibitor IEO368 (4) resulted in macroscopic and microscopic eradication of disease (see figure, p=0.0018 compared to SD). In these conditions, leukemic cells completely disappeared in 4/6 mice after 4 weeks. LSD1 inhibition alone was also effective but did not produce *bona fide* disease eradication.

Importantly, some of the features of the CR-LSD1 interaction could be modeled by combining LSD1 and an IGF1/Insulin inhibitor. *In vivo*, this combination was synergistic and led to durable responses (median survival 121 vs 50 days in untreated controls, p=0.0143, vs 65.5 and 78.5 days with Insulin/IGF1 Inhibitor and IEO368 respectively).

Conclusion: the combination of LSD1 inhibition and insulin/IGF1 signaling reduction by pharmacological or dietary intervention appears as a highly effective therapeutic strategy and deserves further investigation. Ongoing preclinical studies will verify its applicability to other models of AML.

References:

1. Duteil et al, Nat Commun. 2014 Jun 10;5:4093

2. Breccia et al, Blood. 2012 Jan 5;119(1):49-54

3. Westervelt et al, Blood. 2003 Sep 1;102(5):1857-65

4. Varasi et a,l Eur J Cancer Vol 50 supp 6: 185

2. Novel role of obesity in the development of acute promyelocitic leukaemia

Paolo Falvo, Luca Mazzarella, Anna G. Sanarico, Elena Gatti and Pier Giuseppe Pelicci

Enable Congress, Barcelona, oral presentation. 15-17 November 2017

Abstract

Obesity is defined as a pathological state characterized by an augmented presence of fat mass in the body. It is widely known that obesity increases the risk of many cancer types.[1] Clinical data have shown that obesity is strongly correlated with acute promyelocytic leukaemia (APL). These leukaemias carry a reciprocal translocation between the retinoic acid receptor α (RARα) and PML genes, giving rise to the formation of a fusion protein PML/RARα. However, the molecular mechanisms underlying the effects of obesity on APL development are not elucidated.

To recapitulate clinical observations, we aimed at developing and characterizing a mouse model of diet-induced obesity. We used transgenic mice expressing constitutively PML/RARα in hematopoietic system (PML/RARα KI mice) and wild type mice as control.[2] Mice were treated with two different diets: standard diet (SD) and high fat diet (HFD) (60% vs 10% of fats in the chow), and leukaemia free survival was monitored. Interestingly, we observed that PML/RARα KI treated with HFD developed leukaemia earlier (median survival 204 vs 254 days, $p<0.001$) and with higher penetrance (100% vs 70%), as compared to the same mice treated with SD.

We also evaluated the extent of DNA damage in hematopoietic stem cells (HSC) after four months of diet, using the comet assay. Along with a shorter survival time, we also demonstrated that HFD PML/RARα KI mice present 40% increase of DNA damage in HSC as compared to SD PML/RARα mice ($p<0.001$). Finally, we scored whether the diet confers proliferative advantage to PML/RARα bone marrow using colony forming cell assay. We

observed that HFD PML/RARα bone marrow has a stronger clonogenic activity as compared to SD PML/RARα bone marrow (mean 269 ± 61 in SD and 1170 ± 482 in HFD) ($p<0.01$).

Our data suggest that HFD has a double role in PML/RARα KI mice: it increases the penetrance and decreases the latency. Moreover, we demonstrated that the diet increases the amount of DNA damage in HSC of PML/RARα mice and also the clonogenic capacity of PML/RARα bone marrow.

[1] Bhaskaran K, Douglas I, Forbes H, dos-Santos-Silva I, Leon DA, Smeeth L. *Lancet*. (2014); 755-65

[2] Grisolano JL, Wesselschmidt RL, Pelicci PG, Ley TJ. *Blood*. (1997); 376-87

3. Obesity favours leukemogenesis through enhanced preleukemic stem cell self-renewal via polyunsaturated fatty acid-dependent ER stress relief

Luca Mazzarella, Paolo Falvo, Annagiulia Sanarico, Elena Gatti and Piergiuseppe Pelicci

American Association for Cancer Research (AACR) Annual Meeting, 14-18 April 2018 Chicago

Abstract

Obesity increases risk for multiple tumors, but impact on leukemia and its underlying molecular mechanism are poorly understood. Studies from our group and others showed that risk and outcome of Acute Promyelocytic Leukemia (APL) are more strongly associated with obesity than other hematological neoplasms. Intriguingly, in 2 independent cohorts (Italian and TCGA), obesity was associated with ~4 fold higher incidence of internal tandem duplications of the leukemogenic kinase FLT3 (FLT3-ITD), the first example of obesity-associated genetic alterations in cancer (unpublished). Here we propose a molecular mechanisms underlying obesity-associated leukemogenesis through our studies in murine models. Exposure to High fat Diet (HFD), an established model of obesity-related pathology, strongly accelerated disease onset and mortality in 3 murine models of hematological cancer: PML-RARa knockin (PRKI), developing an APL-mimicking disease; FLT3ITD knockin (FIKI) developing myeloproliferation; a new double PRKI-FIKI knockin mouse, developing APL-like disease but, surprisingly, with delayed latency compared to PRKI, presumably due to the known exhaustion of hematopoietic stem cells (HSC) associated with FLT3ITD. Preleukemic HSCs from HFD PRKI mice showed increased DNA damage in Comet assays, but surprisingly this was not associated with increased mutational load as revealed by a novel whole genome sequencing-based method. Instead, HSCs derived from HFD PRKI mice showed enhanced self-renewal in in vitro replating assays. Similarly, in the FIKI model we observed enhanced engraftment in serial competitive transplantation experiments in HFD-fed recipients. Delving more deeply in the molecular mechanisms, through bioinformatic

analysis of RNAseq data from the TCGA we found upregulation of the linoleic acid (LA) pathway in obese APL patients. LA is the richest fatty acid in HFD and in many western diets, thus a likely candidate for mediating HFD activity. LA significantly enhanced PRKI serial replating efficiency; this was abolished by pharmacologically blocking LA metabolism through a 5-lipoxygenase inhibitor or its transcriptional effects through a PPARd inhibitor. In the FIKI model and in a FLT3ITD-inducible cell line, we revealed a previously unappreciated induction of ER stress by FLT3ITD, likely to underlie FLT3ITD-induced HSC exhaustion. HFD (*in vivo*) and LA (*in vitro*) relieved FLT3ITD-induced ER stress, as revealed by the attenuation of markers of adaptive response to ER stress (Unfolded Protein Response and RNA IRE1-dependent RNA decay). In conclusion, our study suggests a novel and somewhat counterinuitive model for obesity-associated cancerogenesis: rather than inducing cellular stress, HFD-induced obesity enhances the self-renewal of preleukemic stem cells through LA-mediated alleviation of oncogene-induced proteotoxic stress

Acknowledgments

I would like to thank my PhD supervisors Professor Pier Giuseppe Pelicci and Luca Mazzarella for their supervisions, their passion in work. I am very grateful for all they taught me, and currently are teaching me. I would like to thank Gioacchino Natoli, and Oscar Fernandèz-Capetillo for being my internal and extern-PhD advisors. During these years, they have given me great suggestions and they have been always avaible for scientific discussion.

I would like to thank our collaborators for their precious work, in particular Marco Peluso for M1dG analysis and Mike Stratton, Sophie Roerink for WGS.

I would like to thank all facilities at IFOM-IEO Campus, which are always helpful and always collaborating, in particular cell tissue staff (Pinuccia, Cristina, Manuela and Donatella), imaging staff (Simona, Mariagrazia) and mouse staff.

I would like to thanks Myriam Alcalay and her group, in particular Debora and Aljcia, for collaborating with me in the last 2 years. If this collaboration has nicely worked, it was only for you! Then I would like to thank Stefania Orecchioni, for her friendship which means so much for me!

Finally, I would like to thank my colleagues from Pier Giuseppe's group for every day collaboration (Elena, Anna Giulia, Errico, Barbara, Giulia) and for all the funny moments during these years.

I would like to thank also my high school Biology professor Maria Carmela Costabile, for having made me love science with her passion in teaching and for having addressing me to proceed with this carreer.

Last but not least, a special thanks to my family, who has pushed me to proceed with this career and not to give up during hard moments!